IN VITRO CO-CULTURE INTERACTION OF ADIPOSE-DERIVED MESENCHYMAL STEM CELLS (ADMSCs) AND THE EFFECTS OF THE SECRETED EXOSOMAL miRNAs ON MCF7 AND MDA-MB-231 DORMANCY

By

NORLAILY MOHD ALI

A thesis submitted to the Department of Pre-Clinical Sciences,
Faculty of Medicine and Health Sciences
Universiti Tunku Abdul Rahman,
in part fulfillment of the requirements of the degree of
Doctor of Philosophy of Medical Sciences

July 2021

ABSTRACT

IN VITRO CO-CULTURE INTERACTION OF ADIPOSE-DERIVED MESENCHYMAL STEM CELLS (ADMSCs) AND THE EFFECTS OF THE SECRETED EXOSOMAL miRNAs ON MCF7 AND MDA-MB-231 DORMANCY

Norlaily Mohd Ali

Breast cancer is the most often diagnosed cancer in women worldwide, and it remains a major health challenge due to cancer relapse. Breast cancer relapses are attributable to the existence of a subpopulation of non-proliferating breast cancer cells that have circulated to other organs and survived chemotherapy. The tumor microenvironment (TME) plays a significant role in driving cancer cells into dormancy and the transition of epithelial-to-mesenchymal (EMT) into aggressive phenotype accountable for cancer-related death. Adipose-derived mesenchymal stem cells (ADMSCs) have received attention in cancer research due to their tumor-homing ability, immunoregulatory activity and secretion of exosomes as biomarker carriers of microRNAs. Understanding cell-cell interactions between ADMSCs and breast cancer cells through the lens of exosomal miRNAs is essential in shaping the therapeutic function of ADMSCs in treating breast cancer metastasis and relapse.

In this study, two different subtypes of established breast cancer cells line were selected to represent the heterogeneity of breast cancer disease and

recurrence, with MCF7 being the luminal, hormonal dependent and non-metastatic while MDA-MB-231 being the basal, hormonal independent and high metastasis. After 48 hours of indirect co-culture, exosomes from the medium of MCF7 and MDA-MB-231 breast cancer cells with ADMSCs were extracted. The extravesical exosomes secreted during the cellular interaction carry many biomolecules, including miRNAs that can contribute to breast cancer tumorigenesis. Thus, we sought to evaluate the proliferation and metastasis changes of selected breast cancer subtypes followed by alteration in miRNAs expression profile via next-generation sequencing (NGS) that contribute to the changes.

Co-culture resulted in differential expression of exosomal miRNAs profiles that differentiate MCF7 and MDA-MB-231 subtypes. Also, there is a consensus of miRNAs that co-expressed in both subtypes. Those signature miRNAs regulate essential signaling pathways and induce cell cycle arrest by inhibiting epithelial-to-mesenchymal transition (EMT). The maintenance and induction of epithelial features in both cells resulted in reduced proliferation and metastasis abilities of BCCs and increased drug resistance. In summary, the works presented in this thesis contribute to the understanding of intercellular interaction between ADMSCs and breast cancer subtypes MCF7 and MDA-MB-231 in 2D-indirect co-culture. The study highlights the essential roles of ADMSCs in inducing breast cancer cell arrest through the secretion of consensus miRNAs via exosomes. Furthermore, the study has identified ideal miRNAs biomarker to be tested in pre-clinical and clinical studies prior to be used for screening, treatment and diagnosis in breast cancer relapse patients.

ACKNOWLEDGEMENT

"Alone, we can do so little; together, we can do so much."

-Helen Keller.

This thesis becomes a reality with the help and support of many individuals. I would like to extend my sincere gratitude to all of them. Foremost, I am grateful to Almighty Allah S.W.T. for the wisdom he bestowed upon me, the strength, the peace of mind and good health in completing the research and thesis. I wish to express my sincere thanks to my supervisor, Professor Dr. Alan Ong Han Kiat for his continuous guidance, advice and faith that have assisted me throughout the project, my co-supervisor, Emeritus Professor Dr. Cheong Soon Keng, for his financial support and advice and my external co-supervisor, Associate Professor Dr. Yeap Swee Keong from Xiamen University Malaysia for his never ending guidance and inspiration.

I would like to thank Cryocord Sdn. Bhd. in providing the adipose-derived mesenchymal stem cells used in this study and Majlis Kanser Nasional (MAKNA) for awarding me with Cancer Research Grant 2014 that financially aid my work. This work was mainly supported by Universiti Tunku Abdul Rahman through UTAR Research Fund (UTARRF) under project number (6200/A23). I would also like to acknowledge MyBrain Ph.D. scholarship (June 2015 –May 2017) for sponsoring my educational journey.

I would like to extend my gratitude to my fellow laboratory mates in FMHS Postgraduate Laboratory, including Boo Lily, Lim Sheng Jye, Choong Pei Feng and another research team from Universiti Putra Malaysia and Nottingham University Semenyih Kampus, Dr. Ho Wan Yong, Dr. Tan Sheau Wei, Dr. Dilan Satharasinghe, Dr. Huynh Ky, Nancy Liew Woan Charn and Koh May Zie for their assistance, sharing of knowledge and encouragement.

Finally, I would like to express my deepest gratitude to my family. Without the support of my family, especially my parents and husband, I would not have completed my postgraduate journey. To my two lovely daughters, Hana and Fyra, who are the joy of my life, I appreciate all your patience during mommy's Ph.D. journey. It requires lots of sacrifices and tricks to juggle the time between being a student and a mother. The unconditional love and unceasing encouragement from my family have kept me going during hard times.

I have been fortunate to have genuinely fantastic supervisors who are aware of my commitments and have been tolerant yet still assured that I have made progress, also, to those who directly or indirectly have lent their helping hands in this venture. This research project is a collective effort of all and I sincerely remember and acknowledge them. Thanks.

APPROVAL SHEET

This thesis entitled **"IN VITRO CO-CULTURE INTERACTION OF ADIPOSE-DERIVED MESENCHYMAL STEM CELLS (ADMSCs) AND THE EFFECTS OF THE SECRETED EXOSOMAL miRNAs ON MCF7 AND MDA-MB-231 DORMANCY"** was prepared by NORLAILY MOHD ALI and submitted as partial fulfillment of the requirements for the degree of Doctor of Philosophy in Medical Sciences at Universiti Tunku Abdul Rahman.

Approved by:

_____

(Prof. Dr. Alan Ong Han Kiat) Date: 14th July 2021
Professor/Supervisor
Department of Medicine
Faculty of Medicine and Health Sciences
Universiti Tunku Abdul Rahman

_____

(Emeritus Prof. Dr. Cheong Soon Keng) Date: 18th July 2021
Senior Professor/Co-supervisor
Department of Medicine
Faculty of Medicine and Health Sciences
Universiti Tunku Abdul Rahman

FACULTY OF MEDICINE AND HEALTH SCIENCES

UNIVERSITI TUNKU ABDUL RAHMAN

Date: 29th July 2021

SUBMISSION OF THESIS

It is hereby certified that **Norlaily Mohd Ali** (ID No: **14UMD07968**) has completed this thesis entitled "IN VITRO CO-CULTURE INTERACTION OF ADIPOSE-DERIVED MESENCHYMAL STEM CELLS (ADMSCs) AND THE EFFECTS OF THE SECRETED EXOSOMAL miRNAs ON MCF7 AND MDA-MB-231 DORMANCY" under the supervision of Prof. Dr. Alan Ong Han Kiat (Supervisor) and Emeritus Prof. Dr. Cheong Soon Keng (Co-Supervisor) from the Department of Medicine, Faculty of Medicine and Health Sciences, Universiti Tunku Abdul Rahman and Assoc. Prof Dr. Yeap Swee Keong (External Co-supervisor) from Xiamen University Malaysia Campus.

I understand that the University will upload a softcopy of my thesis in pdf format into UTAR Institutional Repository, which may be made accessible to the UTAR community and public.

Yours truly,

(Norlaily Mohd Ali)

DECLARATION

I NORLAILY MOHD ALI hereby declare that the thesis is based on my original work except for quotations and citations which have been duly acknowledged. I also declare that it has not been previously or concurrently submitted for any other degree at UTAR or other institutions.

(NORLAILY MOHD ALI)

Date: 29th July 2021

TABLE OF CONTENTS

LIST OF TABLES

LIST OF FIGURES

LIST OF ABBREVIATIONS

2D	2-dimensional
3D	3-dimensional
ABCA3	ATP Binding Cassette Subfamily A Member 3
ABCC2	ATP-binding cassette sub-family C member 2
ABCG2	ATP-binding cassette super-family G member 2
AChE	Acetylcholine esterase enzyme
ACTB	Actin beta
ATCC	American Type Culture Collection
ADMSCs	Adipose-derived mesenchymal stem cells
ABC transporters	ATP-binding cassette transporters
ALDH1A1	Aldehyde dehydrogenase 1 family, member A1
ANOVA	Analysis of variance
ATP	Adenosine triphosphate
BC	Breast cancer
BCC	Breast cancer cell
BP	Biological processes
BRCA1	Breast cancer 1
BRCA2	Breast cancer 2
BSA	Bovine serum albumin
CAPRIN1	Cell Cycle Associated Protein 1
CBL	Gene encoding the protein CBL
CC	Co-culture
CCND2	Cyclin D2

CD24	Cluster of differentiation 24
CD28	Cluster of differentiation 28
CD44	Cluster of differentiation 44
CD105	Cluster of differentiation 105
CDC42	Cell division control protein 42 homolog
cDNA	Complementary deoxyribonucleic acid
CO_2	Carbon dioxide
CSC	Cancer stem cells
Ct	Threshold cycle
Cq	Quantitation cycle
DAPI	4,6-diamidino-2-phenylindole
DE	Differentially expressed
DMEM	Dulbecco's Modified Eagle Medium
DNA	Deoxyribonucleic acid
dNTP	Deoxyribonucleotide triphosphate
dsDNA	Double-stranded DNA
EDTA	Ethylenediaminetetraacetic acid
EGFR	Epidermal growth factor receptor
EMT	Epithelial-mesenchymal transition
ER	Estrogen receptor
ErbB4	Receptor protein-tyrosine kinase ErbB-4
Exo-miRNA	Exosomal micro ribonucleic acid
ERα	Estrogen receptor alpha
FBS	Fetal bovine serum

FC	Fold change
FITC	Fluorescein isothiocyanate
G0	G zero phase
G1	G one phase
GEO	Gene Expression Omnibus
GO	Gene ontology
HER2	Human epidermal growth factor receptor 2
HIF-1α	Hypoxia-inducible factor 1-alpha
IGF1R	Insulin like growth factor1 receptor
KEGG	Kyoto Encyclopedia of Genes and Genomes
MAPK Signaling	A mitogen-activated protein kinase signaling
MAP3K7	Mitogen-activated protein kinase kinase kinase 7
MLH1	MutL homolog 1, mismatch repair gene
MMP	Matrix metalloproteinases
MMP9	Matrix metallopeptidase 9
NEB	New England Biolabs
NIH-3T3	Mouse Swiss NIH embryo derived cell line
RNA	Ribonucleic acid
MCF7	Epithelial luminal cell line positive for estrogen and progesterone receptors
MDA-MB-231	TNBC cell line that lacks ER, PR and HER2 expression
mRNA	Messenger ribonucleic acid
miRNA	Micro ribonucleic acid
MDR	Multi drug-resistant
MET	Mesenchymal-epithelial transition

MF	Molecular function
MLH1	DNA mismatch repair protein, mutL homolog 1
MMR	Mismatch repair
MNCRR	Malaysian National Cancer Registry Report
MTT	4,5-dimethylthiazol-2-yl
NCBI	National Center for Biotechnology Information
NFAT5	Nuclear factor of activated T cells 5
NGS	Next-generation sequencing
PAGE	Polyacrylamide Gel
PARP1	Poly [ADP-ribose] polymerase 1
PARP3	Poly [ADP-ribose] polymerase 3
PBS	Phosphate buffered saline
PCR	Polymerase chain reaction
PE	Phycoerythrin
PR	Progesterone receptor
PTEN	Phosphatase and tensin homolog gene
qRT-PCR	Real-Time Quantitative Reverse Transcription PCR
RIN	RNA integrity number
ROX	Inert fluorescent dye, carboxyrhodamine
RPMI-1640	Roswell Park Memorial Institute (RPMI-1640) cell culture media
SD	Standard deviation
SDS	Sodium dodecyl sulfate
siRNA	Small interfering RNA
SMAD 2	Mothers against decapentaplegic homolog 2

SMAD 4	Mothers against decapentaplegic homolog 4
SNAIL	Zinc finger protein SNAI1
SYBR® Green	Fluorescence reporter dye
SYTO64™	Fluorescence nucleic acid dye
TEM	Transmission electron microscopy
TGFβ	Transforming growth factor-beta
TLR	Toll-like receptor
TME	Tumor microenvironment
TNBC	Triple-negative breast cancer
TP53	Tumor protein 53
TWIST1	Twist-related protein 1
UNG	Uracil-N-glycosylase, incubation step
UV	Ultraviolet
Vybrant™ DiO	Fluorescence cell labeling dye
Wnt Signaling	Wingless-related integration site signaling
ZEB1	Zinc finger E-box binding homeobox 1

CHAPTER 1

INTRODUCTION

Ranked as the fifth leading cause of cancer death globally, breast cancer is the most commonly diagnosed incidence (24.2%) with the highest cancer mortality in women (15%) (Bray et al., 2018). In Malaysia, cancer is the third leading cause of death after cardiovascular disease and septicemia. The annual cancer incidence was growing over the past 10 years (2007-2016) and was reported to be higher in women than men. Malaysian National Cancer Registry Report (MNCRR) estimated that approximately 34 of every 100,000 women had breast cancer from 2012 and 2016 (Azizah, 2016).

Despite substantial progress in the overall survival of many types of cancer due to earlier detection and newer therapies, about 30% of women with breast cancer experience recurrence. Years and decades after curative surgery, chemotherapy and targeted therapy, recurrence and chemoresistance still remain as the primary unmet medical need.

Breast cancer has been generally acknowledged as being heterogeneous in terms of phenotypic, genetic and epigenetic makeup, which is categorized into few subtypes based on receptors expression and proliferative activity with MCF7 being a luminal A-type and MDA-MB-231 as basal B-triple negative breast cancer (TNBC) (Shi et al., 2017). While similar pathological features are

present, patients frequently respond differently to therapies, reflecting that the various cancer subtypes are substantially diverse. MDA-MB-231 was reported to be highly metastatic and aggressive compared to MCF7 and was linked to recurrence and chemoresistance in breast cancer patients (Plava et al., 2019).

Metastasis is the spread of cancer cells throughout the body and is one of the leading causes of cancer recurrence and mortality (Sakha et al., 2016). In the event of metastasis, cells start to lose contact and adhesion facilitated by epithelial-mesenchymal transition (EMT) which leads to the increase of invasion and migration of cancer cells. Many studies have identified the crucial role of EMT in metastasis of breast cancer (Shao et al., 2015; Hu et al., 2018). Tumor cells can enter dormancy, a state of hibernation when cells are under an unfavorable microenvironment. Following this, the cells undergo metastasis latency and once the microenvironmental conditions are favorable, they switch into proliferating cells and initiate the events leading to recurrence (Yadav et al., 2018). Therefore, tumor microenvironment (TME) plays a crucial role in the maintenance of dormancy and recurrence of cancer cells.

A wide range of cellular processes and events in multicellular organisms is mediated by intercellular signaling in the microenvironment. Understanding intercellular signaling between heterogeneous cancer cell communities, as well as the surrounding stromal cells is crucial, particularly in the development, progression and relapse of cancer. TME consists of multiple cellular and non-cellular compartments comprised of extracellular matrix, tumor vasculature, tumor cells, stromal cells, immune cells and fibroblasts.

Mesenchymal stem cells (MSCs) are multipotent stromal cells isolated from a variety of tissues such as bone marrow, Wharton's jelly, dental pulp and adipose tissue. In the tumor niche, MSCs are actively recruited to the site of inflammation and injury, where they express growth factors that expedite the regeneration of tissues (Ramdasi et al., 2015). Several studies have shown that MSCs from various sources release multiple cytokines, growth factors and miRNAs that could be used to treat cancer or as a source of pro-tumor factors (Kucerova et al., 2013; Ono et al., 2014; Reza et al., 2016; Sakha et al., 2016).

Interestingly, the interaction between tumor and surrounding cells particularly adipose-derived mesenchymal stem cells (ADMSCs) in the microenvironment, has been the highlight of cancer research. It involves targeted therapy such as autologous fat grafting in breast reconstruction post-surgery, stem cell transplant in regenerative medicine and anti-cancer cell-based drug (Ramdasi et al., 2015; Cocce et al., 2017).

Collecting evidence suggests that dysregulation of miRNAs expression is associated with tumor formation, growth and metastasis either as promoter or suppressor (Ono et al., 2014; Reza et al., 2016; Sakha et al., 2016). Recently, much interest has been generated in targeting circulating miRNAs, also widely described as extracellular miRNAs secreted out into the microenvironment by vesicular carriers such as exosomes.

Exosomes are small membrane vesicles that encapsulate molecules such as protein, lipids, transcription factors, RNAs and microRNAs and are

secreted by numerous cell types into their surroundings. Exosomal miRNAs are packaged, circulated and incorporated into recipient target cells via exosomes and its content is highly variable depending on cell origin (Milane et al., 2015). In the tumor microenvironment, exosomes were shown to transfer cancer-promoter or suppressor miRNAs as well as other biological molecules through cell-cell interaction (Reza et al., 2016). Therefore, exosomal miRNAs may contribute to cancer therapy and be able to serve as promising cancer biomarkers for early diagnosis and prognosis.

Over the past few years, several studies involving interaction between ADMSCs and breast cancer have been carried out; however, due to the complexity of the cancer pathogenesis, primarily due to their heterogeneity and adaptation to intercellular signaling in TME, most of these studies have failed to show a consensus on the effect of ADMSCs on cancer progression. Moreover, studies involving miRNAs have focused mainly on their specific impact on corresponding target genes instead of looking globally at gene correlation networks. Therefore, sequencing in analyzing miRNAs profiles, particularly for addressing larger sample sizes, has become very advantageous.

The present study hypothesized that circulating miRNAs secreted by ADMSCs could affect the metastasis and dormancy of recipient breast cancer cells. We anticipated that the miRNAs secreted in exosomes by ADMSCs would inhibit the proliferation and metastasis in breast cancer cells by activating epithelial-mesenchymal regulators involved in inducing cells into dormancy.

Identifying differential miRNA expression profiles between breast cancer subtypes is essential for early diagnosis of relapse and the selected tumor suppressor miRNAs or oncomiRNAs can be exploited in targeted therapy by blocking the entry of dormant cells into an actively proliferating state that trigger a recurrence. It aids in lowering recurrence rates among treated breast cancer patients. The development of miRNAs strategy to treat high recurrence and chemoresistant breast cancers that remain incurable despite aggressive therapies can be accelerated by introducing miRNAs-based therapeutics, for which tumor dormancy should be eradicated or removed. Future research in this area may discover novel miRNAs candidates that ultimately offer therapeutic solutions for unmet medical needs in cancer dormancy and drug resistance.

The main objective of the present work was to study the interaction between co-cultured ADMSCs and breast cancer cells and the interplay of miRNAs as the main signaling molecules transported by exosomes.

The specific objectives were:

1. To elucidate the interaction between ADMSCs and breast cancer cells using indirect co-culture and investigate the effects on the proliferation and metastasis of breast cancer.
2. To study the mechanism of ADMSCs in exerting biological functions on two subtypes of BCCs, MCF7 and MDA-MB-231 in the co-culture microenvironment.
    a. To isolate excreted exosomes and profile miRNAs content of exosomes and cellular of ADMSCs and breast cancer using sequencing method.
    b. To assess the alteration of miRNAs expression profiles through bioinformatics analyses in excreted exosomes and recipient cells following co-culture treatment.
    c. To determine the signaling pathways involved during co-culture interaction of two different subtypes of breast cancer with ADMSCs responsible for metastasis and recurrence.
    d. To identify the potential miRNAs involved in cancer inhibition and metastatic ability via transient overexpression.

CHAPTER 2

LITERATURE REVIEW

2.1 Cancer

Cancer is a disease that results when normal cells undergo a random mutation and evolve into abnormal cells. The abnormal cells divide and multiply in an uncontrolled way to form tumors. Certain types of cancerous cells can form visible growths termed tumors, damage the immune system and cause other changes that block the body from functioning regularly, while others do not (Ignatov et al., 2018). Cancer cells often spread into the surrounding tissue or metastasize to distant organs through the blood or the lymphatic system.

Factors contributing to cancer development involve genetic and epigenetic factors that cause mutation to the DNA or genes that govern the cells. The mutations in genes can initiate cancer by accelerating the rate of cell division or by obstructing the mechanism of normal growth through disrupting cell cycle checkpoint or programmed cell death known as apoptosis. The failure of cell cycle arrest and apoptotic control allows cancer cells to survive longer and accumulate mutations (Pfeffer and Singh, 2018).

Cancer development is a multi-step process where oncogenic mutations give rise to cancer cells with different genetic defects, differing within an

individual tumor (Plava et al., 2019). “Initiation” is the first step in cancer development where DNA mutations occur supported by hypoxia, hormones, chemicals, radiation or infection. The irreversible changes of DNA mutation are followed by the second step of cancer formation, the “Promotion” phase. It involves several steps, including the increase in the number of cells, phenotypic changes in cells, *in situ* cancer (confined to the place of origin) and end with invasive cancer (spreading to the surrounding tissues) (Ignatov et al., 2018).

One cancer hallmark is genome instability, which enables cancer cells to accumulate genetic mutations at an abnormal rate. Four main genes are involved in cell division, namely oncogenes such as *RAS* (Degirmenci et al., 2020) and *MYC* (Yang et al., 2020), tumor suppressors genes such as *BRCA1*, *BRCA2* and *TP53* (Godet et al., 2017), DNA repair genes (Majidinia and Yousefi, 2017) and apoptosis genes (Pfeffer and Singh, 2018). A defect in one of these genes can initiate cancer. In normal cells, these critical genes maintain the balance between cell survival and cell death. In tumor cells, oncogenes and tumor suppressor genes are commonly mutated (Harburg and Hinck, 2011).

Another fundamental mechanism in cancer involves dysregulation of epigenetics regulators leading to genome instability. Epigenetic changes affect gene expression in different ways mediated by environmental factors such as age and lifestyle behavior. Although it does not directly affect the primary DNA sequence, the alterations in DNA methylation, histone modifications and nucleosome remodeling affect gene expression to turn the genes “on” and “off

known as gene silencing (Muntean and Hess, 2009; Grønbaek et al., 2007). As reported earlier, increased DNA methylation that results in decreased *BRCA1* gene expression increases the risk for breast and other cancers (Tang et al., 2016).

2.1.1 Epidemiology and Classification of Breast Cancer Cells

Over 200 different types of cancer are categorized by their cell types or place of origin. Breast cancer is the most commonly diagnosed cancer in women worldwide, with an estimated 1.38 million new cases per year. In a recent 2020 statistic report, World Health Organization (WHO) has reported an increase of approximately 2.26 million new cases in both sexes of all ages, as shown in Figure 2.1 (A) (Sung et al., 2021; WHO, 2020). The alarming number has raised concern among clinicians and researchers that drive them to continue making significant progress towards breast cancer.

In Malaysia, cancer is the third leading cause of death after other diseases and is the most prevalent cancer in females, as shown in Figure 2.1 (B). Statistically, one in 20 Malaysian women will develop breast cancer in their lifetime, and 48% are diagnosed with third or fourth cancer stages (Yip et al., 2006). Malaysia has one of the lowest five-year survival rates in the Asia Pacific region, with 49% (Ab, 2017). While the prevalence of breast cancer is rising worldwide, in some continents like Europe, the mortality rate has been decreasing from 2014 and 2019 due to the introduction of hormone replacement therapy as well as early screening and intervention (Malvezzi et al., 2019).

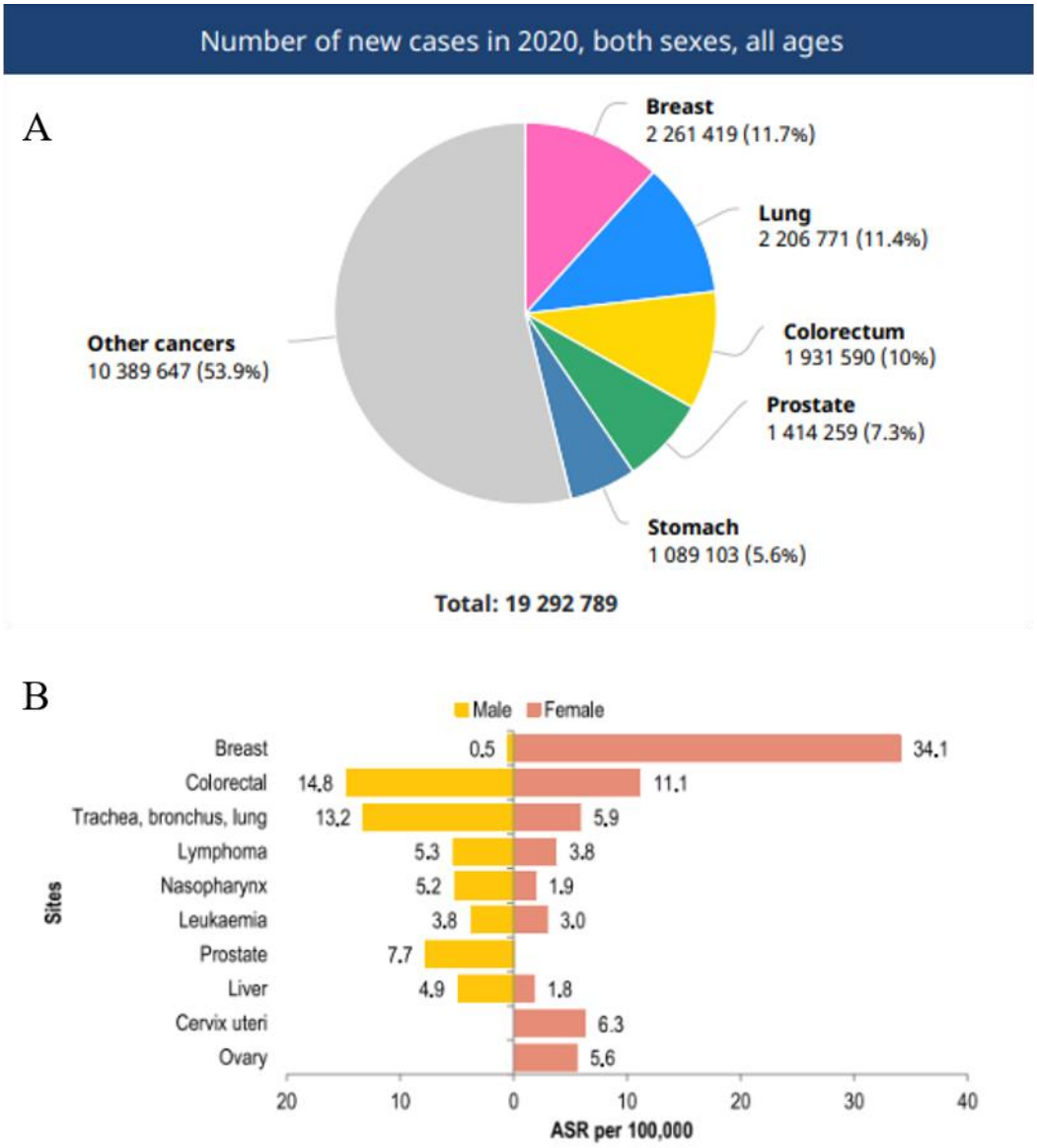

Figure 2.1. Breast cancer statistics. A) Number of new cancer cases worldwide in 2020 in both sexes among all ages. B) Malaysia's top 10 most common cancers. Breast cancer has the highest prevalence, followed by colorectal, lung, lymphoma, nasopharynx, leukemia, kidney, liver, cervix and ovary, adapted from Global Cancer Statistics 2020 and Malaysian National Cancer Registry Report (Ab, 2017; Sung et al., 2021).

The risk of getting breast cancer is associated with specific hormones or factors related to reproduction, environmental factors, and unhealthy lifestyles (Iacoviello et al., 2020). Breast cancer is a malignant growth that frequently but not necessarily originates in the epithelial cells of glandular milk ducts or lobules of the breast tissues.

Breast cancer has been generally recognized as heterogeneous in terms of phenotypic, genetic and epigenetic composition due to random mutations. It can be biologically and molecularly classified based on cell proliferation and metastatic activities and hormonal receptors expression of estrogen (ER), progesterone (PR) and human epidermal growth factor receptor 2 (HER2) (Ahmad, 2013; Ignatov et al., 2018). Breast cancer classifications are very crucial to specify the accurate prognosis and plan an effective treatment. The most established classification includes molecular subtypes of breast cancer and tumor grades.

2.1.1.1 Molecular Subtypes of Breast Cancer

The current molecular classification divides breast cancer into four groups based on their hormonal expression, namely luminal A, luminal B, HER2 (human epidermal growth factor receptor 2) and basal according to the St. Gallen Consensus 2011 (Goldhirsch et al., 2011). Luminal A is the most common subtype that expresses estrogen receptor (ER) and progesterone receptor (PR) but lacks HER2 expression and low expression of the

proliferation-related gene, *Ki-67*. Luminal B is similar to luminal A but has a high expression of *Ki-67* and more aggressive than luminal A.

The third subpopulation exhibits HER2-overexpression and the last one is a basal-like subtype of breast cancer known as triple-negative breast cancer (TNBC) that does not express all three ER, PR and HER2 receptors (Goldhirsch et al., 2011; Al-Thoubaity, 2020). The most common laboratory method to distinguish breast cancer hormonal expression markers is via polymerase chain reaction (PCR) (Kittaneh et al., 2013).

Table 2.1. Molecular subtypes of breast cancer

Subtype	Biomarkers	Prevalence (%)	Response to treatment
Luminal A	ER+, PR+/-, HER2- and *Ki67* low	30-70	Endocrine therapy (tamoxifen and aromatase inhibitors)
Luminal B	ER+, PR+/-, HER2+/- and *Ki67* high	10-20	Endocrine therapy (tamoxifen and aromatase inhibitors), Trastuzumab
HER2-positive	ER-, PR- and HER2+	15-20	Trastuzumab, Chemotherapy
TNBC/ Basal-like	ER-, PR- and HER2-	5-15	Endocrine therapy, Chemotherapy

2.1.1.2 Staging of Breast Cancer

Another common classification used in cancer diagnosis is examining their clinical behavior such as the stage of cancer. It describes the progression and spreading of cancer in the body as summarized from American Joint Committee on Cancer (AJCC) in Table 2.2 (Singletary et al., 2003).

Table 2.2. Breast cancer staging

Stage	Term	Description
0	Carcinoma *in situ*	Abnormal cells are present and confined to the original location.
1	Early stage	Cancer has spread to the other tissue in small areas.
2	Localized	Cancer affecting nearby tissues and lymph nodes.
3	Regional spread	Cancer spread to distant tissues and lymph nodes.
4	Distant spread	Cancer has spread beyond the breast to the other parts of the body.

The frequently studied breast cancer subtypes with distinctive clinical features are MCF7, a luminal A-type and hormone-dependent, and MDA-MB-231 as basal B, hormone-independent TNBC. Other distinct features between the subtypes are in terms of phenotypic and metastasis characteristics, with MCF7 cells expressing epithelial phenotypes and lower metastatic ability while MDA-MB-231 are more mesenchymal and highly metastatic (Yates et al., 2017). Invasive carcinomas like TNBC are cancers in which the altered cells diffuse to surrounding connective tissues and metastasize to distant organs of the body (Xu et al., 2018).

Due to the complex underlying biology in cancer development, the well-established traditional classifications of breast cancer hormonal status and staging biomarkers remain insufficient to reflect breast cancer's diverse biological and clinical heterogeneity, especially in patients with risk of recurrence (Søkilde et al., 2019). In recent years, researchers embark on advanced technology such as exome, mRNA and microRNA arrays and sequencing, genomic DNA copy number and methylation arrays to establish comprehensive and integrated breast cancer data (Curtis et al., 2012; Koboldt et al., 2012). Evolution and advancements in high-throughput molecular procedures and bioinformatics have tremendously improved the understanding of BC biology and change the way oncologists diagnose the disease.

2.1.2 Breast Cancer Treatment

Treatment options for breast cancer depend on several factors, including subtypes (hormone receptor status), stage of the tumor, mutation status of *BRCA1* gene and the age and health condition of the patient. Breast cancers that are confined to the breast or immediate surrounding area are firstly treated with surgery with or without radiation therapy. For recurrent and metastatic cancer, systemic therapy such as chemotherapy, hormonal therapy, targeted therapy and immunotherapy are typically used alone or in combination following surgery (Hurvitz et al., 2013; Othman and Nagoor, 2014).

Treatment for the early stage of breast cancer via hormonal therapy works either by blocking estrogen pathway signaling using Tamoxifen or depriving the estrogen level using aromatase inhibitors or antiestrogens, leading to inhibition of cell proliferation (Jensen et al., 2003; Leung et al., 2017). As for metastatic breast cancer, a combination of chemotherapeutic drugs such as Anthracyclines, cisplatin, doxorubicin, fluorouracil, docetaxel and a few more are used (Cardoso and Castiglione, 2009). The latest advancement in breast cancer treatment is the use of targeted drug therapy. The use of hormonal therapy and chemotherapy alone are sometimes less effective for metastatic, TNBC and recurrence cancer. Therefore, a combination of adjuvant chemotherapy and targeted therapies that specifically target genes, signaling proteins or microenvironment components that support the survival of the cancer subtypes are preferred (Godet et al., 2017).

Breast cancer targeted therapy is a personalized medicine customized for individual needs that involve the use of small molecules or monoclonal antibodies to obstruct the stimulation of breast cancer growth in specific ways. Angiogenesis inhibitors function by blocking the formation of the new blood vessel while monoclonal antibodies block specific target protein that stimulates breast cancer growth, such as Herceptin® targeting HER2 receptor (Higgins and Baselga, 2011; Figueroa-Magalhães et al., 2014; Chan et al., 2017).

Advances in genomic sequencing have contributed significantly to developing a new molecular target that can be utilized as targeted biomarkers for breast cancer intervention. Through sequencing, unlimited genetic variations can be decoded from cancer tissues and circulating cancer cells that may enable the discoveries of mutations responsible for cancer or prediction of drug responses and treatment outcomes (De Abreu et al., 2013; Rabbani et al., 2016).

Despite advanced technologies in cancer treatment, the number of people succumbing to breast cancer is still high. There are challenges to match each individual with the suitable therapy and the risk of breast cancer resistance to the treatment. The main preventive strategy focuses on early detection and early intervention to improve survival rates (Ahmad, 2013). The best solution to address the heterogeneity of breast cancer is by optimizing the efficacy of individualized therapy and developing new predictive markers of sensitivity to differentiate breast cancer subtypes.

Many recent studies have proposed miRNAs as potential biomarkers and therapeutic targets for breast cancer intervention (Graveel et al., 2015; Detassis et al., 2017; Xiong et al., 2017). Differential expression of miRNAs can distinguish not only between cancer and non-cancerous cells (Gao and Liu, 2011) but also between cancer subtypes. A group of researchers has successfully identified signature miRNAs that are differentially expressed and can differentiate between breast cancer subtype basal-like and luminal A of breast cancer (Blenkiron et al., 2007).

The current trend of targeted therapy focuses on miRNAs as critical regulators in cancer therapy due to their roles as tumor suppressors and oncogenes (Kong et al., 2012; Graveel et al., 2015). This substantiates that miRNAs have promising therapeutic application for advanced screening, selection of targeted drug treatment and diagnosis of TNBC, metastatic and recurrence breast cancer cells (Graveel et al., 2015).

2.1.3 Breast Cancer Relapse

Breast cancer remains a substantial scientific, clinical and societal challenge among cancer patients due to cancer relapse. Cancer relapse or recurrence is cancer that has survived and returned after remission following treatment of original cancer. Even after surgery, isolated groups of cells that remain after surgery may survive chemotherapy and radiation therapy that further develop into tumors (Voduc et al., 2010; Belkacemi et al., 2018).

While breast cancer can reappear almost anywhere in the body, liver, bones, lungs, brain and skin are among the common locations for the cancer cells to recur. If it recurs at the same place as original cancer, it is coined as local recurrence. In contrast, if cancer already metastasized to other areas, it is known as a distant recurrence (Smid et al., 2008). The recurrence rates differ widely among cancer types depending on subtypes, stage and metastatic ability, histology, genetic factors, patient-related factors and treatments (Elder et al., 2006; Belkacemi et al., 2018; Ignatov et al., 2018).

The heterogeneity of breast cancer is the main reason for the possible failure of such treatment as universal breast cancer therapy (Chan et al., 2017). The occurrence of cancer relapse could also be attributable to cancer stem cells (CSCs) or acquired aggressive and metastatic phenotype by cancer cells (Al-Ejeh et al., 2011; Yates et al., 2017). In fact, the difference in the degree of tolerance to therapies among heterogeneous BCCs contributed to higher recurrence, particularly in the highly metastatic cells (Ahmad, 2013).

In breast cancer patients, a differential pattern of breast cancer relapse among different subtypes has been reported. The hormonal expression status underlying each subgroup has been closely linked to the recurrence rate after treatment. Patients with ER+ breast cancer have a lower risk of relapse within five years. Almost all late-relapsing patients (later than five years) with luminal tumors had high ER+ and PR+ expressions (Pantel and Hayes, 2018; Wangchinda and Ithimakin, 2016).

Meanwhile, basal-like, ER- and HER2-enriched breast cancer patients tend to recur within the first five years after diagnosis (Riggio et al., 2021). TNBC being the most aggressive breast cancer subtype with clinical features of high invasiveness, high metastatic potential and poor prognosis, is an example of highly prone to relapse. According to the statistic prepared by the American Cancer Society, the 5-year survival rate for women with metastatic breast cancer is 27% worldwide (Fouad and Aanei, 2017). Highly metastatic cells can metastasize to distant sites by activating Epithelial-to-Mesenchymal Transition (EMT) transcription factors that persist in chemotherapy and cause relapse (Lo and Zhang, 2018).

Another possible reason for relapse is due to tumor dormancy. Primary tumors often exploit the inactive condition to resist treatment where cancer cells remain quiescent and undetected for an extended period. Dormant cells remain in a resting state until favorable conditions trigger cancer recurrence (Ahmad, 2013; Yadav et al., 2018; Neophytou et al., 2019).

2.2 Metastasis

Metastasis or the spread of cancerous cells throughout the body remains the most common underlying cause of death in breast cancer patients (Sakha et al., 2016). Patients presenting with distant metastasis are usually diagnosed with Stage IV disease and are unlikely treatable. The metastasis process starts when cancer cells escape the multiple barriers and break away from the primary tumor, circulating through the circulatory and lymphatic system and colonized at a secondary location (Lo and Zhang, 2018).

2.2.1 Metastasis and Tumor Microenvironment

Cancer cells interact and evolve in a complex, surrounding environment known as the tumor microenvironment (TME) for sustainable growth and metastasis. TME consists of both malignant cancer cells and non-malignant stromal cells, including mesenchymal stem cells (MSC), immune cells, fibroblast, endothelial cells, macrophages and the non-cellular components of the extracellular matrix such as collagen, laminin, fibronectin, hyaluronan, and signaling molecules (Quail and Joyce, 2013; Baghban et al., 2020).

To sustain cancer development and metastasis, tumor cells regulate the activity of those cellular and non-cellular components through dynamic signaling networks creating intercellular communication. The signaling networks might involve crosstalks between neighboring cells via cytokines,

growth factors and inflammatory mediators or between distant cells through circulating tumor cells, cell-free DNA and exosomes (Baghban et al., 2020). Alteration of interactions between cancer cells and their microenvironment leads to diverse outcomes in the programmed behavior of the cells.

2.2.2 Mesenchymal Stem Cells in Tumor Microenvironment

Tumors have been described as wounds that do not heal due to the chronic inflammatory response. MSCs are among cells that are actively being recruited to the tumor sites where they are needed to replace damaged tissue in the inflammation area of the active tumor. They indirectly or directly interact with different cell types within the tumor stroma including cancer cells (Ramdasi et al., 2015). MSCs have been isolated from adult tissue such as bone marrow, adipose tissue, dental pulp, and fetal tissue (Wharton's jelly).

They have been extensively explored as therapeutic interventions in many disorders, including cancer (Hmadcha et al., 2020). Due to their ability to self-renew, regulate immune response, differentiate into various cell types and have remarkable migration ability, MSCs have been perceived as crucial players in TME. Numerous researches have highlighted the importance of MSC in TME in tumor development and in cancer recurrence and prognosis of patients (Kucerova et al., 2013; Hass et al., 2019; Hass, 2020).

Although several findings have documented the potential benefits of MSC to treat various diseases such as bone and cartilage diseases, regenerative disease, neurological disorders, cardiac ischemia and diabetes, the therapeutic potential of MSCs in cancer is still debated (Hmadcha et al., 2020). Some studies claimed that MSCs can promote tumorigenic processes by inducing malignant transformation, promoting neovascularization and angiogenesis and maintaining their neoplasticity characteristic (Kucerova et al., 2013).

Moreover, ADMSCs specifically have been shown to suppress apoptosis, promote metastasis formation and enhance chemoresistance to anticancer drugs (Reza et al., 2016). The most recent findings have found the contribution of MSCs in cancer evasion against immune system, cancer stem cell niche, and stemness characteristics (Kletukhina et al., 2019).

On the other hand, other studies have shown the anti-inhibitory effect of MSCs where they induce tumor cell cycle arrest. MSCs were demonstrated to impede the self-renewal ability of cancer cells, proliferation, colony formation and expression of oncogenes (He et al., 2018; Allahverdi et al., 2020). Meantime, both proliferative and inhibitory activities of MSCs have been documented in the same study that described the dual role of MSCs as tumor-favoring and tumor-inhibiting by suppressing proliferation and apoptosis (Li et al., 2011). All these anti-tumor or pro-tumor effects are attributed to the molecules secreted into the immediate microenvironment by MSCs.

2.2.2.1 Human Adipose-Derived Mesenchymal Stem Cells

Adipose-derived MSCs (ADMSCs) are non-tumorigenic cells and share similar characteristics with MSCs isolated from different sources. They have been shown with the ability to differentiate into a variety of specialized cell types and secrete cytokine and growth factors that aid in the tissue regeneration process. Due to their abundance and less invasive harvesting procedure from cosmetic liposuction, ADMSCs have shown great promise in medical application mainly for cell and tissue regeneration in chronic wounds, autologous fat grafting in breast reconstruction post-surgery, immune system regulation, tissue engineering, cell therapy and anti-cancer cell-based drug (Pandey et al., 2011; Al-Nbaheen et al., 2013; Ramdasi et al., 2015; Scioli et al., 2019).

In addition, ADMSCs do not express human leukocyte antigens including HLA-DR molecules and co-stimulatory molecules essential for immune response, making ADMSCs potential candidates for both autologous and allogeneic therapies (Sabol et al., 2018). Despite all the therapeutic potentials of ADMSCs, long-term follow-up of their use have not been thoroughly implemented, raising concern about the safety of their usage (Scioli et al., 2019). Although ADMSCs do not directly initiate cancer or malignant transformation, interactions between ADMSCs and cancer cells in the tumor microenvironment can modulate cancer metastasis and subsequent recurrence (Patrikoski et al., 2019).

Despite having the ability to home or being recruited to the tumor microenvironment, ADMSCs populations are physiologically located in the breast and possibly near any occurring breast cancer site. These features allow both cells to directly or indirectly communicate with each other, affecting both cells' function and activities (Schweizer et al., 2015). MSCs secrete many factors that participate in regulating breast cancer.

Similar to other types of MSCs, ADMSCs secret anti-inflammatory and immunosuppressive cytokines, growth factors and chemokines promoting migration and metastasis of breast cancer (Rowan et al., 2014). ADMSCs also have been reported to positively and negatively regulate breast cancer progression by activating EMT transcription factors after interaction with cancer cells in the tumor microenvironment (Kletukhina et al., 2019; Chen et al., 2019; Schweizer et al., 2015). In fact, ADMSCs can intensify tumorigenic activity, creating an inflammatory microenvironment that facilitates tumor growth and angiogenesis (Jiang et al., 2020). In other contradicting studies, researchers have described that ADMSCs attenuated growth and invasion of breast cancer cells, induces apoptosis by activation of PI3K/AKT and ERK1/2 and their anti-tumor activity in breast cancer (Scioli et al., 2019; Li et al., 2020; Rybinska et al., 2020).

Meanwhile, the mechanism of action ADMSCs on cancer cells has been demonstrated in numerous studies involving a cross-talk between both populations. Such studies proposed two ways of communication courses via direct cell-to-cell contact or contact independent (Rowan et al., 2014; Kuhbier

et al., 2014). For contact independent, exosomes and growth factors have been the most studied signaling factors involved (Wang et al., 2019). Exosomes are secreted to transport small interfering RNAs, microRNAs or chemotherapeutic compounds to the surroundings. Because of this feature, researchers have shifted the focus of breast cancer treatment toward exosomes.

2.2.3 Epithelial-Mesenchymal Transition

2.2.3.1 Epithelial-Mesenchymal Transition in Cancer Metastasis

To overcome the challenges during the metastasis process, cancer cells exploit the fundamental feature of metastatic cancer that is the ability to undergo Epithelial-to-Mesenchymal Transition (EMT) and the reverse mesenchymal-to-epithelial transition (MET) process (Lo and Zhang, 2018). Many signals received from the TME can activate EMT, including *TGFβ, HIF-1α*, *EGF*, *WNT*, and *Notch*, which help promote breast cancer's malignant transformation (Ribatti et al., 2020). EMT is a developmental program where cells undergo changes in cell phenotypes by losing epithelial markers and gaining mesenchymal characteristics that acquire stem-like properties and a migratory phenotype. During the transition, epithelial cells lose cell polarity and cell-cell adhesion and gain migratory and invasive properties to become mesenchymal cells (Tanabe et al., 2020).

Meanwhile, MET is the reverse process of EMT where cells regain epithelial and lose their mesenchymal traits. Both have been shown to play roles in the tumorigenic process in all stages of cancer progression, starting from initiation, primary tumor development, invasion, dissemination, metastasis to colonization. The ability of cancer cells to switch from EMT to MET and vice versa enables metastatic outgrowth at distant sites (Quail and Joyce, 2013; Brabletz et al., 2018).

EMT is regulated at the transcriptional level by EMT-activating transcription factors mainly of the *TWIST, SNAIL, ZEB* families and miRNAs (e.g., the mir200family). The phenotypic changes of EMT include the loss of adherents and tight junction components such as *E-cadherin*, *claudins* and *vimentin*, as well as stem-cell-like properties (Brabletz et al., 2018). Expression of transcription factor *TWIST1* has been shown to promote breast cancer initiation by inhibiting tumor suppressor gene *Tp53*, which subsequently work mutually with oncogenes *HER2* and *H-ras* to accelerate the malignancy (Piccinin et al., 2012; Morel et al., 2012).

Meanwhile, EMT role in triggering metastasis has been demonstrated in xenograft tumor models where the depletion of EMT transcription factors significantly inhibited metastatic dissemination. Conversely, ectopic activation of the EMT transcription factors enhances metastatic dissemination (Ye and Weinberg, 2015). Furthermore, EMT regulator *SNAIL1* has been implicated with the increase of *Matrix metalloproteinase-1* (*MMP-1)* and *Matrix*

metalloproteinase-9 (MMP-9) expression, which aid in the breakdown of ECM that facilitated tumor invasion and metastasis (Ota et al., 2009).

2.2.3.2 Epithelial-Mesenchymal Transition in Chemoresistance of Breast Cancer

Increasing findings also described the potential role of EMT in promoting resistance to therapy and recurrence in patients with breast cancer. One possible mechanism is through activation of EMT regulators including *TGF-β, SNAIL* and *TWIST1* that have been demonstrated to attenuate the cell cycle and conferred resistance to cell death by suppressing *Tp53*-mediated apoptosis death signaling pathways (Vega et al., 2004; Gal et al., 2008; Xu et al., 2018).

Further data reported that EMT induction simultaneously upregulates the expression of several ATP binding cassette (ABC) transporters leading to multidrug resistance in breast cancer cells. *P-glycoprotein* is one of the members of ABC transporter superfamily encoded by multidrug resistance gene 1 (*MDR1*). Tumor cells enriched with *P-glycoprotein* function as efflux pumps of multiple and selected drugs such as doxorubicin, docetaxel and etoposide. Increased efflux of chemotherapeutic agents leads to reduced intracellular drug levels, which directly cause a failure in chemotherapy (Fletcher et al., 2010; Jiang et al., 2017).

Additionally, some findings show EMT supports cancer stem cells (CSC) properties responsible for tumor reoccurrence and can establish metastases (Tanabe et al., 2020). These tumor-initiating cells have been described as capable of mammosphere formation and self-renewal. Furthermore, high expression of CD44+/CD24-, *aldehyde dehydrogenase (ALDH)* and ABC transporter family assist in metabolizing cytotoxic drugs, making CSC resilient to chemotherapy (Huang et al., 2015).

Interestingly, recurrent tumors frequently presented an enhanced expression of EMT gene mainly *vimentin, SNAIL, TWIST* and a decreased of *E-cadherin* (Ahmad, 2013). Thus, it can be concluded that EMT promotes breast cancer resistance in many ways and are the crucial regulator for cancer relapse.

2.2.3.3 Epithelial-Mesenchymal Transition in Cancer Dormancy

With the intervention of MSCs, cancer cells are able to adapt to changes in the tumor environment including therapeutic interventions, where they are able to reach distant organs, penetrate into the stroma and survived initial treatment until there are metastatic relapses years afterward (Park and Nam, 2020). In recent years, studies of bidirectional interaction between breast cancer cells and surrounding MSCs have demonstrated the resistance to chemotherapies due to cell dormancy (Ono et al., 2014; Reza et al., 2016).

Dormant cells acquire the capacity to re-enter the cell cycle, emerge from dormancy, adapt to their new surrounding and initiate colonization in response to signals from MSCs, thereby leading to metastatic outgrowth (Park and Nam, 2020). In indirect co-culture interaction of MSC and breast cancer, Bliss et al. have described the ability of MSC to promote dormancy by releasing exosomes with distinct miRNA content, which facilitates their quiescence (Bliss et al., 2016). Likewise, another research group has demonstrated the role of exosomal MSC in stimulating the cancer dormancy of breast cancer cell MCF7 (Casson et al., 2018).

The definition of dormancy is derived from clinical observations that cancer returns several years after surgery, as illustrated in Figure 2.2. Tumor dormancy is one of the strategies for resistance against various cancer therapies which can be induced by cues from ADMSCs (Bliss et al., 2016). This pathological state is distinct from ‘slow-cycling cells’, such as cancer stem cells (CSC). There are resemblances between the two of them such as rare population, chemoresistant and highly responsible for cancer reoccurrence.

Additionally, many of the biological mechanisms involved in controlling the dormant state of a tumor can also govern CSC behavior, including cell cycle modifications, alteration of angiogenic processes, and modulation of antitumor immune responses. Despite that, fundamental differences exist between the two notions where dormant cells are not expressing stemness markers and CSC are not in a total arrest state, rather in a slow-cycling state (Phan and Croucher, 2020).

Meanwhile, tumor dormancy is an arrest of tumor growth where the cancer cells are in a quiescent state and the oncogenic pathways are suppressed (Yadav et al., 2018). Although the suppression of oncogenic pathway leading to growth arrest, it cannot be considered as an anticancer effect because cell quiescence is a strategy that enables cancer cells to escape from chemotherapeutic agents targeting rapidly dividing cells (Bartosh et al., 2016).

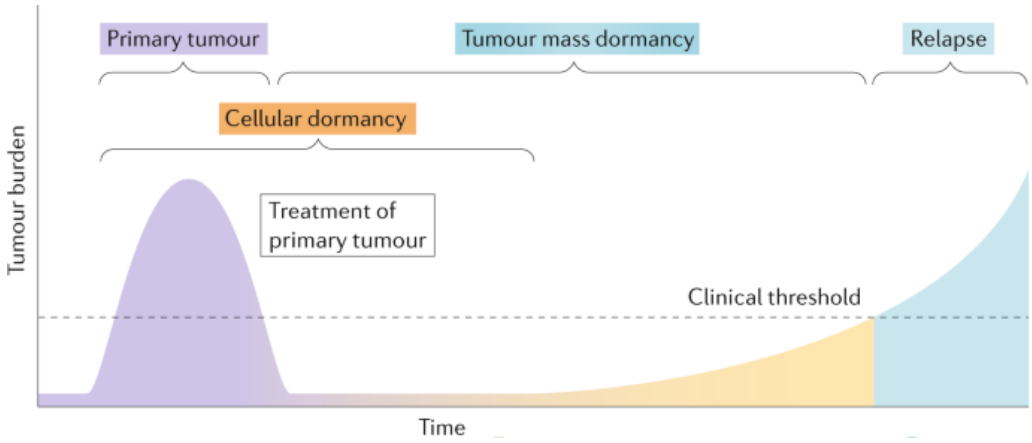

Figure 2.2. Mechanism of cancer cell dormancy. Cellular dormancy at distant sites occurs before treating the primary tumor, where disseminated cancer cells remain dormant for prolonged periods. Once the tumor microenvironment is favorable, dormant cells will enter growth state before becoming detectable as a late metastatic relapse. Adapted from (Phan and Croucher, 2020)

The reversal of EMT is a key driving force in dormant tumor cell proliferation and macrometastasis formation. In head and neck squamous cell carcinoma (HNSCC), paired-related homeobox transcription factor (PRRX1) has been found to be elevated and activate EMT program in maintaining the dormancy via Transforming growth factor-β1 (TGF-β1) signaling. PRRX1 downregulates the expression of miR-642-3p which is associated with tumorigenesis and cell growth (Neophytou et al., 2019).

Another EMT transcription factor, *SNAIL* has been found to impair cell-cycle progression by repressing the transcription of cell division gene *cyclin D2* and suppressing tumor cell proliferation (Vega et al., 2004). A good therapeutic strategy to treat metastatic cancer is by targeting the dormant stage by blocking either the mechanism that sustains metastatic dormancy or promotes escape from dormancy.

2.2.3.4 Regulation of Epithelial-Mesenchymal Transition by MicroRNAs

MicroRNAs (miRNAs) are small, non-coding, single-stranded RNAs that inhibit the expression of target genes by translational repression or mRNA degradation. They predominantly bind to target mRNAs and exert silencing effects on genes, thereby suppressing protein translation (Shi et al., 2017). MiRNAs regulate gene expression in a cell-type-specific manner and govern critical cellular functions such as cell growth, proliferation, migration, disease initiation and cell death (Hu et al., 2018).

Altered miRNA profiles have been correlated with the pathogenesis of many diseases condition and breast cancer. A group of nine circulating miRNAs was reported to be dysregulated in early-stage breast cancer and able to be used to differentiate between healthy controls (Kodahl et al., 2014). By comparing miRNAs profiles between cancer patients and healthy volunteers, researchers hypothesize that miRNAs are promising candidates for diagnostic markers.

Due to the recent advances in molecular profiling, the differential pattern of the molecular signature of miRNAs profiles that were initially detected in cancer cells and tissues is ultimately accessible from patient blood. The presence of dysregulated miRNAs in human circulation was first discovered in 2008 in the serum of lymphoma patients (Lawrie et al., 2008). Since then, miRNAs have emerged as important biomarkers in many diseases such as diabetes, Alzheimer, rheumatoid arthritis and cancer (Kumar et al., 2013; Duroux-Richard et al., 2014; Guay and Regazzi, 2013; Zhang et al., 2015a).

Growing evidence supports that miRNAs are correlated with EMT. MiRNAs involved in EMT regulation are known as EMT inducers or EMT suppressors (Hu et al., 2018). Studies have shown that miRNAs regulate EMT by specifically targeting EMT transcription factors family or by disrupting the integrity of the epithelial structure during EMT progression (Wang et al., 2010; Zaravinos, 2015). The induction of MET by miRNA regulatory networks mainly the miR-200 family, can negatively regulate *ZEB1/ZEB2* genes,

activating TGF-β/BMP signaling to promote MET, affecting breast cancer metastatic colonization and chemoresistance (Saydam et al., 2009; Fischer et al., 2015).

Other miRNAs such as miR-148a, miR-34, miR30a and miR-10b were found to negatively regulate EMT transcription factors *MET/SNAIL* and *TWIST* that prevent EMT and metastasis and increase recurrence in hepatoma, colon and breast cancer (Zhang et al., 2014a; Ding, 2014; Siemens et al., 2011) In addition, in a recently published study, overexpression of miR-509-5p and miR-1243 has been reported to increase *E-cadherin* expression by inhibiting EMT-related genes (Hiramoto et al., 2017). All these studies indicate that miRNAs control EMT transcription factors and are one of the promising tools for EMT regulation.

2.3 Exosomes

2.3.1 Biogenesis, Secretion and Molecular Composition

In cellular microenvironment, MSCs release secretome consists of biomolecules including extracellular vesicles (EVs), soluble factors (peptides, proteins, cytokines, chemokines and growth factors), signaling lipids, DNA, mRNAs and regulatory miRNAs. EVs are lipid bilayer membrane vesicles that consist of microvesicles, exosomes and apoptotic bodies that differ in size, biogenesis and molecular contents, as summarized in Table 2.3 (Zhang et al., 2015b).

Exosomes are small membrane-bound vesicles surrounded by a phospholipid bilayer with a diameter of 30–150 nm. They are in saucer-shaped vesicles and the membrane is commonly embedded with associated proteins such as HSPA8, CD9, GAPDH, ACTB, CD63, CD81, ANXA2, ENO1, HSP90AA1, EEF1A1, PKM2, YWHAE and SDCBP (Taylor et al., 2011; Lobb et al., 2015). Exosomes transfer molecules such as proteins, cytokines, signaling lipids, DNA, mRNAs, and regulatory miRNAs between cells to elicit responses in the target cell. They are formed at the endolysosomal pathway within multivesicular bodies (MVBs) and budding into TME after merging with the plasma membrane (Figure 2.3) (Wang et al., 2019).

Table 2.3. Extracellular vesicles and their characteristics

Vesicles	Biogenesis	Size	Markers	Molecular contents
Exosomes	Endosomal pathway, fusion with the parental cell plasma membrane	30-150 nm	Tetraspanins (CD63, CD81, CD9, TSG101, ALIX	mRNAs, miRNAs, lipids, non-coding proteins, mtDNAs, gDNA, cytoplasmic and membrane proteins
Micro-vesicles	Cell surface; budding of cell membrane	100-1000 nm	Integrins, Selectins (CD62), CD40, Annexin V	mRNAs, miRNAs, non-coding RNAs, lipids, cytoplasmic and membrane proteins,
Apoptotic bodies	Cell surface; outward blebbing of apoptotic cell membrane	1000-5000 nm	Phosphatidyl-serine, Annexin V, histones, DNA	Nuclear fractions, cell organelles

Adapted from **(Zhang et al., 2015b)**

The exosomal contents may vary according to physiological and pathological conditions of the cell origin. Exosomal content released by stromal cells is significantly different from tumor-secrected exosomes. Therefore, exosomes and their biologically active contents are an excellent diagnostic tool for various diseases, including cancer (Zhang et al., 2019).

Exosomes can deliver their cargo content to recipient cells through interactions between the exosomes and cell membrane followed by internalization by recipient cells (Milane et al., 2015). They can be distinguished from other extracellular vesicles by their specific physical and chemical properties and their unique biogenesis within the endosomal pathway (Kowal et al., 2014; He and Zeng, 2016).

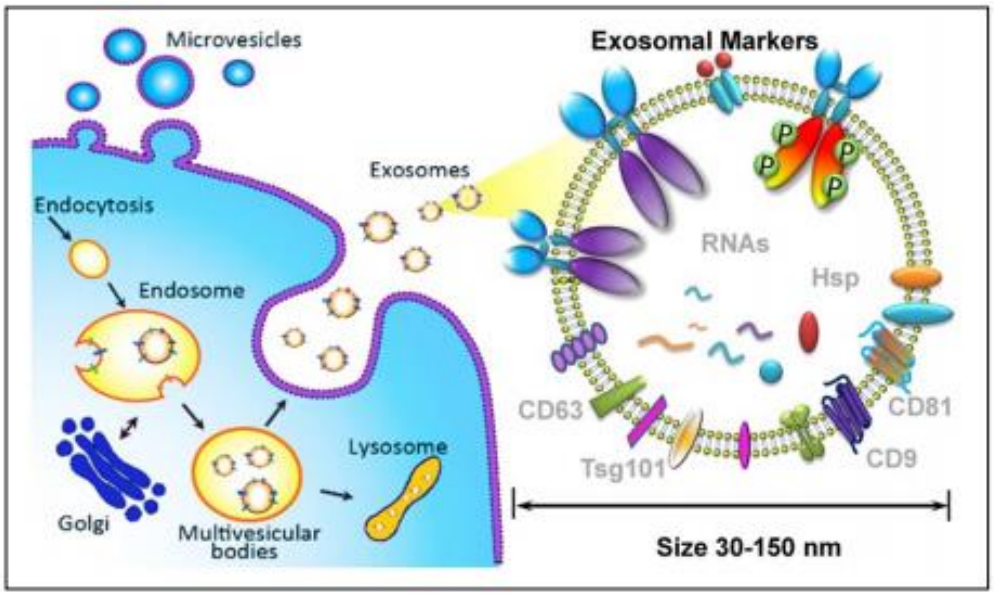

Figure 2.3. Exosome biogenesis, properties, and molecular composition. Adapted from (He and Zeng, 2016).

2.3.2 Exosomes Isolation Methods

For isolation, exosomes can be extracted using a combination of different techniques. Previously, the classical ‘gold standard’ to collect and isolate exosomes was differential centrifugation to remove the larger cells and debris. The method was followed by ultracentrifugation to concentrate the exosomes (Théry et al., 2006). Nevertheless, a recent discovery has demonstrated that ultrafiltration is a faster alternative to ultracentrifugation. Both methods are comparable in yield and quality, yet ultrafiltration is more time-saving (Lobb et al., 2015).

To further maximize the recovery, quality and reproducibility of exosomes, molecular diagnostic companies such as Qiagen (USA), ThermoFisher Scientific (USA), Invitrogen (USA), System Biosciences (USA) and few others have successfully commercialized exosomes isolation kit or isolation reagents. The isolation kits were develop based on different principles such as membrane affinity spin column, charge neutralization-based precipitation, gel-filtration and affinity purification using magnetic beads (Ding et al., 2018; Tang et al., 2017; Patel et al., 2019).

2.3.3 Exosomal MicroRNAs

MiRNAs that are part of exosome cargo are known as exosomal miRNAs or are widely described as circulating miRNAs. Other than using exosomes for transportation, miRNAs utilize the cargo for protection from degradation, thus, increase their stability and resistance against the action of ribonucleases (Sakha et al., 2016).

Localization and sorting of miRNAs into exosomes has been associated with a few modes consisting of ceramide pathways, also recognized as neutral sphingomyelinase 2 (nSMase2)-dependent pathways, sequence motifs present in the mature miRNAs permitting particular binding by sumoylated protein heterogeneous nuclear ribonucleoprotein A2B1 (hnRNPA2B1), EXOmotifs, 3'-end miRNA sequence-dependent pathway and miRNA-induced silencing complex (miRISC)-related pathway. These sorting mechanisms are important in determining the consensus of miRNAs taken up by neighboring or distant cells (Villarroya-Beltri et al., 2013).

2.3.4 Exosomes Mediate Intercellular Communication

Cell communication is the process by which cells interact with adjacent or distant cells via signaling processes. The presence of exosomes in normal biological fluids indicates that they are involved in numerous physiological processes and implicated in immunological and non-immunological processes. Likewise, exosomes are also traceable in the blood of cancer patients and are known to be associated with tumor metastasis, immune response suppression and relapse (He and Zeng, 2016). Even though exosome content released from healthy and cancer cells is very distinct, both can affect each other, creating a bidirectional exchange (Dioufa et al., 2017).

Exosomes have been reported to orchestrate the cellular communication between cancer cells and ADMSCs in the microenvironment. Meanwhile, their exosomal miRNAs are shown to act as signaling molecules that control entire gene networks and are commonly expressed in a cell-type-specific and cancer subtype-specific manner (Shi et al., 2017; Wang et al., 2019). Conventional cell-to-cell signaling pathways involving paracrine signaling by soluble proteins such as cytokines have been the focus of the interaction between ADMSCs and cancer cells. However, more recently, the attention has been shifted to exosomes.

2.3.5 Exosomes as Circulating Biomarkers of Cancer

Exosomes have attracted a lot of attention because of their main roles as mediators of intercellular communication and their potential clinical application as non-invasive biomarkers. As carriers of tumor-specific antigens, tumor-derived exosomes, which are readily available from body fluids, have received a lot of attention as a source of novel biomarkers. Exosomal miRNAs secreted by MSCs from various sources have been shown to act as tumor suppressors or oncogenes (Ono et al., 2014; Reza et al., 2016).

Dysregulation of oncogenes and tumor suppressor genes by miRNAs are well associated with tumor formation, growth and metastasis either as promoters or suppressors (Sakha et al., 2016). Exosomes also play a crucial role in resistance against cancer therapy by carrying miRNAs responsible for dormancy and protection against cancer drugs (Ono et al., 2014).

The non-invasive collection of body fluids such as blood serum, urine, saliva or milk has made exosomal miRNAs evolve as ideal biomarkers for cancer diagnosis (Zhang et al., 2019). Furthermore, detection of circulating miRNAs can aid in predicting the chances of tumor relapse, enable personalized, targeted therapies and monitor the outcome of the therapeutic regime.

2.4 Co-culture Interaction Model

Co-culture is a system employed for remodeling cellular microenvironment and interaction *in vitro* and to study the effects of co-culture on individual cell populations. There are two methods to study the cellular interaction *in vitro*, direct and indirect co-culture. A direct co-culture technique is used for mixing cell types together, whereby the cell types are in direct contact with each other. Although it is commonly employed, analysis of individual cells is complex in general, and at times, changes in protein expression and the like can only be examined at the cell population level. In addition, to monitor activity through direct contact, the indirect effects of humoral factors may also interfere. Thus, although it is an easy procedure to perform, interpreting the analytical methods and results is difficult.

Meanwhile, indirect co-cultures using a transwell system incorporates a physical separation between cell types, such as a semi-permeable membrane. This allows indirect interaction between distinct cell types through paracrine effects. Without cell-cell contact, communication occurs through the secretion and exchange of soluble molecules into the surrounding microenvironment.

Intercellular communication between distinct cell types can occur as one-way interaction. One cell type affects the biology and physiology of another cell type or bi-directional way when both cell types affect each other (Bogdanowicz and Lu, 2013). The maintenance, repair of biological tissues and cell development rely on the interaction of cells with different cell types within

their microenvironment. Thus, establishing a model of indirect co-culture system is an experimental platform for studying cancer progression *in vitro.* Besides, this platform is highly relevant for cancer studies because it reflects the disease progress. Also, the use of human or patient-specific cells to create cellular environments is more representative of human rather than animal-derived cells (Goers et al., 2014; Caddeo et al., 2017).

CHAPTER 3

MATERIALS AND METHODS

3.1 Overview of Methods

An indirect co-culture transwell system was conducted between two types of cells, ADMSCs and BCCs subtypes. MCF7 and MDA-MB-231 cells were used to mimic the microenvironment of cancer cells and investigate the effects of non-contact interaction on cancer progression and metastasis. To further investigate the factors responsible for the co-culture effects, exosomes and its content released by the cells into the microenvironment during the interaction were isolated and analyzed. The presence and intercellular transfer of exosomes were characterized by quantification of acetylcholine esterase enzyme (AChE), transmission electron microscopy (TEM) immunogold staining and membrane staining with Vybrant DiO fluorescence dyes. Meanwhile, the presence of miRNAs was identified based on RNAs integrity and SYTO64™ fluorescence dye staining prior to transcriptomic profiling. Small RNA composition was profiled and dysregulated miRNAs responsible for the biological effects were identified from specific signaling pathways. Finally, the particular roles of miR-941 on BCCs' proliferation and metastasis were evaluated by overexpression of mimic miR-941. The procedures are simplified in Figure 3.1.

Indirect co-culture of ADMSCs and BCCs (MCF7/MDA-MB-231)

⇩

PART 1: Effects of co-culture interaction of ADMSC on proliferation and metastasis of breast cancer cells

1. Cell cycle analysis
2. Cell proliferation
3. Migration
4. Invasion
5. Wound healing
6. Chemoresistant MTT assay
7. Analysis of multidrug-resistant (MDR), cancer stem cells (CSC) and DNA repair genes
8. Analysis of epithelial and mesenchymal genes expression level

⇩

PART 2: ADMSCs-derived exosomes suppressed breast cancer progression and metastatic ability via exosomal miRNAs transfer

1. **Isolation and characterization of exosomes and RNAs**
   - AChE enzyme analysis
   - TEM immunogold staining
   - Vybrant DiO and SYTO64™ fluorescence tracking dyes
2. **Transcriptomic profiling**
   - Library construction
   - Sequencing of small RNAs
   - Bioinformatics analysis
     - Identification of dysregulated miRNAs
     - Prediction of miRNAs-targeted genes
     - Analysis of GO and KEGG signaling pathways
   - Validation by qPCR
3. **Role of specific miRNAs via overexpression study**
   - Overexpression of miRNA mimic
   - Cell proliferation
   - Migration
   - Invasion
   - Wound healing
   - Analysis of epithelial and mesenchymal genes expression

Figure 3.1. Flow chart of research methodology of the study

3.2 Cells Culture

3.2.1 Breast Cancer Cells Lines

The human breast cancer cell lines, MCF7 (ATCC® HTB-22™) and MDA-MB-231 (ATCC® HTB-26™) were bought from American Type Culture Collection (ATCC, USA). Both epithelial cell lines were selected according to their metastatic characteristic with MCF7 (low metastatic) and MDA-MB-231 (highly metastatic). According to the documentation, MCF7 was derived from 69 years old Caucasian female mammary adenocarcinoma and molecularly classified as luminal A subtype with the presence of estrogen receptor (ER) and progesterone receptor (PR) but lack of HER2 (human epidermal growth factor receptor 2) expression. MCF7 represented the less aggressive and better prognosis breast cancer model. Meanwhile, the MDA-MB-231 cell was derived from 51 years old Caucasian female with metastatic mammary adenocarcinoma. This cell is widely known as triple-negative breast cancer (TNBC) due to the lack of all three receptors; ER, PR and HER2 expression. MDA-MB-231 represents the more aggressive form of breast cancer attributed to highly invasive and poorly differentiated (Xu et al., 2018).

3.2.2 Adipose-Derived Mesenchymal Stem Cells

Primary human ADMSCs were obtained from Cryo Cord Sdn Bhd. The cells were given at passage two and the source is from a young age donor. These ADMSCs were selected for this interaction model due to their feasibility to be expanded in culture. The research was approved by the UTAR Scientific and Ethical Review Committee (U/SERC/14/2012) in compliance with the guidelines regarding the use of primary stem cells for research.

3.2.3 Preparation of Culture Media

Basal media Dulbecco's Modified Eagle Medium (DMEM) with high glucose and Roswell Park Memorial Institute (RPMI) 1640 medium (Sigma, USA) were prepared following the manufacturer's instruction. DMEM high glucose powder was dissolved in 900 mL of deionized water supplemented with 3.7 g of sodium bicarbonate (NaHCO3) (Merck Millipore, USA). RPMI was dissolved in 900 mL of deionized water supplemented with 2 g of sodium bicarbonate. The pH of the medium was adjusted to 7.2 ± 2 before topping up with 1 L of deionized water.

The medium was filtered-sterilized through a 0.22 μm cellulose acetate filter unit (Sartorius) attached to a vacuum pump system (Gast, Michigan, USA). Complete culture medium for cancer cell lines was further supplemented with 10% (v/v) exosomes-depleted fetal bovine serum (FBS)

(System Biosciences, USA) and 1% of 100 U/mL Penicillin-Streptomycin (Gibco). Exosomes-depleted FBS was preferred instead of normal FBS to minimize the level of bovine exosomal miRNAs contamination in the supplemented media and subsequently to avoid misinterpretation of analyzed data.

3.2.4 Thawing of Cryopreserved Cells

Cryopreserved vials stored in a liquid nitrogen tank were thawed immediately in a 37°C water bath (Memmert, Germany). Vials were handled with an aseptic technique using 70% ethanol and continued with cell culture procedures in a Class II Biosafety cabinet (ESCO, Singapore). The thawed cells were transferred into sterile 15 mL centrifuge tubes (BD Biosciences) containing 9 mL of pre-warmed complete medium.

The cell suspensions were centrifuged at 2,000 rpm for 5 minutes using a benchtop centrifuge (Allegra® X-15R, Beckman Coulter). After centrifugation, the supernatants were discarded and the cell pellets were suspended in 1 mL of complete medium and transferred to T75 culture treated flasks in a ratio of 1:3. The cells were maintained at 37°C in a 5% CO_2 incubator (ESCO).

3.2.5 Cell Maintenance and Subculture

Breast cancer cell lines MCF7 and MDA-MB-231 were cultured as 2D monolayer and maintained in a complete medium of RPMI-1640 and DMEM high glucose, respectively, at 37°C with 5% of CO_2. Meanwhile, primary ADMSCs were maintained in MesenPRO RS medium (Thermo Fischer Sc., UK) supplemented with 2 mM GlutaMAX (Invitrogen) with 5% CO_2 at 37°C and the passage number was maintained under 12. MesenPRO medium contains a low serum concentration (2%) formulated to cater to the growth of human ADMSC. The mediums were changed twice weekly and subcultured upon 80% confluent.

Briefly, the medium was discarded and the cells were rinsed with 1x phosphate buffer saline (Amresco, USA) to remove traces of serum. Phosphate buffer was discarded and 1 mL of TrypLE solution (Thermo Fischer Sc) was added into the flask. The flasks were incubated at 37 °C to allow the cells to detach from the flask and dissociate into single cells. The flask was monitored under an inverted light microscope (Nikon, USA) to check for detachment. Next, a complete medium was added into the flask to inactivate the enzymatic activity. The cell suspension was spun at 2,000 rpm for 5 minutes. Unwanted culture supernatant was removed and the pellet was re-suspended in complete medium before 10% of the cells were re-seeded back into the new flask.

3.2.6 Mycoplasma Test

All cell lines were routinely mycoplasma tested using Myco-Alert™ Mycoplasma Detection Kit, Catalog #: LT07-118 (Lonza, USA). Briefly, cells culture supernatant was centrifuged at 200 x *g* for 5 minutes and 100 µL cleared supernatants were transferred to a 96-well plate loaded with 100 µL MycoAlert reagent.

After 5 minutes of incubation, the plates were read using luminescence Infinite® 200 PRO plate reader (Tecan, Switzerland) at an interval of 1s. Subsequently, 100 µL of MycoAlert substrate were added to the wells and the second reading was taken after 10 minutes. Viable mycoplasma present in cell supernatant will be lysed and the enzyme will react with reagent substrate to converts ADP to ATP which can be detected by luciferase enzyme. A ratio of less than 0.9 was considered mycoplasma-free after dividing the second reading with the first.

3.3 Transwell Co-culture Assay

ADMSCs were seeded in 6 well-transwell inserts (Corning, USA) containing polycarbonate membranes (1.0 μm pore size) at a density of 2 x 10^5 cells/mL with MCF7 or MDA-MB-231 cells pre-plated in the basolateral compartment at a density of 3 x 10^5 cells/mL (Figure 3.2). The cells were co-cultured for 48 hours in DMEM complemented with 10% exosome-depleted fetal bovine serum (System Biosciences, USA), 100 U/mL penicillin and 100 ug/mL streptomycin at 5% CO_2 at 37 ^{0}C. BCCs that were cultured alone were used as the negative control.

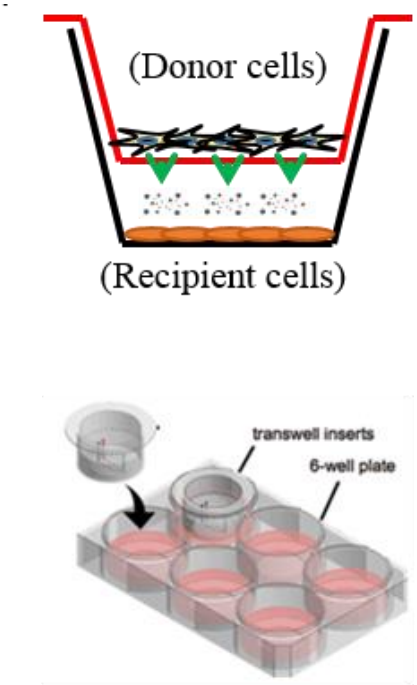

Figure 3.2. Schematic representation of transwell indirect co-culture between breast cancer cells and ADMSCs containing polycarbonate membranes 1.0 μm pore size.

3.4 Mesenchymal Stem Cells Characterization

3.4.1 Immunophenotyping

Human ADMSCs phenotypes were determined using flow cytometry by detecting the cell surface markers expression using fluorochrome-conjugated primary cocktails containing CD90+, CD44+ and CD105+ from FlowCellect™ human MSC characterization kit (Merck, USA). Cells were incubated with 18 μL of antibody working solution (Anti-human CD105-conjugated with FITC, anti-human CD90-conjugated with PE and anti-human CD44-conjugated with Alexa fluor 647) for 30 minutes in the dark at 4°C and analyzed using BD FACs Canto™ II Flow Cytometer (BD Biosciences, USA).

The antibody panel used was composed of antibodies against CD90 CD44 and CD105 as positive MSC markers present on the surface of ADMSCs. The purity of ADMSCs was determined as >85% positive for CD90, CD44 and CD105 surface antigen expression prior to co-culture. The list of antibodies used has been listed in Appendix A.

3.4.2 Multipotent Differentiation

The multipotency of ADMSCs was assessed for lipid droplets (adipocytes) and calcium deposition (osteoblasts). For *in vitro* differentiation into osteoblasts, cells were induced with osteogenic induction medium (OIM), composed of DMEM complemented with 10% FBS, 50 mg/mL ascorbate-2 phosphate, 10^8 M dexamethasone, and 10 mM β-glycerophosphate. For *in vitro* differentiation into adipocytes, cells were induced with adipogenic induction medium (AIM), composed of DMEM complemented with 10% FBS, 50 mg/mL ascorbate-2 phosphate, 10^7M dexamethasone, 50 mM indomethacin, 0.45 mM 3-isobutyl-1-methylxanthine (IBMX) and 10 mg/mL insulin. Change of medium was performed every three days until 21 days, when the matrix mineralization and lipid droplets were fully formed.

3.5 Analysis of Exosomes

3.5.1 Isolation of Exosomes

Prior to exosome collection, cells were seeded in exosome-depleted FBS (System Biosciences, USA) containing medium and further co-cultured for 48 hours until 80-90% confluency. The conditioned medium was harvested through serial centrifugation at 300 x *g* at 4℃ for 10 minutes and followed by 3000 x *g* at 4℃ for 15 minutes to precipitate cell debris.

The cell-free supernatant was pre-filtered using a 0.4 µm syringe filter before exosome isolation using ExoEasy Maxi kit (Qiagen, Germany). The kit uses membrane affinity spin columns and specialized buffers to efficiently isolate and purify exosomes from the pre-filtered cell culture supernatant.

Briefly, isolated supernatant was mixed with exosome isolation buffer XBP at (1:1) and the tube was gently inverted five times. Next, the mixture was aliquoted to the column and centrifuged for 1 min at 500 x *g* in a swinging bucket rotor. A 10 mL of buffer XWP was added to wash the column and centrifuged at 5,000 x *g* for 5 minutes and the flow-through was discarded. Exosome was eluted in 100 µL of phosphate-buffered saline (PBS) for further exosome characterization. The isolation process was summarized in Figure 3.3.

Figure 3.3. Schematic representation of exosome isolation process. Cells supernatant was pooled and collected into tubes, cells pellets and debris were removed by serial centrifugation, followed by ultrafiltration to further eliminate the larger vesicles. Finally, the supernatant were run through membrane affinity column ExoEasy Maxi kit to concentrate the exosomes.

3.5.2 Characterization of Exosomes

To further confirm the presence of exosomes extracted from culture supernatant, size distributions, morphology and protein surface markers of isolated exosomes were assessed.

3.5.2.1 Quantification of Acetyl Choline Esterase enzyme (AChE)

To measure AChE enzyme activity that is highly enriched within exosomes, AChE Colorimetric Assay Kit (Abcam, USA) was purchased. The protocol uses DTNB to measure the thiocholine byproduct from the breakdown of acetylthiocholine by AChE. The absorption concentration of 5,5'-dithio-bis-2-nitrobenzoic acid (DTNB) adduct at a wavelength of 410 nm that is comparative to the AChE activity was used to quantify the amount of thiocholine formed. Briefly, assay buffer, 20x DTNB, 50 units/mL Acetylthiocholine stock solution and 1000 mU/mL standard solution were prepared. A serial dilution of acetylcholinesterase standard was performed. A volume of 50 μL of acetylthiocholine reaction mixture was incubated with AChE standard and culture medium for 30 min before absorbance was taken at 415 nm using Infinite® 200 PRO plate reader (Tecan, Switzerland). The average absorbance was determined from standard and the dose-response curve was plotted. From the trendline equation of the AChE standard, the value of AChE activity of the culture medium was calculated to represent the number of exosome particles.

3.5.2.2 Transmission Electron Microscopy with Immunogold-Labeling

To further assess the size distributions, morphology and protein surface markers of nano-scale biological structures such as exosomes, it requires the use of very high-resolution microscope, such as a transmission electron microscope (TEM) for visualization. The short wavelength of electron beams is used to illuminate the sample and form images (Zhang et al., 2018a).

Before visualization, sample processing steps are necessary which primarily involve fixation, antibody staining and dehydration. Briefly, isolated exosomes were diluted in PBS and fixed in a solution containing 4% paraformaldehyde. For immunogold-staining, a fixed exosome was mounted onto formvar/carbon-coated copper 300 mesh grid for 5 minutes at room temperature. Grids were blocked with PBS-BSA for 5 minutes upon removal of the surplus samples using filter paper. Next, the grids were incubated with primary anti-mouse monoclonal CD63, CD81 and CD9 (15 µL; 1:5 dilution in PBS-BSA) for 1 hour at 37℃. After incubation, grids were rinsed thrice with PBS-BSA, followed by incubation with secondary antibody goat-anti mouse IgG conjugated to 10 nm gold particle (15 µL; 1:20 dilution in PBS-BSA) for another 1 hour at 37℃. After washing, the grids were fixed in uranyl acetate [1% (w/v)] for 5 minutes and air-dried before being viewed using TEM at 80-120k Volt (Hitachi HT7700, Japan). Negative staining was used as a control. The list of antibodies used has been listed in Appendix A.

3.6 Characterization of Co-culture Breast Cancer Cells

3.6.1 Internalization of Exosomes and RNAs

To track the transfer of exosomes containing RNAs from one cell to another, cells were fluorescently labeled with cell membrane labeling solution *Vybrant-DiO* and nucleic acid labeling solution SYTO64™ (Thermo Fischer Sc., UK). ADMSCs were pre-stained with 5 µM of Vybrant-DiO or 1 µM of SYTO64™ in a flask and incubated at 37℃ for 2 hours.

After removing fluorescence dyes, stained cells were harvested and co-cultured with breast cancer cells for 48 hours. The uptake of exosomes and RNA was observed using a fluorescence microscope (Carl Zeiss, Germany) with green (484-501 nm) and red wavelength (599-619 nm) filters. Next, an opposite staining method was performed on another group of breast cancer cells in order to confirm the direction of exosome and RNAs uptake. Cancer cells were pre-stained with Vybrant-DiO or SYTO64™, harvested and co-cultured with unstained ADMSCs (Santos et al., 2018).

3.6.2 Cell Proliferation Analysis

Cell proliferation was measured using Cell counting kit-8 (CCK-8) (Sigma-Aldrich, USA) by utilizing the water-soluble tetrazolium salt WST-8 (2-(2 methoxy-4-nitrophenyl)-3-(4-nitrophenyl)-5-(2,4-disulfophenyl)-2H-tetrazolium-monosodium salt). A volume of 100 µL of cells (1.0×10^4 cells/well) was seeded in 96-well plates and incubated in an incubator for 24 hours, 37℃ at 5% CO_2.

After 48 hours of co-culture treatment, 10 µL of CCK-8 reagent was mixed with cells and incubated for 4 hours. The reduced formazan crystal (orange color) was measured using Infinite® 200 PRO microplate reader (Tecan, Switzerland) at a wavelength of 450 nm. The amount of the formazan dye produced in cells by dehydrogenases is relative to the number of alive cells.

3.6.3 Cell Cycle Analysis

The cells were harvested and washed with 1x PBS following treatment using BD Cycletest™ Plus DNA Kit (BD Biosciences, USA). Briefly, cells were dissociated with 250 µL of solution A (trypsin) for 10 minutes at room temperature. Next, the cells were treated with 200 µL of solution B (trypsin inhibitor with RNase A) for 10 minutes and finally with 200 µL of solution C (propidium iodide) for 10 minutes in the dark and on ice. The cells were

analyzed using BD FACS Canto™ II Flow Cytometer (BD Biosciences, USA). A total of 10,000 events were recorded and the results were analyzed using BD CellQuest software (BD Biosciences). The experiment was performed in triplicates.

3.6.4 Chemoresistant MTT Assay

Control and co-culture breast cancer cell lines with a concentration of 5 x 10^3 cells in 100 µL per well were seeded into 96-well plates at 5% CO_2, 37℃ for 24 hours, at a cell density of 70% confluence. The cells were separately treated with doxorubicin, tamoxifen, cisplatin and 5-Hydroxy-[1,4] Naphtho-quinone (5HNQ) also known as juglone.

After 48 hours of incubation, 20 µL of 5 mg/mL tetrazolium salts (3-(4,5-Dimethylthiazol-2-yl)-2,5-diphenyl-tetrazolium bromide) MTT solution (Sigma-Aldrich) was added to each well and further incubated for 4 hours. The formed formazan precipitate was dissolved in 100 µL of dimethylsulfoxide before absorbance at 570 nm was taken with Infinite® 200 PRO microplate reader (Tecan, Männedorf, Switzerland). All experiments were carried out in triplicate. The viability of the cells was calculated as shown in the formula below. The dose-response graph of concentrations of the drug versus percentage of viability of the cells was constructed and IC_{50} values were determined using Microsoft Excel.

3.6.5 3D Spheres Formation Assay

To investigate the effects of cells interaction with ADMSCs on sphere forming ability of cancer cells, co-cultured cancer cells were enriched to form 3D tumorspheres. Approximately 5000/ mL single cells of control and co-cultured cancer cells were seeded in a non-adherent ultra-low attachment plate, serum-free medium of DMEM/F12 complemented with 20 ng/mL human recombinant epidermal growth factor and basic fibroblast growth factor (Invitrogen, USA), 1 x B27 (Thermo Scientific, USA), 10 µg/mL insulin, 0.5 µg/mL hydrocortisone, 100 U/mL penicillin and 100 µg/mL streptomycin and 0.4% bovine serum albumin (Sigma, UK).

Tumorspheres were maintained at 5% CO_2, 37℃. One mL of fresh stem cell media was added every 2-3 days. After 21 days, the spheres were counted and disaggregated into singles cells and re-seeded to generate a secondary spheroid. The number of spheres with diameter size larger than 50 µm was counted under an inverted microscope.

$$\text{Cell Viability} = \frac{\text{Absorbance of treated well}}{\text{Absorbance of control well}} \times 100\%$$

3.6.6 Expression of Multidrug Resistant (MDR), Cancer Stem Cells (CSC) and DNA Repair, Epithelial and Mesenchymal Genes

3.6.6.1 Total Ribonucleic Acids (RNAs) Extraction

RNAs extraction was performed using Qiagen RNeasy ® Mini Kit (Qiagen, Germany) according to the manufacturer's protocol. Approximately 3 x 10^6 cells were harvested via trypsinization and the resulted pellets were lyzed in 600 µl RLT Buffer. ß-mercaptoethanol was added to the RLT buffer prior to usage. Cells were disrupted and homogenized using QIAshredder (Qiagen, Germany) and centrifuged at maximum speed, at room temperature for 2 minutes. The flow-through was collected and transferred to the column, followed by centrifugation at 5,000 x *g* for 5 minutes. The flow-through was collected again and one part of 70% ethanol (~600 µl) was added to the flow-through and resuspended.

Then, the mixture was transferred to the RNeasy spin column in a 2 mL collection tube, spun for 8,000 x *g* for 15 seconds and the flow-through was discarded. Next, 700 µL of RW1 buffer was added to the column and centrifuged at 8,000 x *g* for 15 seconds. Flow-through was discarded after centrifugation followed by washing with 500 µL of RPE buffer. After centrifugation, flow-through was discarded and another 500 µL of RPE buffer was further added to the column. The column was centrifuged at 8,000 x *g* for 2 minutes and flow-through was discarded.

The column was then placed in a new microcentrifuge tube and 20 µL of RNase-free water was added to it. The column was incubated for 2 minutes at RT before centrifugation at 8,000 x *g* for 1 minute to elute the RNAs. The eluted RNAs were stored at -80℃ for future use.

3.6.6.2 Quantification of Total Ribonucleic Acids (RNAs)

The concentration of the extracted RNAs was quantified using Qubit 2.0 Fluorometer (Invitrogen, USA). Briefly, the extracted RNAs were diluted to 5 ng in 2 µL of nuclease-free water and mixed with 198 µL of Qubit working reagent. The low and high standard tubes were simultaneously prepared with 10 µL of standard reagent mixed with 190 µL of Qubit working reagent. The mixtures were vortexed and incubated at room temperature for 2 minutes before the measurement was taken using Qubit. The final concentration of samples was calculated by multiplying the value with the dilution factor performed earlier.

Next, the purity of the extracted RNAs was determined by measuring the reading ratio of absorbance 260 and 280 nm (A_{260}/A_{280}) using NanoPhotometer UV/Vis spectrophotometer (Implen, Germany). RNAs isolates with a ratio between 1.8 and 2.0 were used for the downstream gene expression study.

3.6.6.3 cDNA Conversion of Messenger RNAs

Reverse transcription was performed to convert extracted RNA into cDNA prior to PCR experiments. Total RNAs were first converted into cDNAs using iScript™ Reverse Transcription Supermix (BioRad, USA). Reverse transcription mixture was prepared as outlined in Table 3.1 and run on a PCR thermal cycler (Takara Bio, USA) at 25℃ for 5 minutes, followed by reverse transcription at 46℃ for 20 minutes and inactivation at 95℃ for 1 minute.

Table 3.1. Reverse Transcription Reaction Mixture

Component	Volume/Reaction
Total RNA	x μL (up to 1 μg)
5X iScript Reverse Transcription Supermix	4 μL
RNase-free water	Add to 20 μL
Total volume	20 μL

3.6.6.4 Quantitative Real-Time Polymerase Chain Reaction (qRT-PCR)

Cells were assessed for the expression levels of multidrug-resistant (MDR), cancer stem cells (CSC) and DNA repair genes via qPCR. Quantitative PCR (qPCR) enables determination of the relative concentration of the amplified DNA in the sample by utilizing: i) the fluorescent reporter dye (SYBR® Green) that binds to double-stranded DNA (dsDNA) or ii) fluorogenic single-stranded oligonucleotide probe that binds only the DNA sequence between the two PCR primers (TaqMan® probe).

Both quantification methods are reliable and commonly used in RT-PCR. In this study, both platforms were employed for qPCR. It was not intended to compare the efficiency or sensitivity between the two different methods but rather due to the availability of interest primers. Next, the fluorescent signals were plotted against the quantitation cycle (Cq), reflecting the copy number of the target. Briefly, the synthesized cDNAs were diluted to 200 ng and amplified using MDR, CSC and DNA repair primers (Appendix B, Integrated DNA Technologies, Singapore).

The mRNA expression level of MDR, CSC, epithelial and mesenchymal genes was quantified using SYBR-Green mix (PCR Biosystems, UK) according to the volumes in Table 3.2. No template control (NTC) was included in each assay by substituting the cDNA with RNase-free water. Amplification was run for in ABI thermal cycler (StepOne Plus, Thermo Fisher Scientific, USA) as outlined in Table 3.3.

Meanwhile, the DNA repair genes expression was evaluated via TaqMan™ Gene Expression Assays (Applied Biosystems, USA) containing a pair of PCR primers and a TaqMan probe with a FAM™ dye label on the 5' end and minor groove binder (MGB) and nonfluorescent quencher (NFQ) on the 3' end in a single tube. Briefly, Taqman® Gene Expression Assay (20x), cDNA samples and Taqman® Fast Advanced Master Mix (2x) were mixed together. An appropriate number of replicates and reactions were prepared according to the volumes in Table 3.4 and run in the thermal cycler (StepOne Plus, Thermo Fisher Scientific, USA) as outlined in Table 3.5.

The melt curve analysis was carried out for each assay in both qPCR platforms. Relative quantification was analyzed by geometric average Cq of the mRNAs normalized by the average of reference mRNAs (ACTB). The fold expression was calculated using the $2^{-\Delta\Delta Ct}$ method.

Table 3.2. SYBR Green PCR Biosystems reaction set-up (mRNA)

Components	Volume per reaction	Final concentration
2X SYBR Green PCR Mix (ROX-high)	5 µL	1x
Forward primer (10 µM)	0.4 µL	200 nM
Reverse primer (10 µM)	0.4 µL	200 nM
cDNA template (100 ng/µL)	2 µL	200 ng
RNase-free water	2.2 µL	-
Total volume	10 µL	

Table 3.3. Thermal Cycler protocol for SYBR Green PCR Biosystems qPCR

Step	Temperature	Duration	Cycle
DNA Polymerase Activation	95℃	2 min	1
Denaturation	95℃	5 sec	40
Annealing/Extension	62℃	25 sec	

Table 3.4. TaqMan® qRT-PCR reaction set-up

Component	Volume/ Reaction	Final Concentration
TaqMan® Fast Advanced Master Mix (2x)	10 µL	1x
TaqMan® Gene Expression Assay (20x)	1 µL	1x
cDNA template (10 ng/µL)	2 µL	20 - 50 ng
RNase-free water	7 µL	-
Total volume	20 µL	

Table 3.5. Thermal Cycler protocol for TaqMan® qPCR

Step	Temperature	Duration	Cycle
UNG incubation	50℃	2 min	Hold
DNA Polymerase Activation	95℃	20 sec	Hold
Denaturation	95℃	1 sec	40
Annealing/Extension	60℃	20 sec	

3.7 Cell Metastases

3.7.1 3T3 Condition Medium

To stimulate the invasion and migration of MCF7 cells, a chemoattractant of conditioned medium from NIH-3T3 fibroblasts was used in the transwell invasion and migration assays. Cells were maintained in HG-DMEM supplemented with 10% fetal bovine serum (Thermo Fischer Sc, USA), 100 U/mL penicillin and 100 µg/mL streptomycin at 5% CO_2 at 37℃. When cells are nearly confluent, conditioned medium was harvested, sterile-filtered and stored at 4℃.

3.7.2 Transwell Invasion and Migration Assays

Transwell invasion assay was carried out by coating 8.0 µm pore size polycarbonate membrane inserts of 24-well (Corning) with matrigel basement membrane matrix (BD Biosciences) at 37℃ for a minimum of 3 hours. Control or co-culture cells were suspended in 200 µL of serum-free medium and seeded at a density of 1.0×10^5 cells/well in the upper chamber.

Meanwhile, the lower chamber contained a growth medium with 10% FBS or NIH-3T3 condition medium. Cells were further incubated for 24 hours to allow them to invade the matrigel. After removing media from both the lower well and the transwell insert, the migrated cells were fixed with 4%

formaldehyde for 2 minutes, permeabilized with 100% methanol for 20 minutes and stained with diluted crystal violet 15 minutes in the dark. In between, the fixed cells were rinsed with PBS. Non-invaded cells at the surface of the membrane were scraped off using a cotton swab. Migration assay was performed similarly, without matrigel. Images of cells that migrated and invaded through the membrane were captured at wavelength 590 nm using an inverted microscope (Nikon, USA).

3.7.3 Wound Healing Assay (Scratch Assay)

To monitor cell migration with a third independent method, an *in vitro* wound-healing assay was performed. After 48 hours of cancer cells cultured with ADMSCs, the culture insert was detached, followed by the creation of wound/gap using a P1000 pipette tip by scratching the center of the well. The cells were rinsed with PBS to clear the detached cell and replenished with a new medium. Wound/gap was monitored at 24 hours interval (0 hours, 6 hours and 24 hours) using an inverted microscope at 10x magnification (Nikon, USA) and the percentage of migration was assessed by calculating the ratio of gap distance relative to the original wound area in at least five fields using Image J software (NIH).

3.7.4 Expression of Epithelial (CD24) and Mesenchymal (CD44) Surface Markers by Flow Cytometry Analysis

The epithelial (CD24) and mesenchymal (CD44) surface markers of cancer cells were analyzed using a flow cytometer. Control and co-cultured MCF7 and MDA-MB-231 cells were harvested and dissociated using tyrpLE to produce single-cell suspension as described in Section 3.2.5. Later, they were concentrated and resuspended in 100 μL of 0.5% BSA – PBS solution buffer at a concentration of 5 x 10^5 cells/mL per tube. Cell surface levels were determined with combinations of fluorochrome-conjugated monoclonal antibodies obtained from BD Biosciences (San Diego, USA) against human CD44, CD24 and their respective isotype controls.

A volume of 10 μL of CD44-conjugated FITC antibody and 10 μL CD24-conjugated PE were mixed with the cells and incubated at 4℃ in the dark for 30 minutes. Separate tubes were prepared to run individual surface markers. Afterward, cells were centrifuged and washed in the wash buffer and the pellets were suspended with 300 μL wash buffer prior to acquisition on a BD FACS Canto™ II Flow Cytometer (Becton Dickinson, USA). The list of antibodies used has been listed in Appendix A.

3.7.5 Expression of Epithelial and Mesenchymal mRNA Level

Total Ribonucleic Acids (RNAs) were extracted, quantified and converted to cDNA as previously described in Section 3.6.6. The epithelial and mesenchymal mRNAs expression level of control and co-cultured cells were screened using primers from Integrated DNA Technologies, Singapore as stated in Appendix C. The expression level was quantified using SYBR-Green mix (PCR Biosystems, UK). Relative quantification was analyzed by geometric average Cq of the mRNAs normalized by the average of reference mRNAs (ACTB). The differences in fold expression were calculated following the $2^{-\Delta\Delta Ct}$ method.

3.8 Exosomes Functionality Study

To further confirm the role of exosomes mediating crosstalk between ADMSCs and cancer cells in the co-culture microenvironment, isolated exosomes from the co-cultured medium were collected as described previously in Section 3.5.1. Next, breast cancer cells were pre-seeded in 6 well-plates at a density of 3×10^5 cells/mL, 24 hours prior to the addition of exosomes.

An aliquot of 100 µL of exosomes was added into the culture of breast cancer cells to allow exosome uptake by cancer cells. (Tang et al., 2018). After 48 hours of interaction, exosome functionality assay was conducted on recipient cancer cells focusing on similar biological activities; cell

proliferation, migration, invasion, wound healing properties as well as RNA expression of epithelial and mesenchymal genes as described in Section 3.6.2, 3.7.2, 3.7.3, and 3.7.5.

3.9 MicroRNAs Expression Study

3.9.1 Isolation of Cellular and Exosomal miRNAs

MicroRNAs populations from cells and exosomes were extracted using miRNeasy ® Mini Kit (Qiagen, Germany), allowing purification of miRNA with total RNA for qRT-PCR and sequencing applications. Pellets of cells were lysed with QIAzol reagent and homogenized using QIAshredder (Qiagen, Germany) centrifuged at maximum speed, at room temperature for 2 minutes. The flow-through was collected and transferred to the column, followed by centrifugation at 5,000 x *g* for 5 minutes at room temperature.

Meanwhile, exosome aliquots were transferred to the column, followed by centrifugation at 5,000 x *g* for 5 minutes without going through QIAzol lysation. A total of 90 µL of chloroform was added to the lysates and shaken vigorously for 15 seconds to form three layers of phase separation. Lysates were centrifuged at 12,000 x *g* for 15 minutes at 4℃. Subsequently, the colorless top layer of lysates was carefully transferred into a new microcentrifuge tube and mixed with 1.5 x volumes of 100% ethanol to form precipitates.

The mixtures, including precipitates, were transferred to elution column and were washed with 700 μL of RWT buffer and centrifuged at 8,000 x *g* for 15 seconds. Flow-through was discarded after centrifugation. Next, 500 μL of RPE buffer was added to wash the column and centrifuged at 8,000 x g for 15 seconds. After the centrifugation, flow-through was discarded and another 500 μL of RPE buffer was added to the column.

The column was centrifuged at 8,000 x *g* for 2 minutes and flow-through was discarded. The miRNeasy spin column was transferred to a new collection tube and centrifuged at full speed, at room temperature for 1 minute to remove any possible carryover. The column was then placed in a new microcentrifuge tube and 20 μL of RNase-free water was added to the column. The column was incubated for 2 minutes at room temperature before centrifugation at 8,000 x *g* for 1 minute to elute the miRNA. The eluted miRNA was stored at -80℃ for future use.

3.9.2 Quantification of Small RNAs and Their Integrity

The concentration and purity of the extracted total RNAs were measured using Qubit 2.0 Fluorometer (Invitrogen, USA) as described earlier in Section 3.6.6.2. Prior to sequencing, RNAs integrity was examined using Total RNA 6000 Pico assay together with Agilent 2100 bioanalyzer (Agilent Tech, Germany). This crucial step ensures the integrity and the concentration of small RNA meet the minimal requirement for sequencing.

For cellular RNAs, a minimum ratio of 18S to 28S ribosomal subunits RNAs integrity number (RIN) must be above 7 to be classified as intact RNAs and any value lower than that was considered degraded RNAs. As for exosomal RNAs, the RIN of all samples was below 7, primarily due to the deficiency of ribosomal RNAs in the exosome itself. The small RNAs fraction (<200 bp) contains miRNAs in their primitive (pri-miRNA), precursor (premiRNA) and mature (miRNA) forms.

3.9.3 MicroRNAs Profiling via Next-Generation Sequencing (NGS)

3.9.3.1 Library Construction and Sequencing of Small RNAs

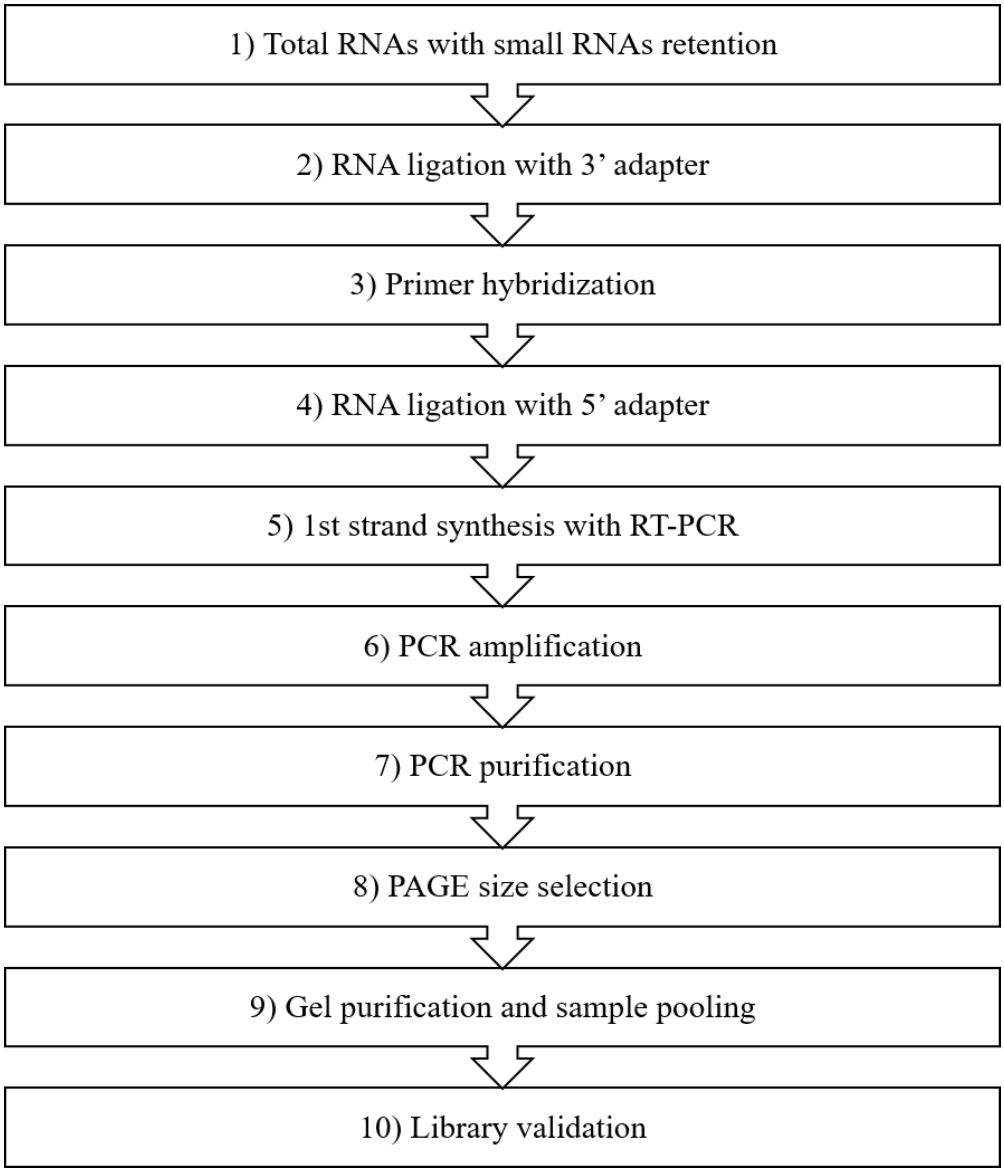

Figure 3.4. Small RNAs library preparation for sequencing. RNA samples were constructed into a library using NEBNext® Multiplex small RNA.

To evaluate the differences in the miRNA profile among cells and their respective exosomes of the co-culture conditions, small RNA sequencing technology was employed using miSeq (Illumina, USA). A total of 100 ng of cellular and exosomal RNAs were prepared for small RNA sequencing library following manufacturer's protocol, NEBNext® Multiplex small RNA library prep set for Illumina (New England Biolabs, USA).

As outlined in Figure 3.4, starting with 3′ adapter ligation, 1 μL of 3′-SR adapter was combined with 100 ng total RNA in a 6 μL volume, heated to 70℃ for 2 minutes and directly placed on ice. In a separate microcentifruge tube, 10 μL of 3'-ligation reaction buffer were mixed with 3 μL of 3'-ligation enzyme and added to the RNA/3′adapter mix and incubated at 25℃ for 1 hour. Then, 4.5 μL of nuclease-free H_2O and 1 μL SR RT primer was added and further heated for 5 minutes at 75℃, 15 minutes at 37℃ followed by 15 minutes at 25℃.

Next, 5' adapter ligation was carried out. After denaturation of 5'-SR adapter at 70 °C for 2 minutes and directly placed on ice, 1 μL of 5'-ligation reaction buffer and 2.5 μL of 5'-ligation enzyme mix were combined with 3'-ligated sample and incubated for 1 hour at 25℃. Reverse transcription of the sample was carried out to synthesize first-strand cDNA by mixing with 8 μL of first-strand synthesis buffer, 1 μL of murine RNase inhibitor and 1 μL of ProtoScript II reverse transcriptase and incubated for 1 hour at 50℃.

The cDNA was further amplified by mixing with 50 µL of Long Amp Taq master mix, 2.5 µL of SR primer, 2.5 µL of designated Index primer (1-12) and 5 µL of nuclease-free H_2O to make a total volume of 100 µL. The PCR amplification was run on a thermal cycler (Takara Bio, USA) as outlined in Table 3.6.

Table 3.6. Thermal Cycler protocol for NGS library construction-PCR amplification

Step	Temperature	Duration	Cycle
Initial denaturation	94℃	30 sec	1
Denaturation	94℃	15 sec	15
Annealing	62℃	30 sec	
Extension	72℃	15 sec	
Final extension	70℃	5 min	1

The resulting PCR products were purified using a QIAQuick PCR purification kit (Qiagen, Germany) and the concentration was subsequently checked using High Sensitivity DNA chips (Agilent, Germany) and a bioanalyzer. Purified PCR samples (25 μL) with a similar range of concentrations were grouped together, mixed with 5 μL of gel loading dye and run on a 6% Polyacrylamide gel. The gel was run for 1 hour at 120 V with DNA-Mspl Digest as molecular weight standards for gel electrophoresis.

Isolation of miRNAs was performed via size selection by staining the gel with SYBR gold nucleic acid gel stain for 15 minutes and cutting the gel in between 140–150 nucleotides bands. The library was extracted from the gel using 250 μL DNA gel elution buffer. The eluted miRNAs were washed in ethanol and air-dried to yield the pellet before re-suspended in Tris-HCl buffer.

A final quality check of the purified library was performed on a bioanalyzer using High Sensitivity DNA chips. A total pool of 4 nM of different libraries with equimolar ratios was combined into a single multiplexed library and sequenced using a MiSeq Reagent Kit v3 150 cycle and run using Miseq System (Illumina, USA).

3.9.3.2 Bioinformatics Analysis of miRNAs Sequencing Data

The analysis pipeline presented here aims to measure miRNAs expression profiles and assess differential expression between samples as simplified in Figure 3.5. Raw reads were preprocessed by removing a 3' adapter using *Cutadapt* version 1.16 (Martin, 2011) and filtered using *Fastx* toolkit version 0.0.14 (Gordon and Hannon, 2010).

The remaining reads were inspected for quality control using *Fast QC* software *(http://www.bioinformatics.babraham.ac.uk/projects/fastqc/)*, a quality control tool for analyzing high-throughput sequence data and then the reads were assigned to separate output files based on different barcodes used. The clean data were obtained by filtering out low-quality reads and bases with less than 16 and more than 26 nucleotides prior to mapping miRNA read sequences to the human genome.

Reads were aligned to the human reference genome (*UCSC 38*) using *Mapper* and precursor mature miRNA reference (*miRBase 21*) using *miRDeep2* version 2.0.0.8. (Friedländer et al., 2011). After data processing, expression statistical significance (*p-value*) for the normalized reads was calculated to generate differential expression profiles. Differentially expressed genes were selected if the fold changes (FC) in expression was > 2 with a p value < 0.05. The sequencing data are available in the NCBI *Gene Expression Omnibus* (GEO) database under the series accession identifier GSE156380.

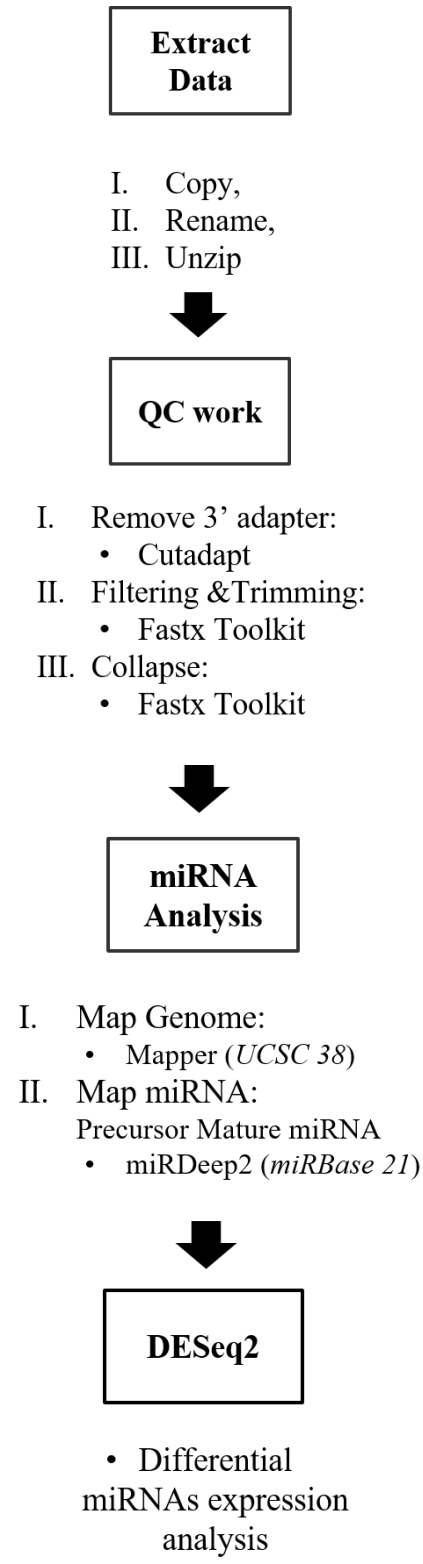

Figure 3.5. Flow chart of miRNAs sequencing analysis pipeline

3.9.3.3 Prediction of Highly Dysregulated miRNAs Target Genes

A target gene prediction platform, *miRSystem* was used to predict the potential regulation of mRNAs by dysregulated miRNAs available freely at http://mirsystem.cgm.ntu.edu.tw/. The program integrates seven prediction platforms: DIANA, miRanda, miRBridge, PicTar, PITA, rna22, and TargetScan allowing query of multiple miRNAs for the associations between them and their target genes (Lu et al., 2012). Hierarchical cluster analysis (HCA) is an algorithmic approach to identify groups with varying degrees of (dis)similarity in a data set represented by the color matrix (heat map) and diagram that shows the hierarchical relationship (dendrograms). Both heat maps and dendrograms generated by hierarchical clustering were carried out using *Heatmapper* (Babicki et al., 2016).

3.9.3.4 Gene Ontology and KEGG-Pathway Enrichment Analysis

To gain a better understanding of the potential role of exosomal miRNAs in co-culture interaction, *Panther DNA* database *(http://pantherdb.org)* was used to carry out functional annotation and enrichment analysis of their target genes identified in the GO enrichment analysis. Functional annotation was categorized by biological process and molecular function. The selection focused on the top 10 GO terms with the smallest *p-value*. The selected GO terms signify the annotation of the functional enrichment of targeted genes,

while a lower *p-value* indicates a superior functional enrichment of a relative term (Mi et al., 2013).

Meanwhile, the biological pathways enrichment, *Kyoto Encyclopedia of Genes and Genomes (KEGG)* were performed using the *miRSystem* RNA database among the genes targeting by queried miRNAs that integrate information from pathway prediction program KEGG (http://www.kegg.jp) (Lu et al., 2012). The workflow is summarized in Figure 3.6.

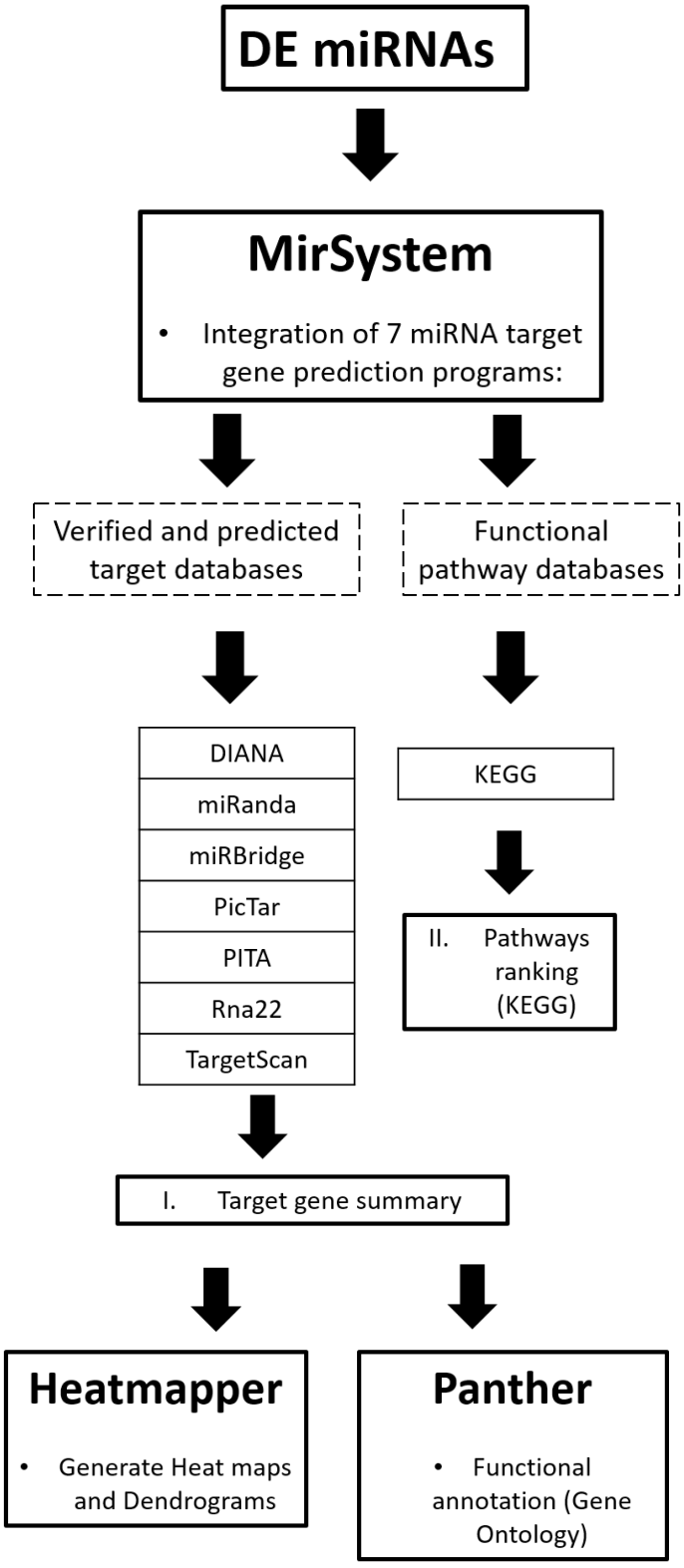

Figure 3.6. Overview of target genes prediction and enrichment analysis. Target genes, functional annotation (KEGG and GO) and heat map were generated using *miRSystem*, *Panther* and *Heatmapper* platforms.

3.9.3.5 Validation of miRNAs Sequencing by qRT-PCR

Five differentially expressed miRNAs from NGS results were selected for further verification by qRT-PCR (Appendix D) using samples from cells and exosomes from both MDA-MB-231 and MCF7 cell lines. The miRNAs were selected for validation based on statistical significance ($P < 0.05$) and their crucial role in biological or signaling pathways altered in co-cultured treatment with respect to control condition. Isolated miRNAs as described in Section 3.9.1 were first converted into cDNA using All-in-One™ miRNA First-Strand cDNA Synthesis Kit (GeneCopoeia, USA).

Briefly, a solution with 2 μg of total RNA, 1 μL of 2.5 U/μL Poly A Polymerase, 1 μL of RTase Mix and 5 μL of 5×PAP/RT Buffer and RNAse-free water to a final volume of 25 μL was prepared. The reaction was incubated for 60 minutes at 37℃ and at 85℃ for 5 minutes in a thermal cycler.

Subsequently, the synthesized cDNAs were further diluted (100ng) and amplified using the specific primers from GeneCopoeia, USA (Table 3.10). The miRNA expression level was quantified using SYBR-Green mix (PCR Biosystems, UK) as described earlier in Section 3.6.6.4 with qRT-PCR reaction set-up (Table 3.7) and similar thermal cycler protocol (Table 3.3). Relative quantification was analyzed by geometric average Cq of the miRNAs normalized by the average of reference miRNAs (RNU6b) and fold expression was calculated using the $2^{-\Delta\Delta Ct}$ method.

Table 3.7. SYBR Green PCR Biosystems qRT-PCR reaction set-up (miRNAs)

Components	Volume per reaction	Final concentration
2X SYBR Green PCR Mix (ROX-high)	5 μL	1x
All-in-One^{TM} miRNA qPCR primer	1 μL	200 nM
Universal Adapter (2 μM)	1 μL	200 nM
cDNA template (100 ng/μL)	2 μL	200 ng
RNase-free water	1 μL	-
Total volume	10 μL	

3.10 Transfection of MicroRNAs

Upon bioinformatics and miRNAs verification, miR-941 was selected for transfection study on the basis that it was previously reported to contribute to the suppression of cell proliferation, migration and invasion of hepatoma and gastric cancer cells (Zhang et al., 2014b; Kim et al., 2014). For the transient gain of function experiments, with the aim to ectopically overexpress the miR-941, breast cancer cells were transiently transfected using the reverse transfection protocol as recommended following HiPerFect Transfection Reagent (Qiagen) instructions.

A specific miR-941 mimic (10 nM, Syn-Hsa-mir941, Qiagen) was used for transfection with the following sequence: MIMAT0004984: 5'CACCCGGCUGUGUGC-ACAUGUGC-3'.A 25 nM of AllStars Cell Death siRNA (Cat.no: 1027298) or AllStars Negative Control siRNA (Cat.no: 1027280) (Qiagen, USA) or miR-941 mimic was mixed with 3 μL of HiPerFect (Qiagen, USA) transfection reagent and vortexed. The complexes were incubated at room temperature for 10 minutes before introduced into the cells. Transfected cells were incubated under normal conditions (37℃, 5% CO_2) for 48 hours.

After successful transfection, downstream assays consist of proliferation, migration, invasion, wound healing properties as well as mRNAs expression of epithelial and mesenchymal genes were performed as described previously in

Section 3.6.2, 3.7.2, 3.7.3, and 3.7.5. Transfection efficiency was measured by observation of the level of cell death at the transfection endpoint.

3.11 Statistical analysis

All experiments were repeated a minimum of three times and data were presented as mean ± standard deviation. For the comparisons between two groups, a Student's t-test approach was used. Comparisons between more than three groups were statistically calculated using one-way ANOVA followed by Bonferroni's post hoc testing. All data were analyzed for significance using GraphPad Prism version 8.0.1 with $p\text{-}value < 0.05$ was considered significant.

CHAPTER 4

RESULTS

PART 1: Effects of Co-culture Interaction of ADMSCs On Proliferation, Metastasis and Dormancy of Breast Cancer Cells

4.1 Indirect Co-culture Allow Interaction Between ADMSCs and Breast Cancer Cells In The Microenvironment

Non-contact co-culture model using the transwell system was set up to recapitulate the interaction between stromal ADMSCs and breast cancer in the microenvironment (Figure 3.2). Transwell inserts made of 1.0 μm porous polycarbonate membranes were used to isolate the two distinct cells and allow them to communicate through secreted signaling molecules in an immediate environment. Prior to co-culture, ADMSCs characterization was performed. ADMSCs displayed fibroblast-like morphology with a long-spindle shape at passage 5 (Figure 4.1 A).

Positive staining of Alizarin Red and Oil Red O shows that the cells were able to convert to calcium deposition osteocytes and lipid vacuoles adipocytes in a week after differentiation, respectively (Figure 4.1 B, C). Immunophenotyping analysis shows that most cells are positive for CD90, CD44 and CD105 surface antigen expression with >85% before co-culture (Figure 4.1 D, E). These results confirmed the properties of ADMSCs.

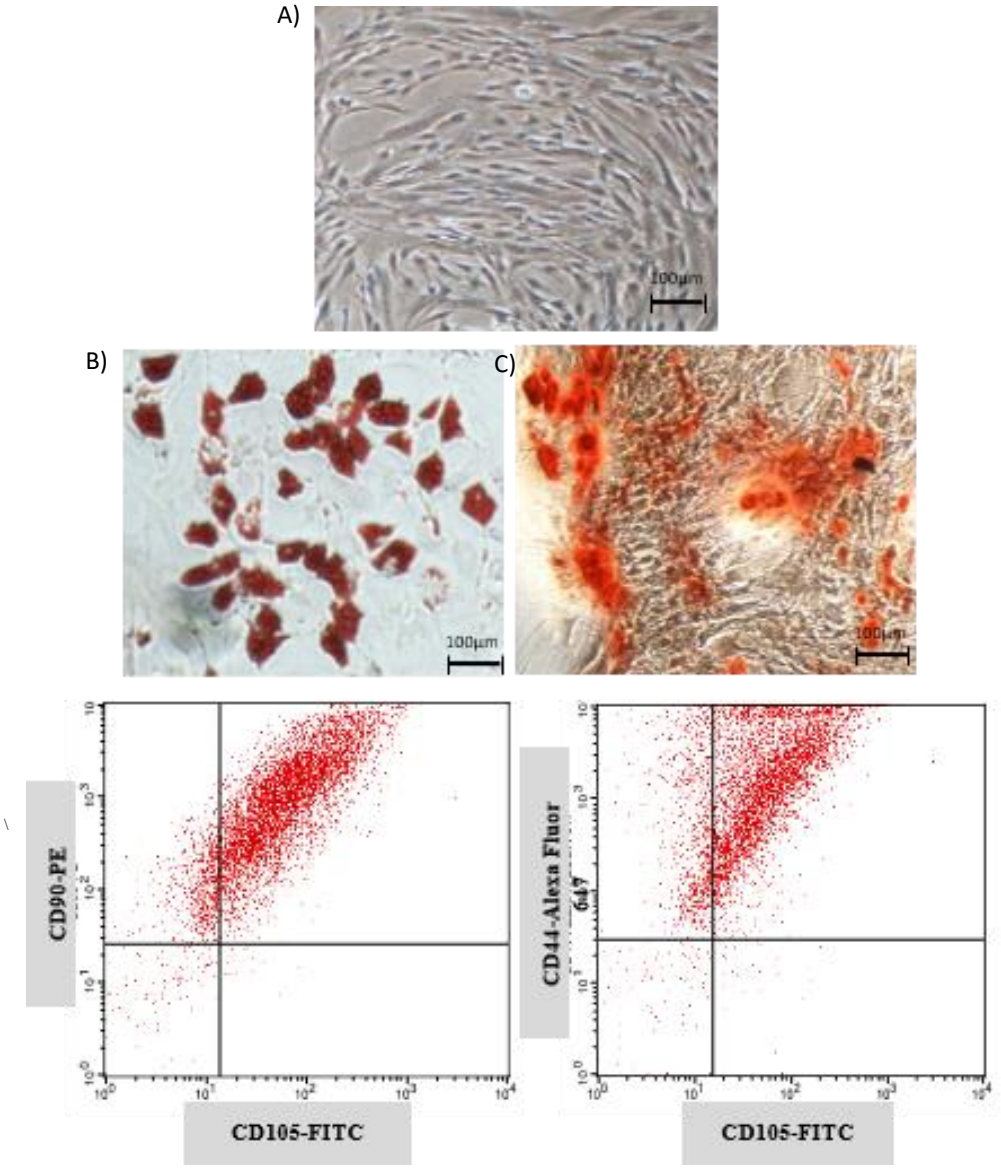

Figure 4.1. Characterization of ADMSCs. A) Primary ADMSCs after reaching confluence at passage 5. B) Osteogenic differentiation marked with Alizarin Red dye following calcium deposition. C) Adipogenic differentiation marked with Oil Red O dye to visualize the lipid droplets following differentiation. Scale bar= 100 µm. D, E) Representative images of ADMSCs analyzed for CD105, CD90 and CD44 expression level using flow cytometer.

4.2 Co-culture Promotes Cancer Dormancy and Chemoresistance

4.2.1 Co-culture Inhibits The Proliferation of Cancer Cells Leading to Dormancy

The effects of co-culture interaction on cancer proliferation were assessed using a CCK-8 colorimetric assay. We speculated that the proliferation effect on cancer growth might be correlated with the distribution of the cell cycle. After 48 hours of co-culture, significant inhibition of MDA-MB-231 and MCF7 cell proliferation was found in ADMSCs' presence compared to when being cultured alone (Figure 4.2). Furthermore, the MDA-MB-231 cells' morphology shifted from spindle-shaped fibroblast to cobblestone epithelial-shape with scattered colonies and lesser adherence. In MCF7, the shape mostly remains the same, but there is an increase in the appearance of apoptotic and detached cells. In addition to that, the analysis of the cell cycle showed significant (p<0.05) G0/G1 phase arrest in both cancer cells (Figure 4.3) and was accompanied by a decline in cell growth (S phase).

To demonstrate the concept of reversible dormancy, post-co-cultured BCCs were re-cultured in 96-well plates without the presence of ADMSCs. Results show that both cells display higher proliferation activity when re-cultured alone (Appendix E). This illustrates that ADMSCs may serve as an inhibitory niche that inhibits cell growth of BCCs.

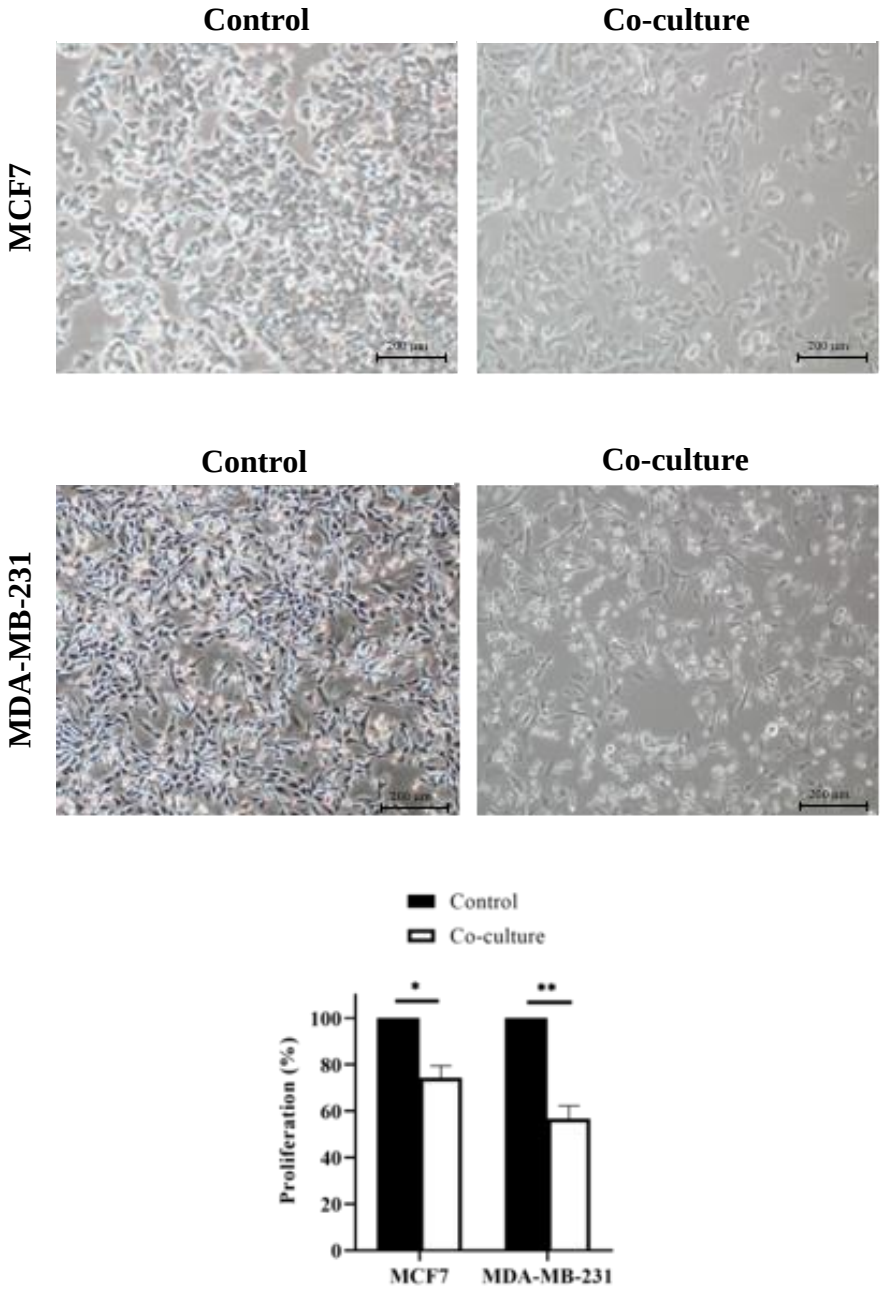

Figure 4.2. Inhibition of breast cancer cells' proliferation. A) Cell proliferation of MCF7 at 48 hours before and after co-culture. B) Cell proliferation of MDA-MB-231 at 48 hours before and after co-culture (10 x magnification). C) Percentage of cell proliferation. The results were analyzed using a t-test with mean values ± SD. *p<0.05 and **p<0.01 compared with the non-co-culture group.

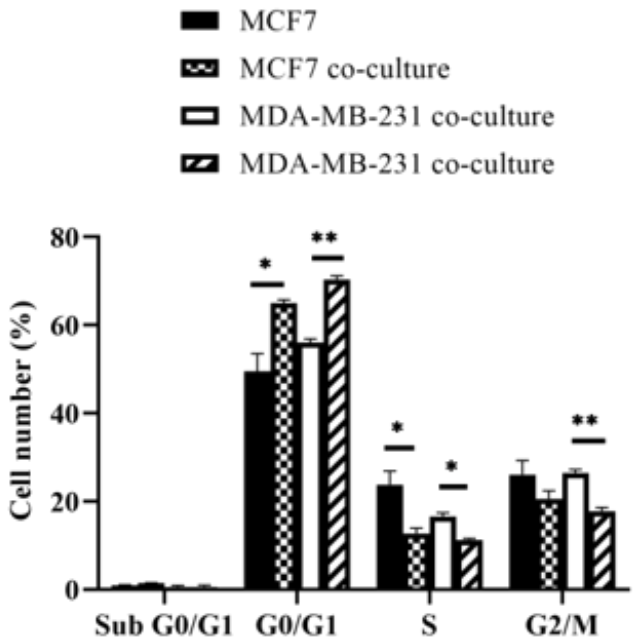

Figure 4.3. Distribution of cell cycle. Cell proliferation of both cancer cells was arrested at G_0/G_1 phase after 48 h of co-culture. The results were analyzed using a t-test with mean values ± SD. *$p<0.05$ and **$p<0.01$ compared with the non-co-culture group.

4.2.2 Co-culture Promotes Breast Cancer Chemoresistance

Meanwhile, after co-culture, both cells demonstrated higher IC_{50} values of doxorubicin (DOXO), tamoxifen, cisplatin and 5HNQ compared to non-co-culture cells after 48 hours of incubation (Table 4.1). After cells expansion in spheres-enriched condition medium, co-cultured MCF7 cells formed small (~50 µm in length), densely packed spheres and extremely low in number compared to co-cultured MDA-MB-231 where they formed large (70-170 µm in length), loose clusters of cells and significantly higher spheres forming ability (Figure 4.4 and Appendix F).

Gene expression of multiple drug resistance (MDR)-ABC transporter genes, CSC genes and DNA repair genes were screened after co-culture treatment. Two of three MDR genes, *ABCC2* and *ABCG2* were consistently up-regulated in both cells. The expression levels of CSC-associated surface markers, *CD44* and *ALDH1* were significantly down-regulated in MDA-MB-231 cells. Meanwhile, two of four genes involved in DNA repair and cell cycle, *PARP1* and *CCND2*, were significantly dysregulated in both cells (Figure 4.5). Overall, all genes involved in the development of chemoresistance and the regulation of cell survival were significantly dysregulated.

Table 4.1. Chemotherapy resistance in breast cancer cells before and after co-culture interaction with ADMSCs. Inhibition concentration at 50% (IC_{50}) values of drugs in co-culture-treated cells increased after 48 hours of incubation. The results were analyzed using a t-test with mean values ± SD. $^{**}p<0.01$ and $^{***}p<0.001$ compared with the non-co-culture group.

	DOXO (µM)	Tamoxifen (µM)	Cisplatin (µM)	5HNQ (µM)
MCF7	1.6 ± 0.3	9.5 ± 1.2	31.5 ± 4.3	8.5 ± 1.4
MCF7 co-culture	12.4 ± 2.7***	18.8 ± 1.0**	42.0 ± 4.3***	14.1 ± 1.7
MDA-MB-231	0.5 ± 0.2	10.6 ± 0.4	47.5 ± 2.5	6.0 ± 0.8
MDA-MB-231 co-culture	1.5 ± 0.2	21.3 ± 2.0***	63.0 ± 3.0***	21.1 ± 1.8***

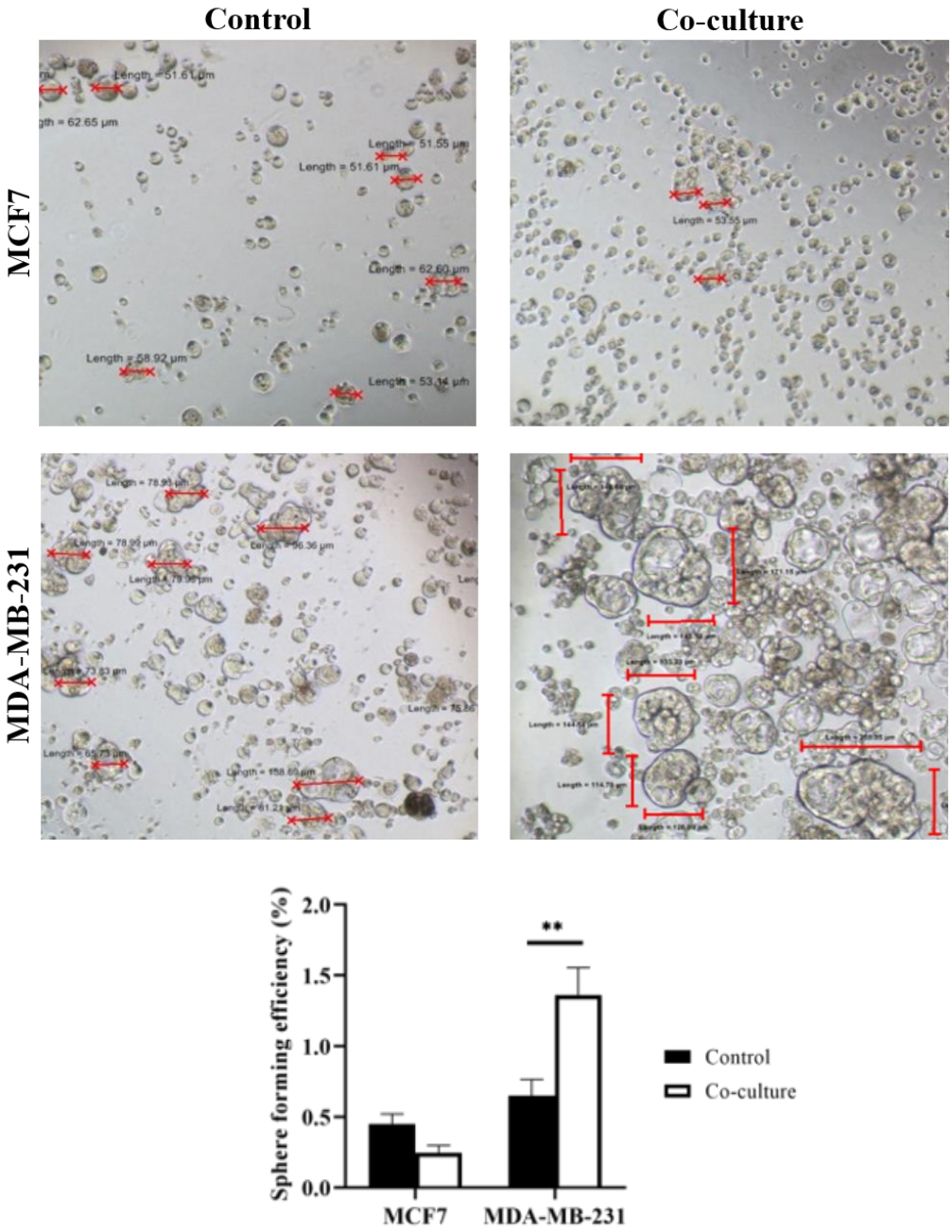

Figure 4.4. Representative images of spheroids formed in 3D culture. Bright-field microscopy images of spheroids formed on day 14 in a spheroidal culture of BCC lines MCF7 and MDA-MB-231 before and after co-culture, with 10X magnification. (Bars=length in µm). Percentage of spheres forming efficiency in a bar chart. The results were analyzed using a t-test with mean values ± SD. ***p*<0.01 compared with the non-co-culture group.

MCF7

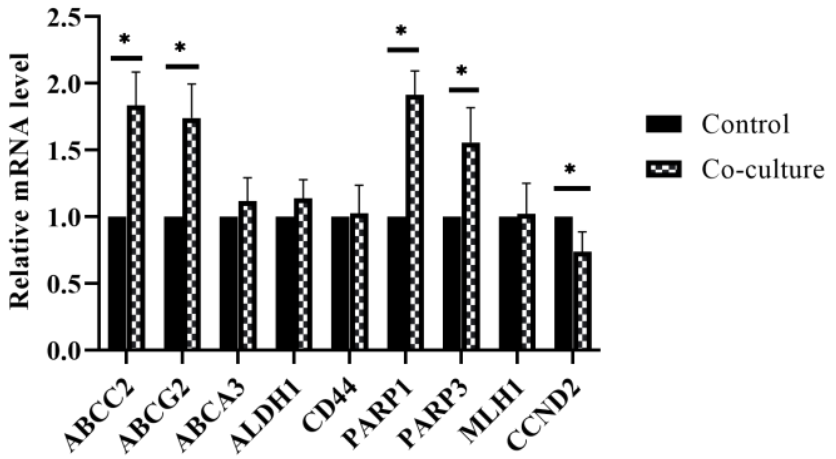

MDA-MB-231

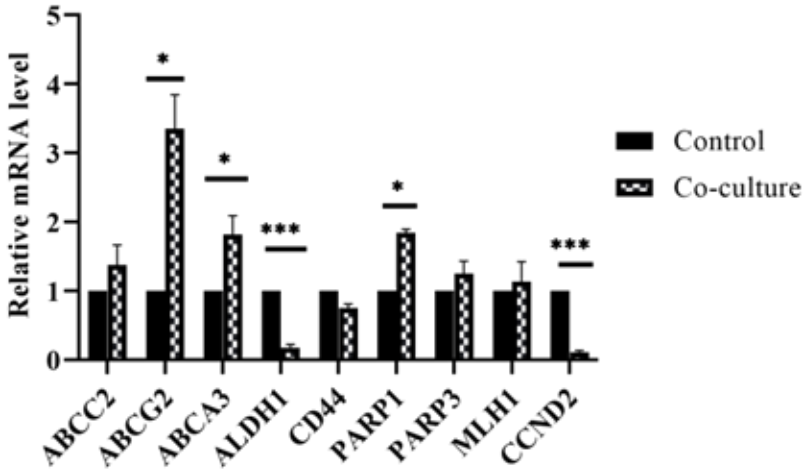

Figure 4.5. Dysregulation of MDR, CSC and DNA repair gene expression in co-cultured Breast Cancer Cells; A) MCF7 and B) MDA-MB-231 cells. The results were analyzed using a t-test with mean values ± SD. *p<0.05 and ***p<0.001 compared with the non-co-culture group.

4.3 Co-culture Suppresses Breast Cancer Metastasis Through Mesenchymal-Epithelial Transformation

Transwell assay demonstrated that co-culture with ADMSCs decreased the migratory and invasiveness of breast cancer cells (Figure 4.6 A, B). The mouse origin medium was used as the chemo-attractant and inducer in invasion and migration assays as both of cells have low invasion and migration abilities. It has been reported previously that the use of NIH-3T3 medium as chemo-attractant displayed enhanced migration and invasion of MCF cells. As shown in Figure 4.6 (C), co-culture delayed the migratory distance of cancer cells in the wound gap created in scratch assay compared to the control cells for the time course over 24 hours.

In conjunction with that, we speculate that ADMSCs may alter the expression of epithelial (*CD24*) and mesenchymal (*CD44*) surface markers and genes associated with epithelial (*E-cadherin, OLCN*) and mesenchymal (*SNAIL, ZEB2, Vimentin and SMAD4*) regulatory networks. To explore the involvement of the EMT/MET regulatory network in suppressing cancer progression, epithelial and mesenchymal surface markers gene expressions required for initiation of metastasis were evaluated. The majority of MCF7 cells expressed epithelial surface marker, *CD24* before and after co-culture, yet no significant increase on the level of the mesenchymal marker, *CD44* (less than 8%) (Figure 4.7).

In addition, stable expression of epithelial genes *E-cadherin* and *OCLN* and a significant reduction in all mesenchymal genes were detected (Figure 4.8). In the case of MDA-MB-231 cells, ADMSCs increased the expression of CD24 by 32%, increased *E-cadherin* and *OLCN* by three and seven-folds respectively and reduced *SMAD4*. Overall, ADMSCs maintain the epithelial identity and suppress the expression of mesenchymal genes in MCF7 cells. Meanwhile, ADMSCs enhanced the expression of epithelial in MDA-MB-231 cells while suppressing the mesenchymal markers. In MDA-MB-231, ADMSCs lead the transition of EMT to MET state, whereas, in MCF7, the cells maintain the MET state accordingly.

A)

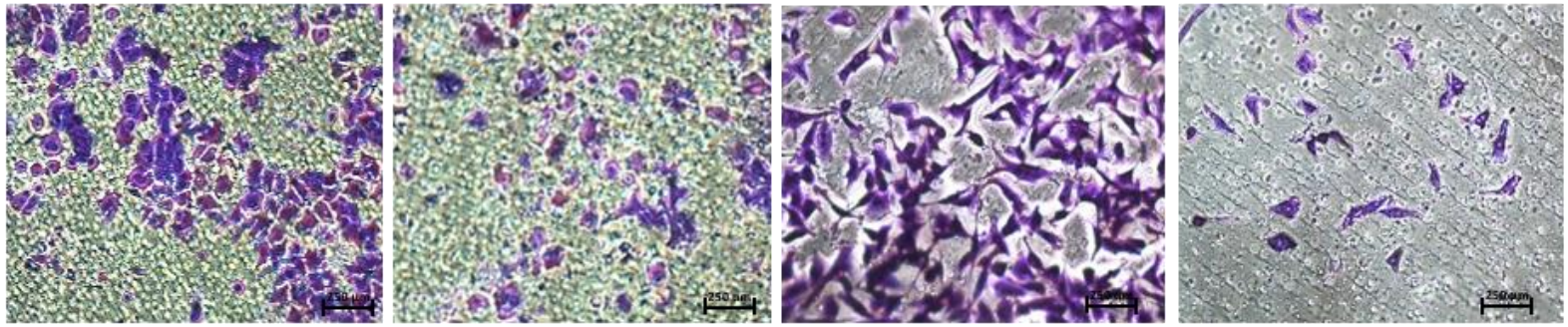

MCF7 | MCF7 co-culture | MDA-MB-231 | MDA-MB-231 co-culture

B)

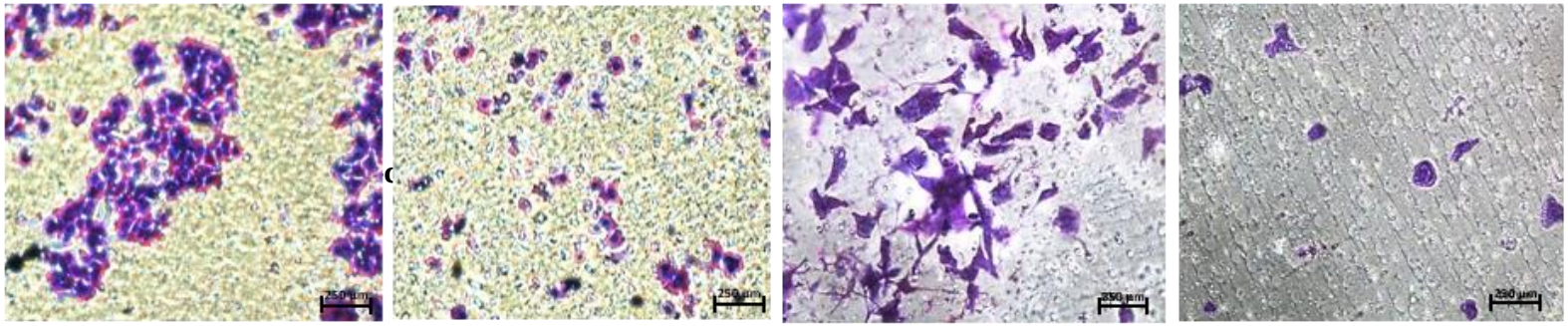

MCF7 | MCF7 co-culture | MDA-MB-231 | MDA-MB-231 co-culture

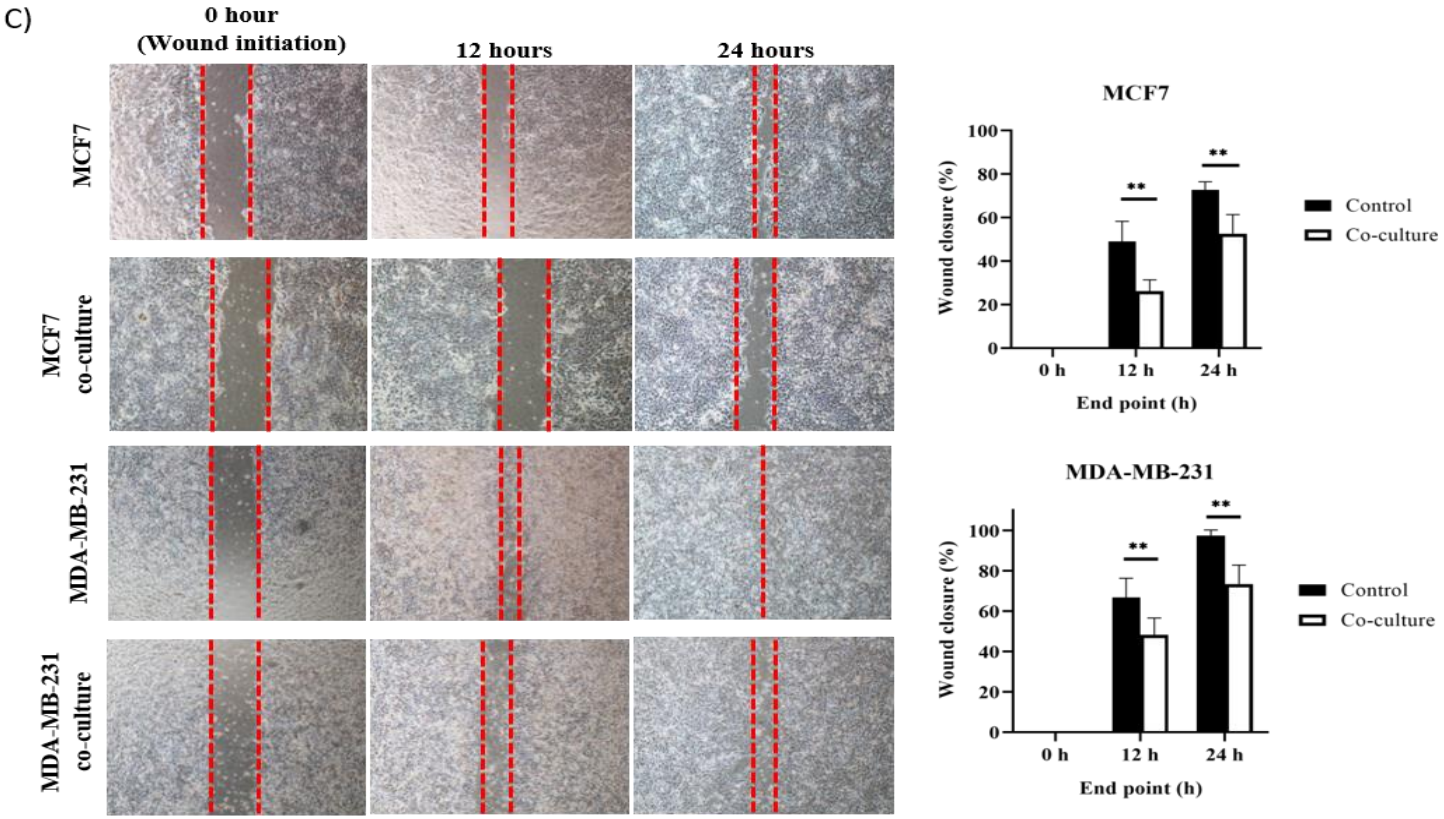

Figure 4.6. Metastasis capacity of cancer cells co-cultured with ADMSCs. Representative images of breast cancer cells analyzed for (A) migration ability, (B) invasion ability (20x magnification) (C) wound healing ability (10x magnification).

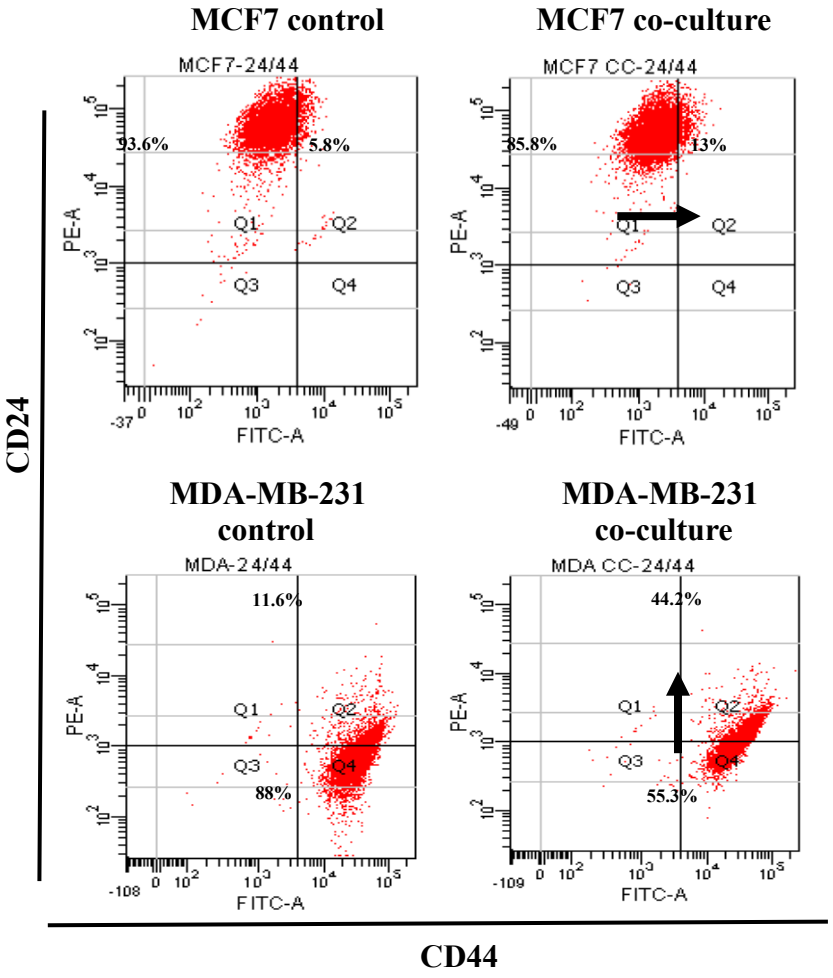

Figure 4.7. Alteration in epithelial (*CD24*) and mesenchymal (*CD44*) surface markers expressions. Representative image of *CD24* and *CD44* expression in Breast Cancer Cells before and after co-culture interaction with ADMSCs analyzed using flow cytometer.

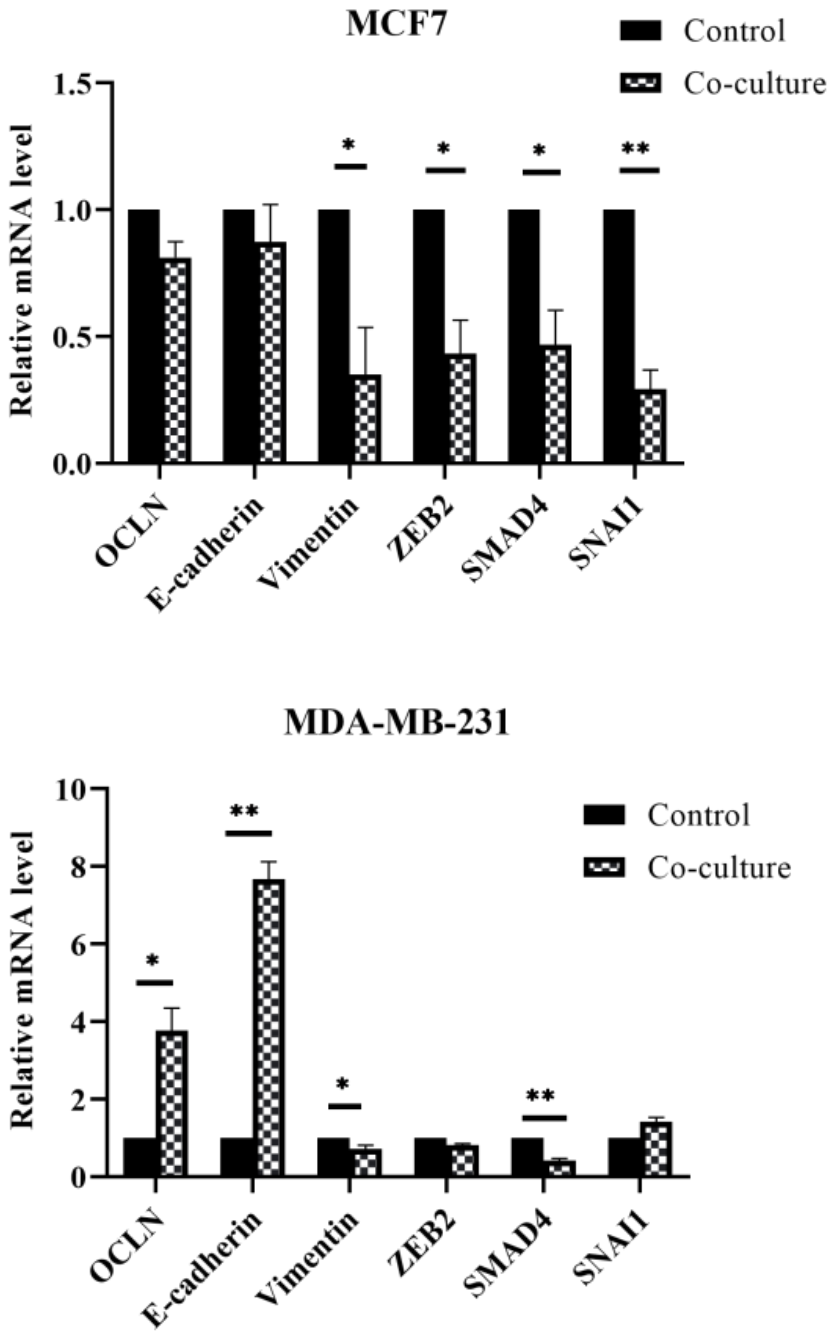

Figure 4.8. Alteration in epithelial and mesenchymal genes expression level. The results were analyzed using a t-test with mean values ± SD. *p<0.05 and **p<0.01 compared with the non-co-culture group.

4.4 Indirect Co-culture Allow Interaction Between ADMSCs and Breast Cancer Cells via Exosome Transfer

Earlier, we found that culturing breast cancer with ADMSCs reduced proliferation and metastasis of cancer cells, suggesting that a factor secreted by ADMSCs was responsible for acquiring the dormant state of MCF7 and MDA-MB-231 cells. Thus, exosomes secreted during the co-culture interaction were further investigated.

Exosomes collected from supernatants of ADMSCs, MCF7, MDA-MB-231 and the respective co-cultures were successfully isolated using serial centrifugation followed by membrane affinity spin column. The presence of exosomes was verified through the detection of AChE enzymatic activity of exosome membrane protein. The enzyme assessment of exosomes indicated a slightly higher number of vesicles secreted by ADMSCs and co-culture cells than cancer cells alone (Figure 4.9 A).

Another way to confirm the presence of exosomes is by looking at the size and structure *via* electron microscopy imaging (TEM) (Figure 4.9 B). Representative images show that isolated vesicles are primarily exosomes enriched with tetraspanin membrane protein markers CD81, CD9, CD63 and TSG101 shown by conjugated-gold particles in all exosome samples. Next, fluorescence dye staining with Vybrant Dio and SYTO64™ was carried out to track the direction of exosome and RNA transfer. Culturing cells with fluorescence-labeled exosomes in only one cell type and detecting the presence

of fluorescence in cells in another chamber allowed the confirmation of exosomes passing through the transwell filter. Interestingly, both unstained cancer cells fluoresce green and red after 48 hours of co-culture with pre-stained exosomes-ADMSCs.

Meanwhile, minimal fluorescence signals were detected in unstained ADMSC when cancer cells were pre-stained and co-culture for 48 hours with ADMSCs (Figure 4.10). This indicates that most exosomes particles that carry RNA molecules were secreted by ADMSCs (act as donor cells) into the microenvironment and were taken up by breast cancer cells (act as recipient cells).

A)

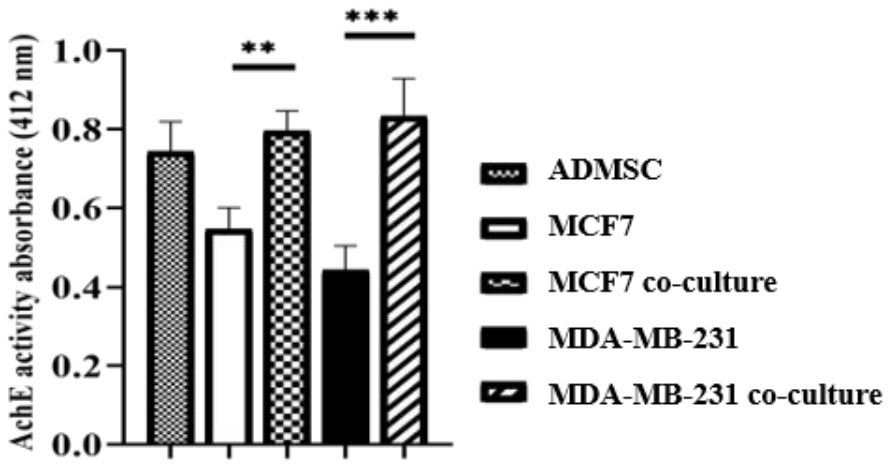

B)

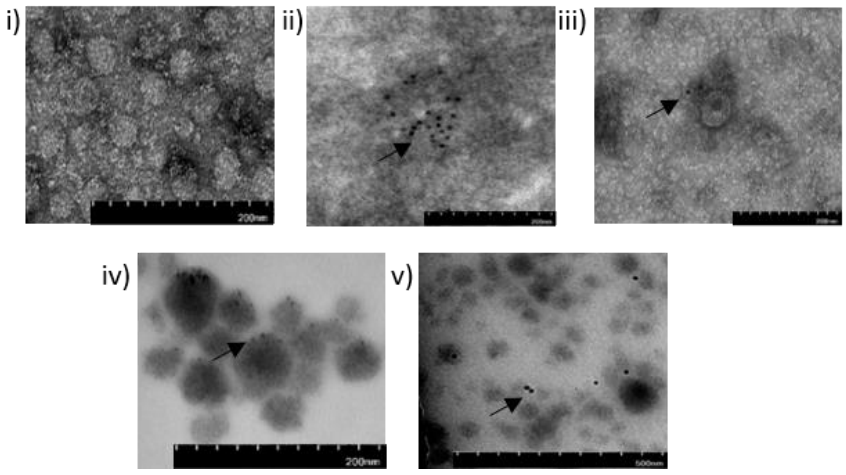

Figure 4.9. Characterization of exosomes. (A) A graph showing the enzymatic activity AChE of isolated co-culture exosomes. (B) Representative images of transmission electron microscopy (TEM) of cells-derived exosomes; i) negative staining, ii-v) exosomes stained with gold-conjugates secondary antibody to anti-CD81, anti-CD9, anti-CD63 and anti-TSG101 (80k x magnification). The arrow indicates the golden particles of the secondary antibody. The results were analyzed using t-test and ANOVA with mean values ± SD. $^{**}p<0.01$ and $^{***}p<0.001$ compared with the control group.

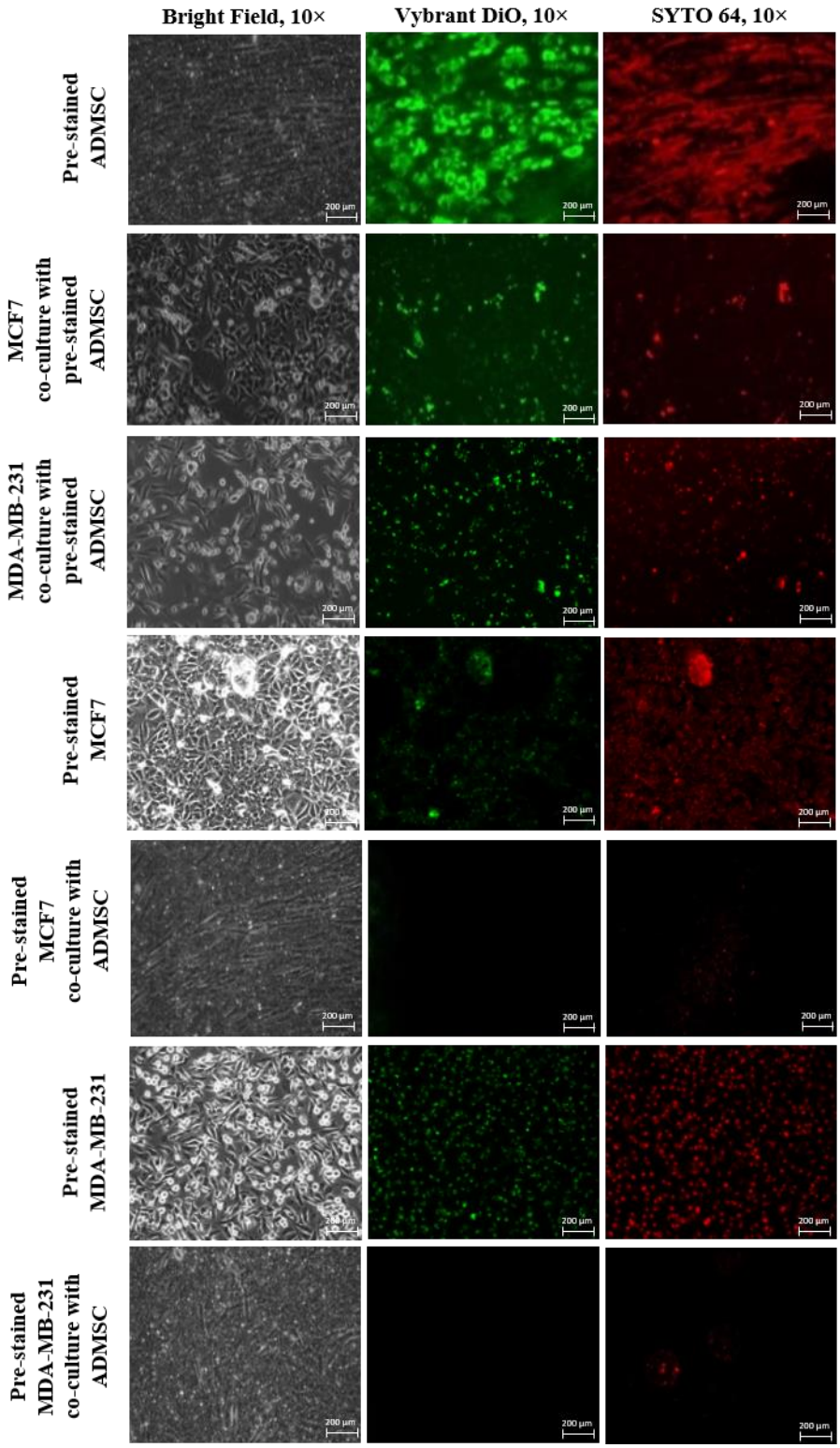

Figure 4.10. Intercellular transfer of exosomes. Intercellular transfer of exosomes and RNAs was visualized through membrane and RNAs staining with Vybrant DiO and SYTO64™ fluorescence dyes (10x magnification).

4.5 Intercellular Transfer of Exosomes and RNAs From ADMSCs to Breast Cancer Cells Facilitate Dormancy Acquisition and Metastasis Inhibition

To investigate the presence of two-way cross-talk and functionality of exosomes in mediating the interaction, we treated BCCs with exosomes derived from the culture medium of; i) ADMSC-derived exosomes, ii) MCF7 co-culture-derived exosomes and iii) MDA-MB-231 co-culture-derived exosomes. The results were analyzed against control (no addition of exosome). Comparable to indirect transwell co-culture, the addition of exosomes aliquot from 48 hours of co-culture resulted in the transformation of breast cancer phenotypes; changes in morphology, reduction in proliferation (Figure 4.11), migration (Figure 4.12 A), invasion (Figure 4.12 B) and wound healing (Figure 4.13).

Overall, co-culturing cancer cells with exosomes-derived co-culture showing similar effects on cells' morphology, proliferation rate and metastasis ability. Similar results but with lesser inhibition levels were seen in cells treated with exosomes of ADMSCs. It explains the importance of cell communication in exerting specific effects on cancer progression. During co-culture, cancer cells interact with ADMSCs in response to changes in the microenvironment that inhibit the progression of cancer cells.

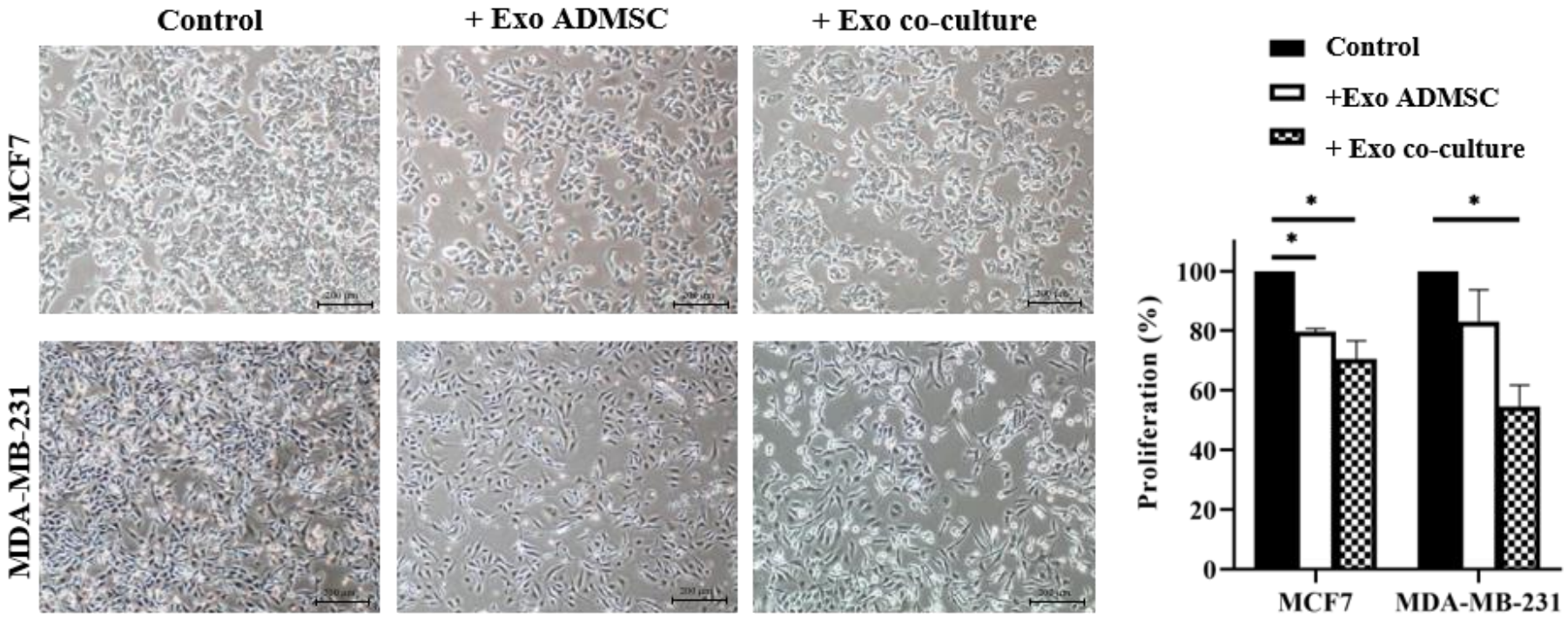

Figure 4.11. Exosomes functional test on cell proliferation. The changes in the morphology and proliferation of breast cancer cells were observed after treatment with exosomes derived from ADMSCs and co-culture cells. The results were analyzed using t-test and ANOVA with mean values ± SD. *p<0.05 compared with the control group.

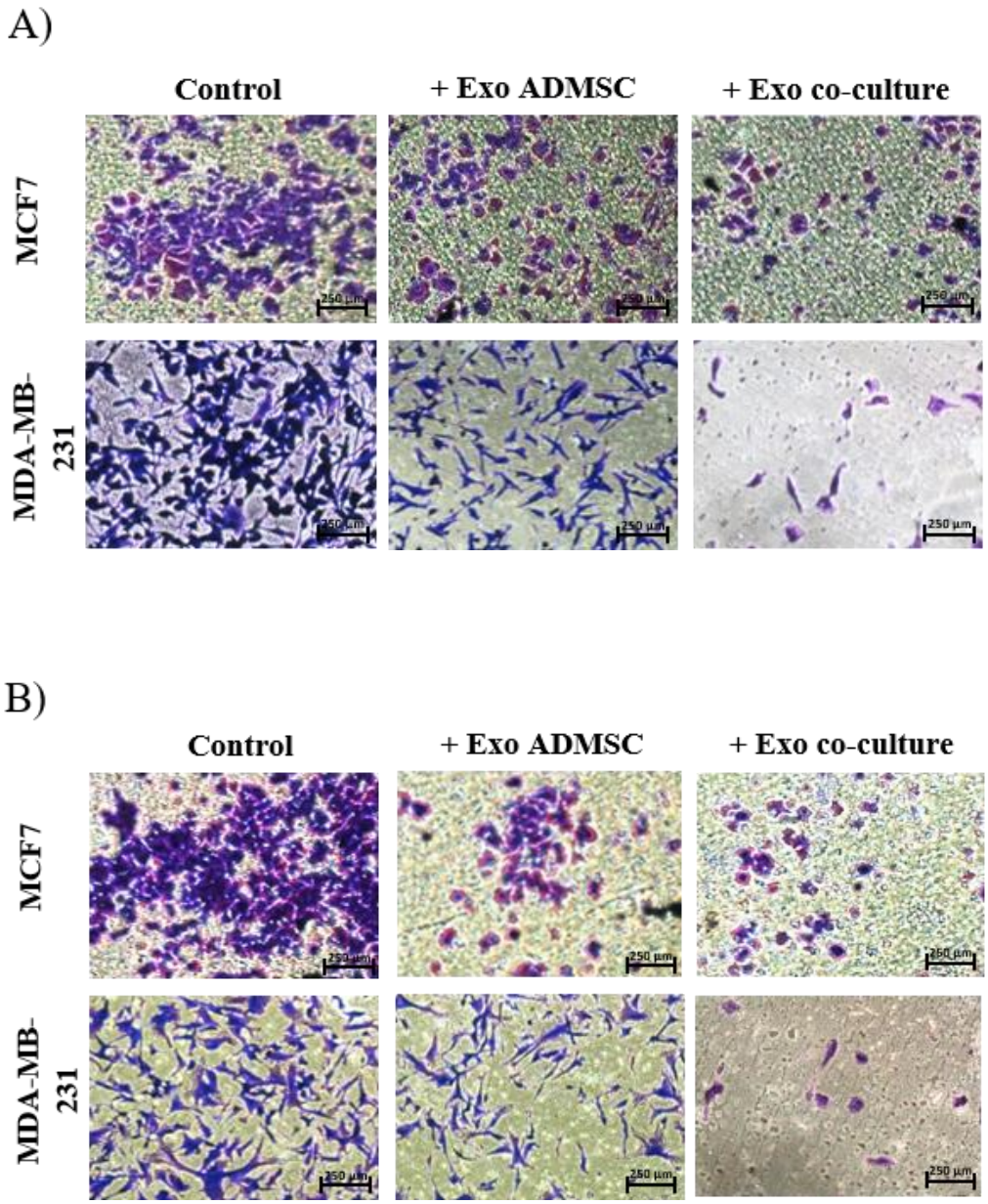

Figure 4.12. Exosomes functional test on cell migration and invasion. Representative images of breast cancer' A) migration and B) invasion abilities were observed after treatment with exosomes derived from ADMSCs and co-culture cells.

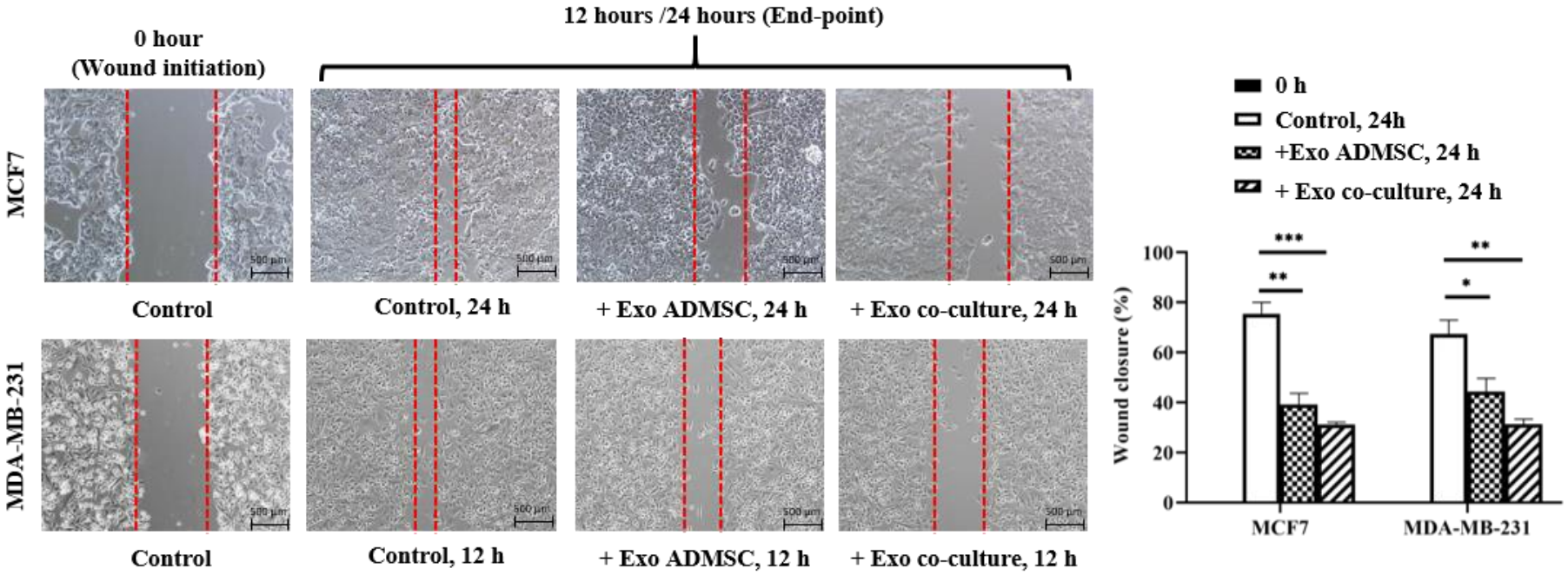

Figure 4.13. Exosomes functional test on wound healing ability. A gap was created on breast cancer cells, followed by treatment with exosomes derived from ADMSCs and co-culture cells. The results were analyzed using t-test and ANOVA with mean values ± SD. *p<0.05, **p<0.01 and ***p<0.001 compared with the control group.

RESULTS

PART 2: Evaluation of EMT/MET Pathway from miRNAs Expression Profile of Indirect Co-culture Cells Using Next-Generation Sequencing

4.6 The Distribution of Small RNAs Between Cells and Exosomes

To further investigate the role of exosomes in mediating communication between ADMSCs and breast cancer cells, it is crucial to examine the RNAs content inside the vesicles that may play a role in cancer dormancy. Total RNA was isolated from exosomes released by ADMSCs, breast cancer and co-culture cells. The results of the bioanalyzer show that exosomes and cells consist of a different composition of RNA population. Ribosomal RNA (rRNA) population (28S and 18S subunits) is highly enriched in cellular RNA, while exosomes majorly consist of short nucleotides. (Figure 4.14 A). The miRNA population in both cells and exosomes was confirmed to be present at less than 40 nucleotides, with exosomes enriched in tRNAs at approximately 60 nucleotides.

Prior to sequencing using NEB and Illumina platforms, a minimum cut-off RNA integrity number (RIN) for cells was set to be seven and <three for exosomes due to the low amount of rRNA detected in exosomal RNA. The variation in RNA size distribution between exosome and cell was detected. Intense bands of shorter than 200 nucleotides were observed in exosomes

indicating a small RNAs population, while longer length (1.9-4kb) nucleotides were observed in cellular RNAs (Figure 4.14 B).

After demultiplexing and trimming, the quality was assessed using FastQC > 30. All reads from 30 samples (including replicates) were mapped to known small RNAs of the human genome and annotated to mature miRNA. The small RNA population mainly consists of 5S rRNA, transfer RNA (tRNA), micro RNA (miRNA), small nucleolar RNA (snoRNA), messenger RNA (mRNA), small nuclear RNA (snRNA) and yRNA (Figure 4.15).

The proportion of small RNA population is different between exosomal and cellular RNA, where miRNA and tRNA dominate exosomal RNA and miRNA and rRNA dominate cellular RNA. This presumably explains that miRNAs are one of the significant components that are being transported between the cells. Nevertheless, the “unknown” or unannotated sequence fragments accounting for a quarter of mappable reads in all cells and exosomes libraries (11-34%) were secreted into exosomes by the cells, indicating a significant number of novel small RNAs or miRNAs candidates that could potentially have regulatory functions.

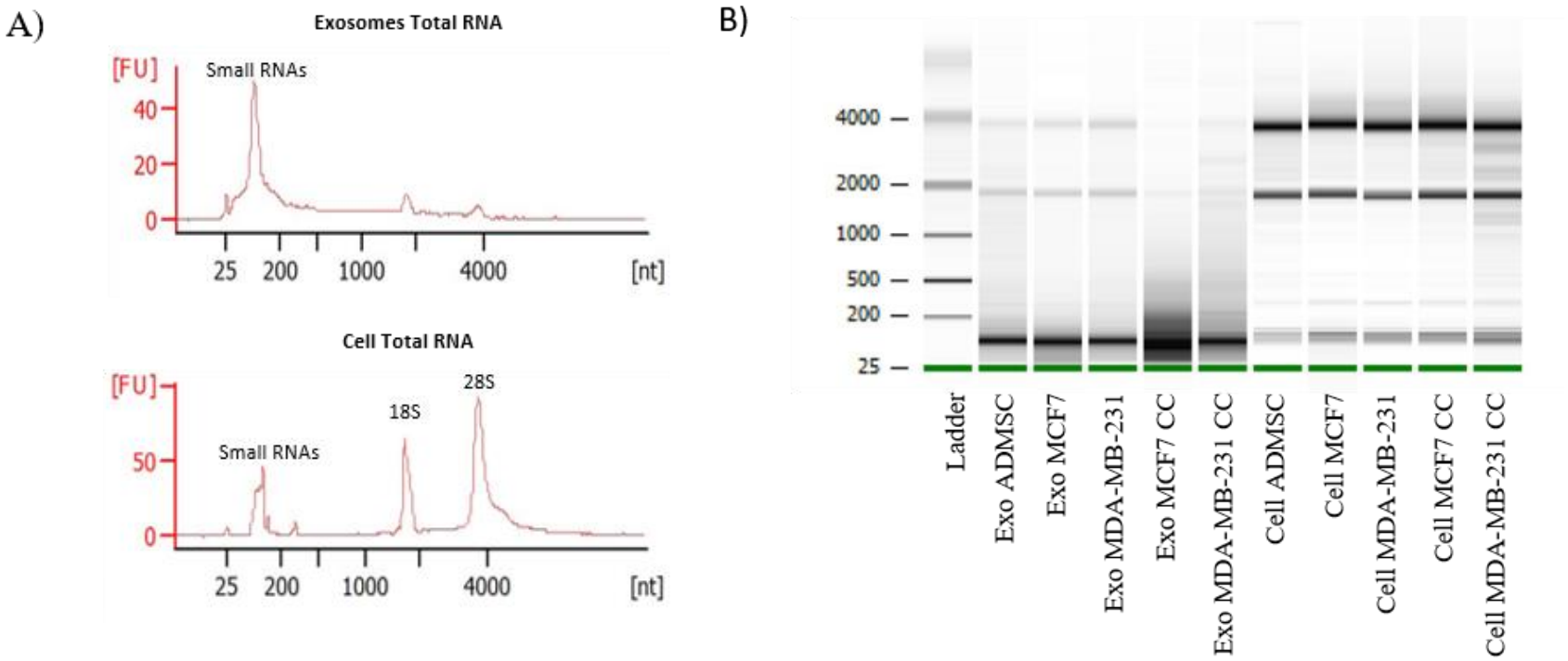

Figure 4.14. Characterization of RNAs and small RNAs composition. (A) Representative peaks of total RNAs in cells and exosomes by bioanalyzer, respectively. Exosomes lack detectable 18S and 28S rRNAs compared to cell total RNAs, while the miRNA population is present in both at <40 nucleotides. (B) Length distribution of total RNAs in all samples of exosomes and cells.

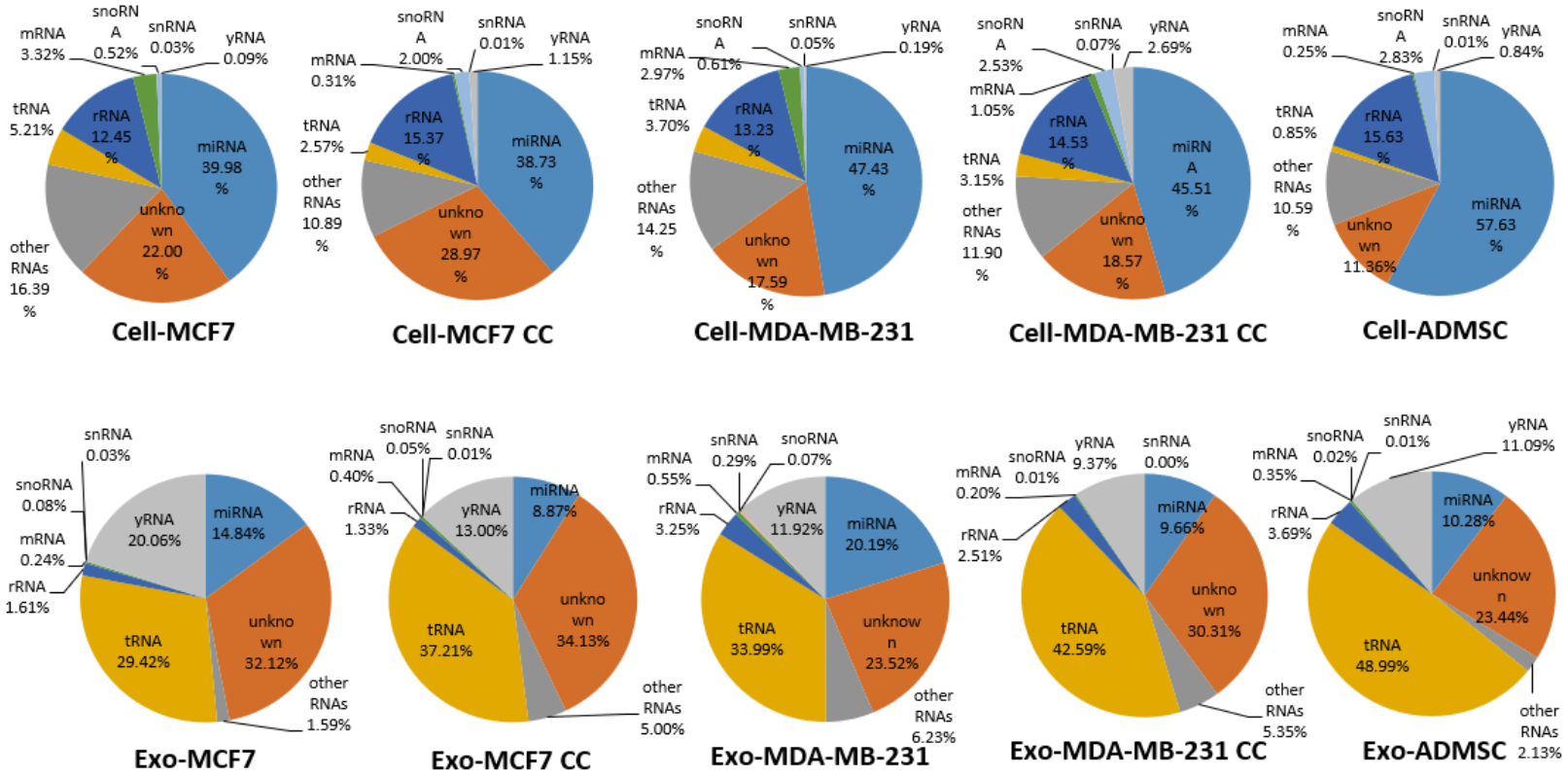

Figure 4.15. Distribution profiles of small RNAs population. Transcriptome profiling of small RNAs was performed using Next-Generation Sequencing. Small RNAs population in cells and exosomes predominantly consist of miRNA, tRNA, yRNA, mRNA and rRNA.

4.7 Alteration of miRNAs Expression Profile in Cells and Exosomes Following Co-culture

Even though exosomes are enriched in small RNA fragments, the relative miRNA composition is smaller in exosomes (8-20%) than in cells (38-57%) (Figure 4.15). Based on the differentially expressed miRNA heat map and hierarchical clustering, three distinct patterns between parental cells, co-culture cells and exosomes were detected (Figure 4.16). Among the cells, parental MCF7 and MDA-MB-231 have a clear separation from ADMSCs, co-culture MCF7 and co-culture MDA-MB-231 cells.

The fact that ADMSCs are in the same cluster as the co-culture cancer cells show that the donor (ADMSCs) and recipient (co-culture cancer) cells share similar miRNA expression. To conclude the role of exosomes as carriers in transporting miRNAs between cells, their content should closely resemble those of the parent cells. In this case, hierarchical clusters of co-culture exosomes are closer to ADMSCs than parental cancer cells, portraying that co-culture exosomes' content is mainly derived from ADMSCs rather than later. Interestingly, even though exosomes libraries are clustered within the same hierarchical group, there is a distinct miRNAs signature between exosomes derived from breast cancer subtypes, ADMSC and co-culture cells.

The change in miRNA levels of exosomes and cells following co-culture is crucial to be explored as it may contribute to the overall effects of ADMSCs on breast cancer cells proliferation and migration. To do so, differential

expression in co-culture exosomes miRNA profiles were normalized against ADMSCs exosomes and overlapped with co-culture cells normalized against non-co-culture cancer cells, which resulted in the changes of consensus miRNAs (Figure 4.17).

Based on the constructed Venn diagram of top 50 miRNAs differentially expressed with fold change > 2 or <-2, 14 miRNAs were found to be upregulated and 13 miRNAs were downregulated in MCF7 cells. Meanwhile, nine miRNAs were upregulated and two miRNAs were downregulated in MDA-MB-231 cells (Table 4.2). Of the 38 miRNAs differentially expressed in both cells, subsequent overlapping resulted in only five miRNAs common to both cancer cells (miR-200a-5p, miR-941, miR-629-5p, miR-10b-5p and miR-486-5p), indicating that both sets of dysregulated miRNAs exclusively target different groups of genes (Table 4.3). Taken together, alteration in the content and regulation level of miRNAs in exosomes after co-culture interaction for 48 hours sequentially affects the miRNAs content of recipient cancer cells.

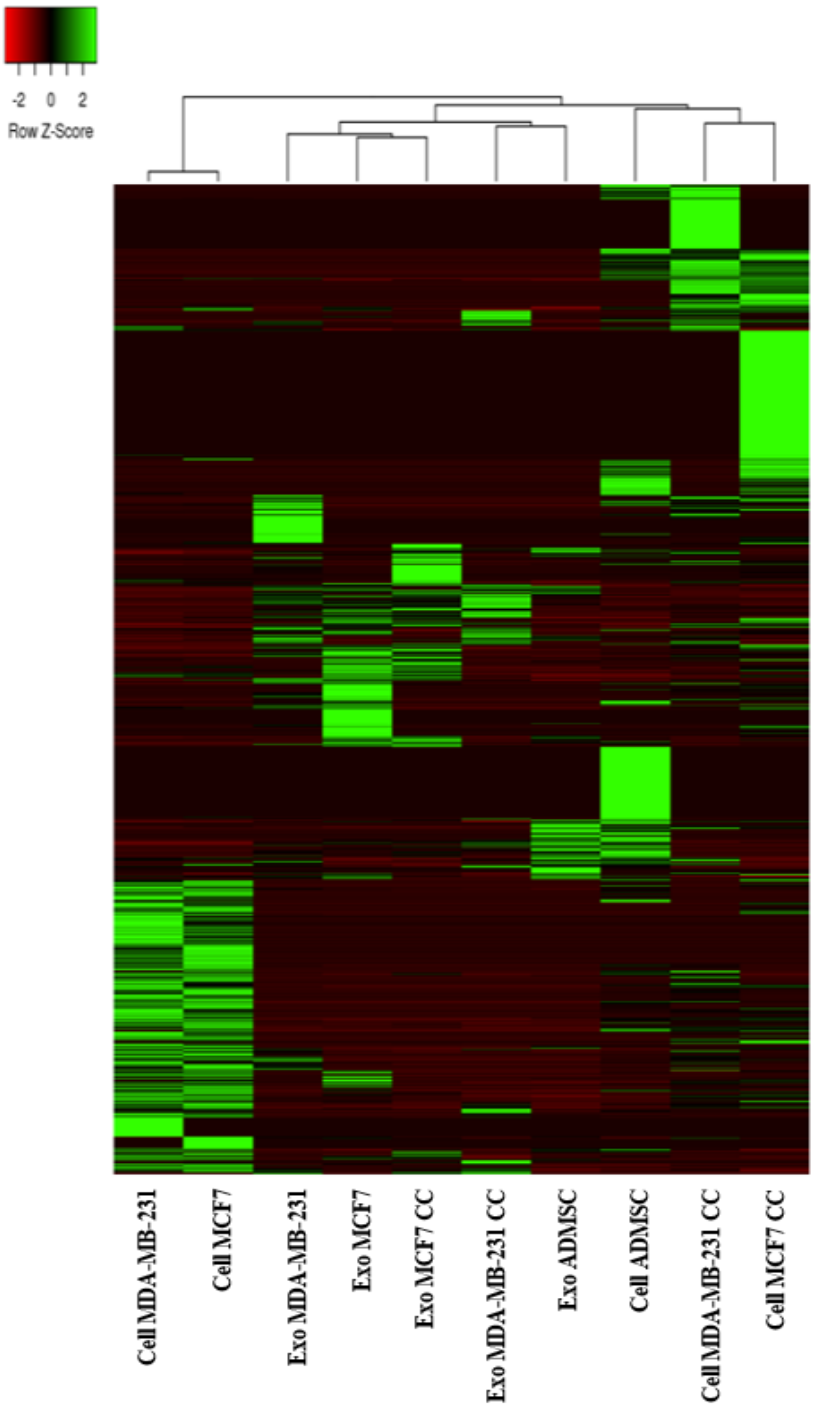

Figure 4.16. Differential miRNA expression of cells and exosomes derived from ADMSCs, breast cancer and co-culture. Heat maps and dendrograms generated by hierarchical clustering of miRNAs expression profiles signifies the different expression pattern and cluster of cells and exosomes.

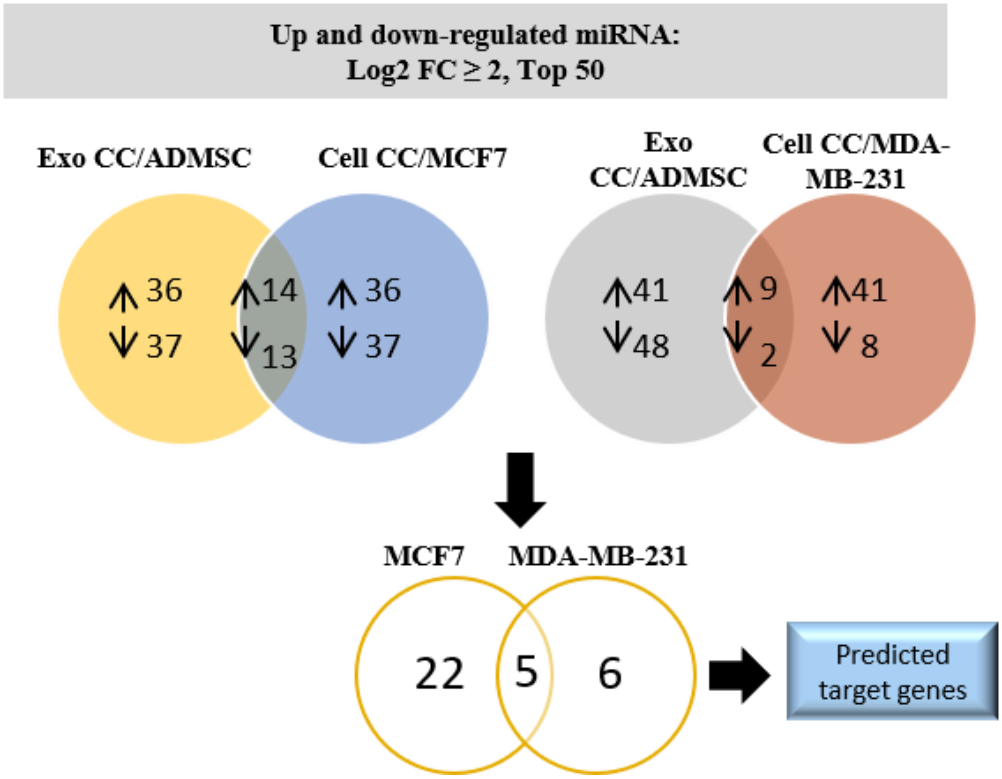

Figure 4.17. Top 50 of highly dysregulated miRNA in cells and exosomes derived from ADMSCs, breast cancer cells and co-culture. The Venn diagram represents the differentially expressed miRNA (Up- and down-regulated) in exosomes (co-culture normalized against ADMSCs) overlapped with cells (co-culture normalized against breast cancer cells). Further overlapping of the mutually dysregulated miRNA generates five miRNAs shared by both cancer cells (highlighted in Table 4.2). Predicted target genes were generated from the dysregulated miRNAs (Table 4.3).

Table 4.2. List of differentially expressed miRNAs in exosomes. Co-culture-treated cells were normalized against ADMSCs overlapped with co-culture-treated cells normalized against A) MCF7 and B) MDA-MB-231. MicroRNAs highlighted in bold are five mutually dysregulated in both cancer cells.

A)

Up/down-regulated miRNA	Exo-ADMSC Fold change > 2	p-value	Cell-MCF7 Fold change > 2	p-value
hsa-miR-200a-5p	**4.99**	**0.006**	**9.84**	**0.000**
hsa-miR-203a-3p	3.01	0.179	8.24	0.000
hsa-miR-941	**3.10**	**0.066**	**7.62**	**0.005**
hsa-miR-200a-3p	3.50	0.062	6.93	0.000
hsa-miR-629-5p	**2.89**	**0.100**	**6.86**	**0.000**
hsa-miR-200b-3p	4.43	0.002	6.81	0.000
hsa-miR-589-5p	2.00	0.441	6.17	0.002
hsa-miR-200c-3p	5.30	0.012	5.69	0.002
hsa-miR-3615	3.32	0.122	5.60	0.002
hsa-miR-7-5p	3.20	0.005	4.73	0.000
hsa-miR-185-5p	3.91	0.017	3.65	0.001
hsa-miR-1268b	2.22	0.315	3.57	0.058
hsa-miR-1268a	2.22	0.315	3.57	0.058
hsa-miR-375	3.76	0.045	3.41	0.018
hsa-miR-222-5p	-2.06	0.232	-5.18	0.001
hsa-miR-10a-5p	-2.30	0.028	-5.24	0.000
hsa-miR-221-5p	-3.61	0.026	-5.54	0.000
hsa-miR-143-3p	-2.58	0.032	-5.87	0.000
hsa-miR-199b-3p	-2.00	0.259	-6.19	0.000
hsa-miR-199a-3p	-2.00	0.259	-6.20	0.000
hsa-miR-199a-5p	-2.31	0.173	-7.06	0.000
hsa-miR-100-5p	-2.28	0.000	-7.19	0.000
hsa-miR-486-5p	**-2.89**	**0.004**	**-7.46**	**0.000**
hsa-miR-125b-1-3p	-2.00	0.000	-7.89	0.000
hsa-miR-155-5p	-13.68	0.000	-9.34	0.000
hsa-miR-10b-5p	**-2.80**	**0.011**	**-10.22**	**0.000**
hsa-miR-224-5p	-3.30	0.001	-23.77	0.000

B)

Up/down-regulated miRNA	Exo-ADMSC Fold change > 2	p-value	Cell-MDA-MB-231 Fold change > 2	p-value
hsa-miR-941	**3.58**	**0.114**	**12.89**	**0.000**
hsa-miR-629-5p	**4.82**	**0.006**	**9.61**	**0.000**
hsa-miR-146a-5p	6.31	0.000	8.46	0.000
hsa-miR-1180-3p	4.13	0.128	8.39	0.001
hsa-miR-1246	4.15	0.008	7.64	0.000
hsa-miR-1290	4.74	0.027	7.46	0.002
hsa-miR-200a-5p	**3.05**	**0.150**	**6.85**	**0.000**
hsa-miR-1301-3p	3.07	0.308	6.04	0.034
hsa-miR-7704	6.22	0.000	6	0.002
hsa-miR-486-5p	**-2.72**	**0.052**	**-6.97**	**0.000**
hsa-miR-10b-5p	**-3.93**	**0.004**	**-11.16**	**0.000**

Table 4.3. Top 10 exclusive dysregulated miRNA-targeted genes. Predicted genes highlighted in bold are mutually targeted by miRNAs in both cancer cells.

Target gene (MCF7)	Gene description	Dysregulated miRNAs	O/E ratio
ACVR2A	activin A receptor, type IIA	10	0.916248
CBL	Cbl proto-oncogene,E3 ubiquitin protein ligase	8	0.52331
CAPRIN1	cell cycle associated protein 1	7	0.562918
MAP3K7	mitogen-activated protein kinase kinase kinase 7	6	1.13509
CDC42	cell division cycle 42	6	0.777232
PTEN	phosphatase and tensin homolog	6	0.633646
SMAD2	SMAD family member 2	6	0.400451
IGF1R	insulin-like growth factor 1 receptor	6	0.392482
ErbB4	v-erb-b2 avian erythroblastic leukemia viral oncogene homolog 4	6	0.372997
NFAT5	nuclear factor of activated T-cells 5, tonicity-responsive	6	0.308160

Target gene (MDA-MB-231)	Gene description	Dysregulated miRNAs	O/E ratio
CADM1	cell adhesion molecule 1	3	0.841896
NFAT5	nuclear factor of activated T-cells 5, tonicity-responsive	3	0.378196
GAB1	GRB2-associated binding protein 1	2	0.977964
MAP3K7	mitogen-activated protein kinase kinase kinase 7	2	0.92871
BRCA1	breast cancer 1, early onset	2	0.768397
PTEN	phosphatase and tensin homolog	2	0.518440
ARHGAP5	Rho GTPase activating protein 5	2	0.494601
CD28	CD28 molecule	2	0.428873
CAPRIN1	cell cycle associated protein 1	2	0.394774
SMAD2	SMAD family member 2	2	0.327642

4.8 Biological Pathway Potentially Influenced by Dysregulated miRNAs-Mediated Breast Cancer Cells' Dormancy

Earlier, it is noted that the majority of exosomes trafficking directed from ADMSCs towards cancer cells contributed substantial dysregulation in miRNAs expression of recipient cancer cells. Thus, we further analyzed the potential biological function of that direction for both MCF7 and MDA-MB-231 cells. MiRNAs regulate the expression of specific genes via hybridization to mRNAs to promote their degradation to inhibit their translation or both.

Bioinformatics searches showed a total of 3857 and 832 putative target genes were identified in MCF7 and MDA-MB-21 and 554 genes shared by both. The top 10 targeted genes with highly significant O/E ratios were summarized in Table 4.3. From that, five of the target genes were mutually predicted in both cells. Predicted genes targeted by dysregulated oncomiRs or tumor suppressor miRNAs were mainly targetting cell cycle regulators such as *CAPRIN1, CDC42, PTEN, IGF1R, BRCA1* and *CD28*, which could lead to cancer dormancy. Other predicted genes such as *CBL, MAP3K7, SMAD2* and *ErbB4* regulate multiple cellular processes; apoptosis and cell proliferation. Meanwhile, *CADM1* and *NFAT5* are critically involved in the migration and invasion of cancer cells.

Of the top 10 predicted targets in the 10 Gene Ontology (GO) terms in molecular function (MF), the percentage of binding and catalytic activity are the same for both cells (80%). However, 20% of the genes differed in

molecular transducer activity in MCF7 and transcription regulator activity in MDA-MB-231 cells (Figure 4.18). The predicted genes associated with the biological process (BP) for both cells type were primarily enriched in cellular process, biological regulation, metabolic process, response to stimulus and signaling.

KEGG annotation revealed the exclusive and shared pathways of the ten most enriched KEGG pathways in both cancer subtypes (Table 4.4). The shared pathways are related to tumor development and EMT-related pathways such as TGF-β and Wnt signaling, cancer classical pathways (ErbB, MAPK, pathways in cancer) and pathways related to primary intercellular signaling (neurotrophin signaling).

MCF7 exclusively targeted the predicted genes involved in proliferation and EMT/MET pathways, such as axon guidance and focal adhesion, together with cancer metabolic processes (insulin signaling pathways). On the other hand, MDA-MB-231 targeted predicted genes involved in physiological functions such as toll-like receptor (TLR), B cell receptor and T cell receptor and protein related to cancers (chemokines signaling pathways). Although some of the cascade and signaling pathways are dissimilar between two cells, they were all crucially involved in regulating cancer proliferation, metastasis and dormancy, leading to resistance. Taken together, exosomes from co-culture mediate the transfer of miRNAs that contribute to the dormant state of breast cancer cells.

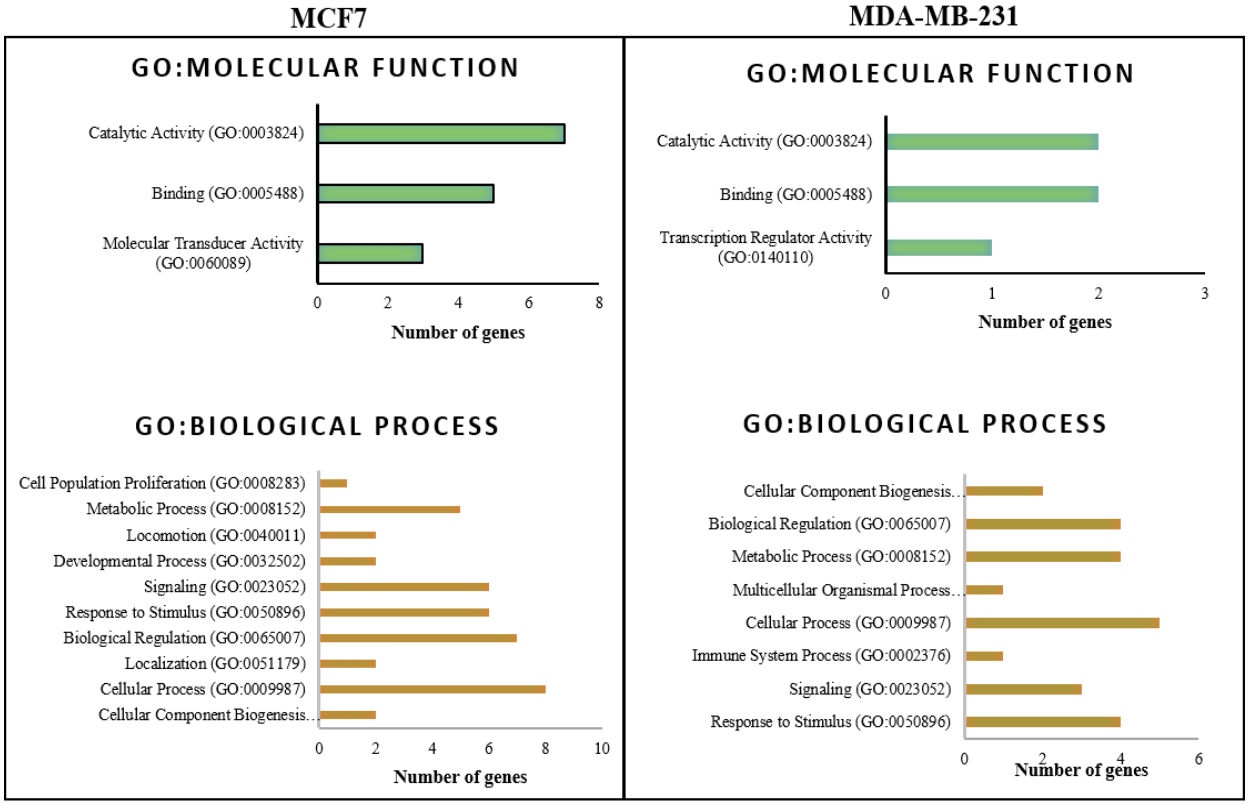

Figure 4.18. GO annotation for predicted target genes of differentially expressed miRNAs. Most significant GO annotation associated with molecular function and biological process, respectively, along with the number of genes that matched each GO term.

Table 4.4. KEGG pathway enrichment for predicted target genes of differentially expressed miRNAs. Ten most enriched KEGG pathways displaying mutual signaling pathways shared by both and exclusive pathways according to breast cancer type.

	KEGG pathways
MCF7	Focal Adhesion
MCF7	Insulin Signaling Pathway
MCF7	Axon Guidance
MCF7, MDA-MB-231	TGF-β Signaling Pathway
MCF7, MDA-MB-231	Wnt Signaling Pathway
MCF7, MDA-MB-231	MAPK Signaling Pathway
MCF7, MDA-MB-231	ErbB Signaling Pathway
MCF7, MDA-MB-231	Pathways In Cancer
MCF7, MDA-MB-231	Neurotrophin Signaling Pathway
MCF7, MDA-MB-231	Renal Cell Carcinoma
MDA-MB-231	Toll-like Receptor Signaling Pathway
MDA-MB-231	B Cell Receptor Signaling Pathway
MDA-MB-231	T Cell Receptor Signaling Pathway
MDA-MB-231	Chemokine Signaling Pathway

4.9 Specifically Upregulation of miR-941 in the Co-culture of Exosomes and Cellular Breast Cancer Cells

4.9.1 miR-941 Expression in Co-culture of Exosomes and Cellular Breast Cancer Cells

Among the commonly dysregulated miRNAs, miR-941 (the highest fold change in recipient cells) was selected as an upregulated miRNA marker that could represent both BCC types, which are significantly involved in exosomal trafficking. Also, we selected miR-941 on the basis that it was previously reported to contribute to the suppression of cell proliferation, migration and invasion of hepatoma and gastric cancer cells (Kim et al., 2014; Zhang et al., 2014). Specific mir-941 miRNA-pathway network analyses showed that miR-941 participates in regulating B and T-cell receptor signaling, ErbB and MAPK signaling pathways (Appendix G).

To confirm our selection of miR-941 and validate sequencing findings, the miRNAs expression level in cells and exosomes was performed using qRT-PCR. As compared to control, miR-941 was significantly upregulated ($p^* < 0.05$) in co-cultures and exosomes, therefore is a potential upregulated miRNA diagnostic marker (Figure 4.19).

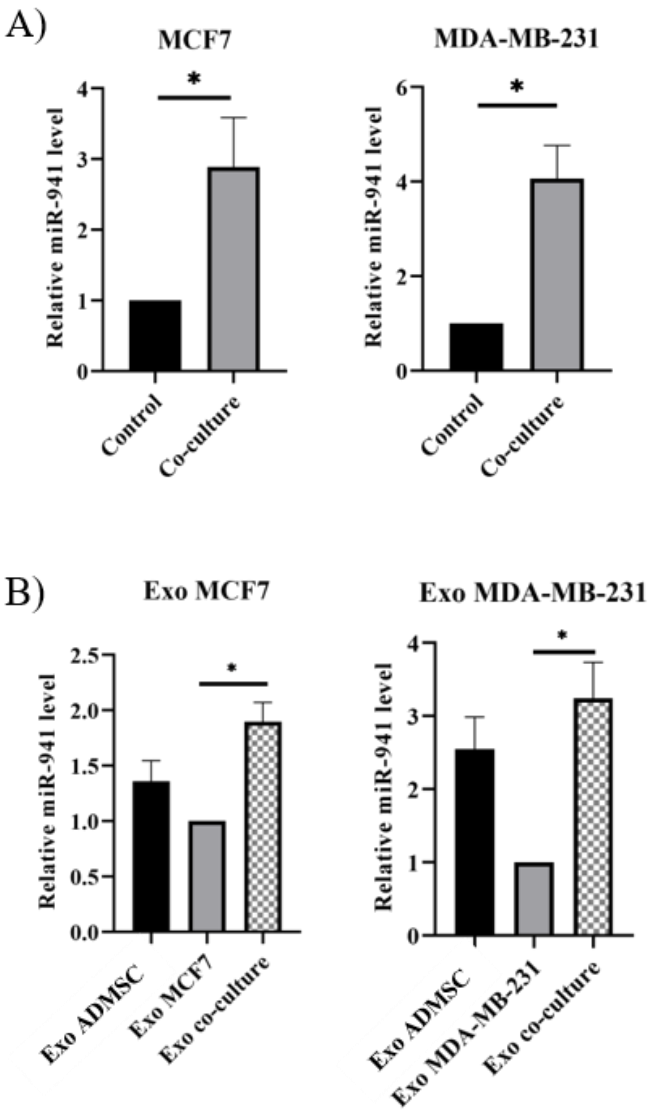

Figure 4.19. Relative miRNA-941 expression in cells and exosomes. Both co-culture-treated A) cells and B) exosomes expressed a higher level of miRNA-941 compared to control (non-co-culture) (*p<0.05).

4.9.2 Validation of Transcriptomic Sequencing using qPCR

To confirm the findings obtained from miRNA sequencing, qPCR is utilized. Two mutual miRNAs expressed in both MCF7 and MDA-MB-231 cells, miR-941 and miR-10b-5p were selected for validation. In addition, another three miRNAs (miR-760, miR-146a-5p and miR-205-5p) were chosen based on their suppression ability on breast cancer metastasis. An internal control RNU6b was employed for the assay. Overall, Figure 4.20(A) shows that miR-941 was the most steadily upregulated, whereas miR-10b-5p was the only downregulated miRNA of validated qPCR analysis. Meanwhile, miR-146a-5p was highly upregulated in the co-culture of MDA-MB-231 cells and exosomes but was downregulated in MCF7 cells.

The results suggest that ADMSCs can selectively signal the secretion of specific miRNAs into the microenvironment via exosomes depending on the breast cancer subtype. Similarly, cancer cells can selectively uptake specific miRNAs depending on the cancer subtype. In conclusion, qRT-PCR results correlated well with sequencing data (Figure 4.20(B)), indicating the reliability of sequencing-based expression analysis. ADMSCs secrete exosomes that suppress metastasis through miRNAs specific effect impeding migration, invasion and proliferation activities of breast cancer cells.

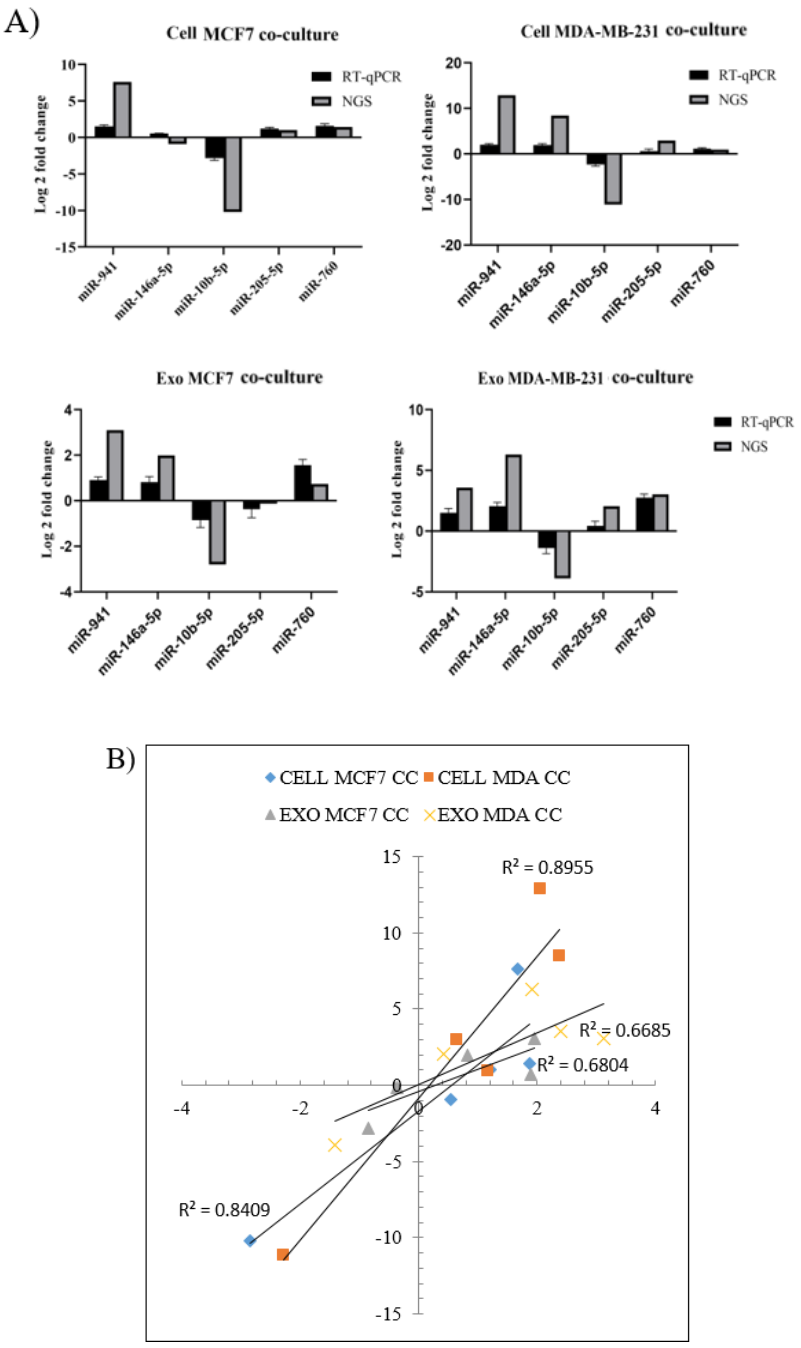

Figure 4.20. RT-qPCR validation and correlation plot. A) Reproducibility of NGS sequencing. B) Comparison of miRNA expression between NGS and qPCR analysis. Corresponding R^2 values were determined by linear regression analysis.

4.10 Tumor Suppressor miRNA (miR-941) Regulates Dormancy by Suppressing Cancer Cells Viability and Metastasis via MET Regulations

4.10.1 miR-941 Inhibits the Viability and Metastasis Ability of Brest Cancer Cells

We next sought to determine the role of miR-941 as tumor suppressor miRNA and a potential biomarker for breast cancer survival. We overexpressed miR-941 mimic into two breast cancer subtypes for 48 hours and assessed their relative levels. As shown in Figure 4.21, both cells have successfully been transfected and induced with significantly higher levels of miR-941 than the negative control. Overexpression of miR-941 has negatively impacted the viability and proliferation rate of both subtypes (Figure 4.22). Furthermore, overexpression of miR-941 reduced cell migration (Figure 4.23(A)) and invasion (Figure 4.23(B)). In the wound healing assay, wound closure by miR-941 cells transfected with the negative control was almost complete by 12/24 hours and comparable to the untreated controls.

On the contrary, both miR-941 mimic transfected-cells traveled into the wound site at a slower rate. Their ability to repopulate wounded areas was greatly reduced compared to untreated and negative control cells (Figure 4.24). In general, overexpression of miR-941 developed a similar, low metastatic potential in both breast cancer subtypes and was comparable to co-culture cells.

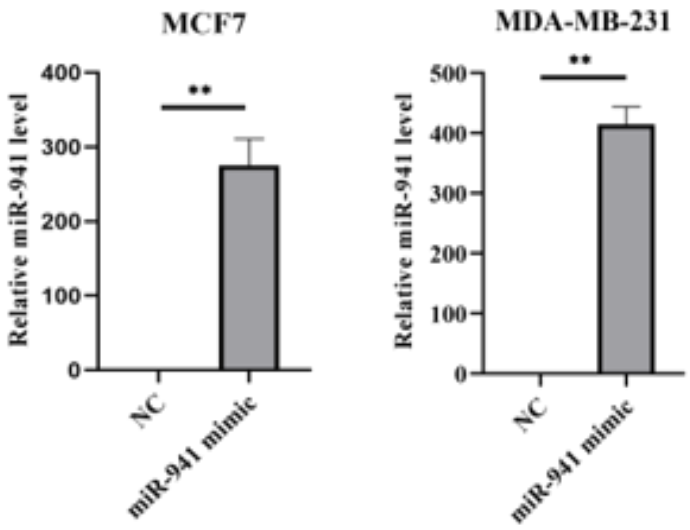

Figure 4.21. Relative expression of miR-941 in breast cancer cells after transfection. Cells were transfected with non-targeting negative control (NC) miRNA (AllStar Negative Control siRNA) or miR-941 mimic for 48 hours and analyzed with RT-PCR. The results were analyzed using a t-test with mean values ± SD. ** $p<0.01$ compared with the control group.

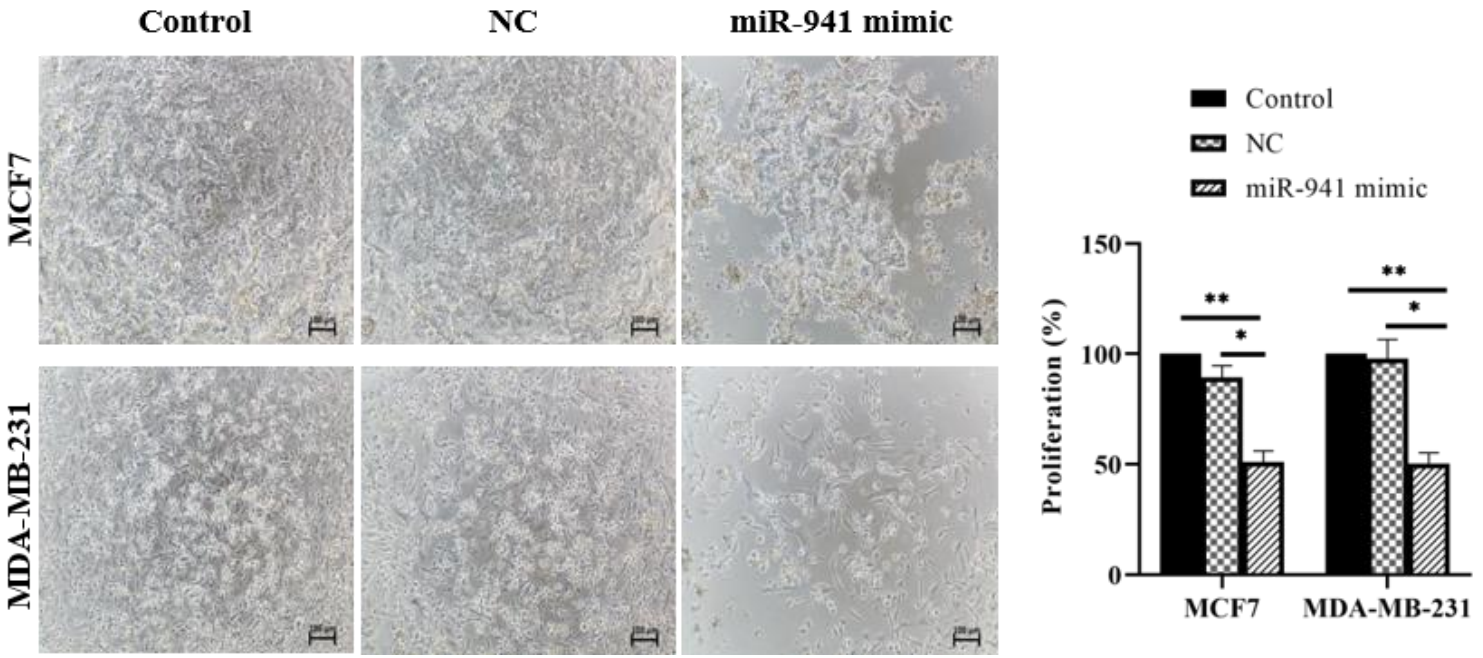

Figure 4.22. The effect of miR-941 mimic transfection on the proliferation of breast cancer cells. The viability and proliferation of miR-941 mimic- transfected-cancer cells were significantly inhibited compared to non-targeting negative control (NC) miRNA transfected-cells (AllStar Negative Control siRNA). Images were viewed using an inverted microscope (magnification x10) and analyzed using t-test and ANOVA with mean values ± SD. *p<0.05 and **p<0.01 compared to the control group.

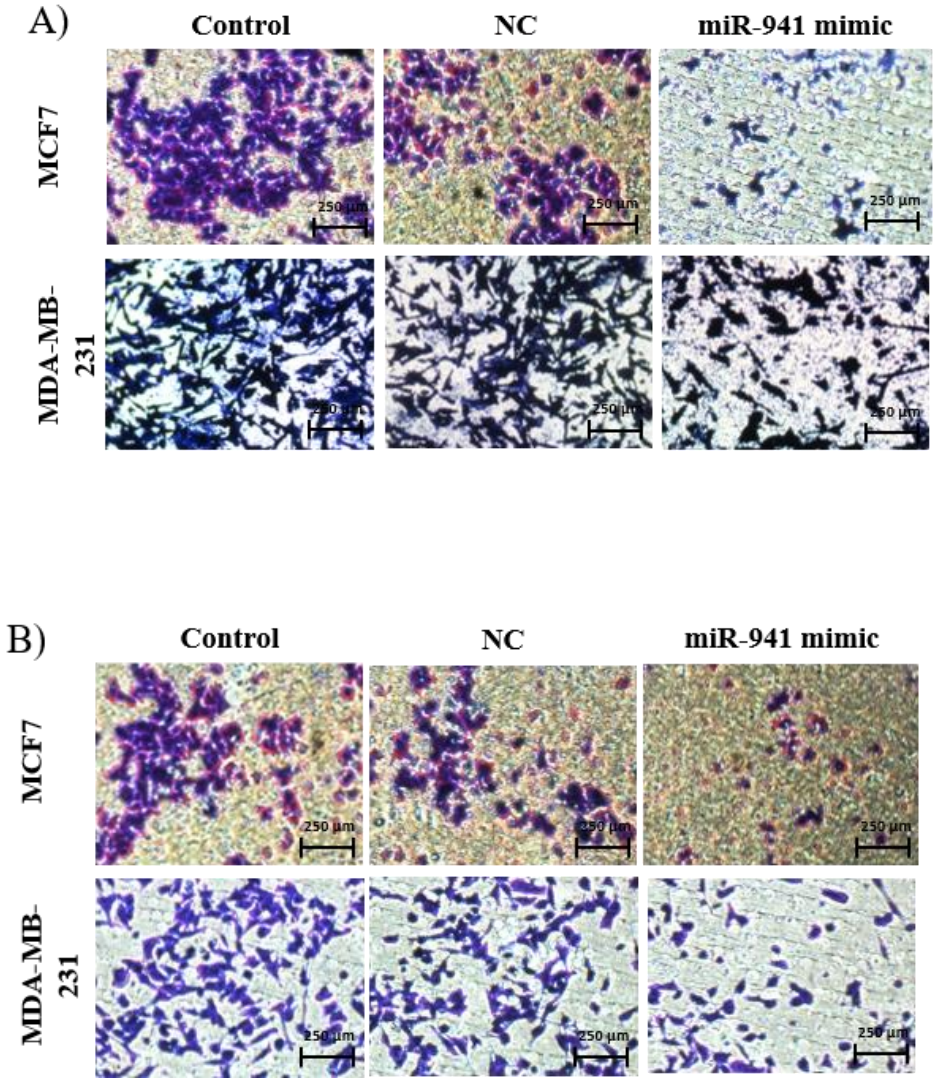

Figure 4.23. The effect of miR-941 mimic transfection on migration and invasion of breast cancer cells. Suppression of A) migration and B) invasion was observed in miR-941 mimic transfected-breast cancer cells compared to non-targeting negative control (NC) miRNA (AllStar Negative Control siRNA) transfected-BCCs (magnification x10).

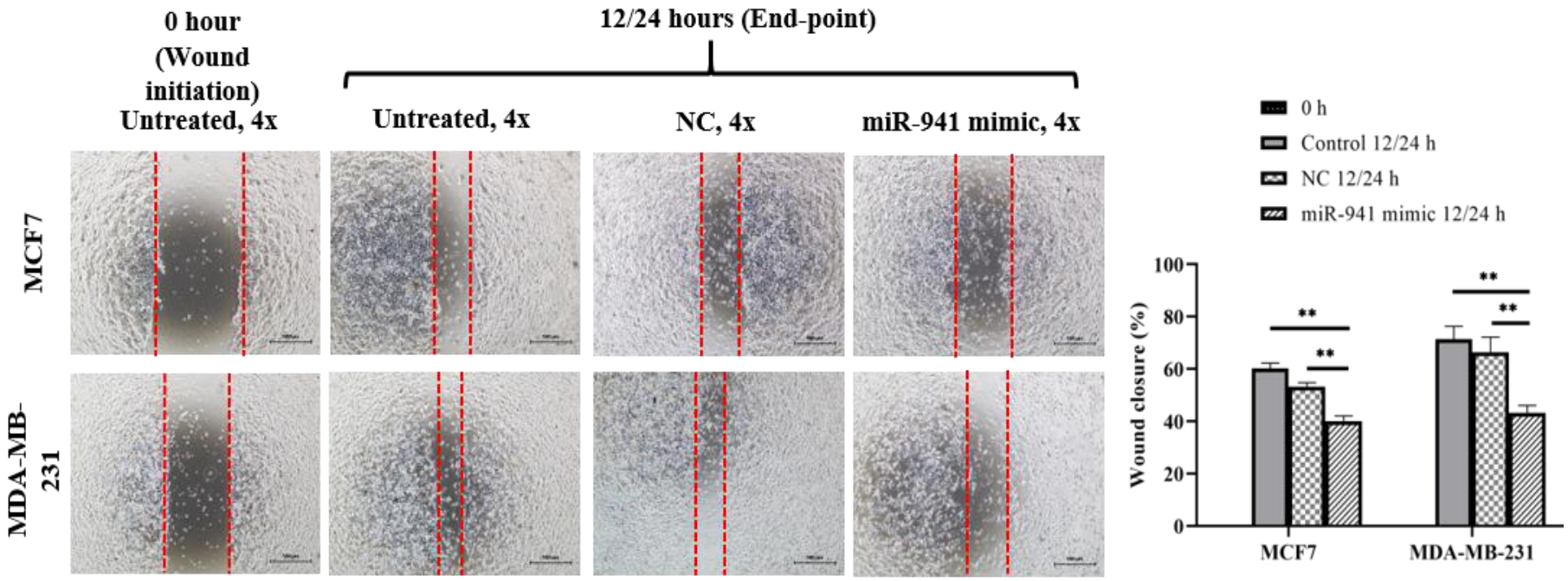

Figure 4.24. The effect of miR-941 mimic transfection on wound healing and migration. Suppression of wound healing and migration abilities was observed in miR-941 mimic transfected-cancer cells compared to non-targeting negative control (NC) miRNA transfected-cancer cells (AllStar Negative Control siRNA). The results were analyzed using a t-test and ANOVA with mean values ± SD. ** $p<0.01$ compared with the control group.

4.10.2 Validation of Differentially Expressed Genes Associated in Epithelial-Mesenchymal Process

To identify the role of miR-941-induced MET regulation, epithelial and mesenchymal markers were screened. Overexpression of miR-941 significantly enhanced *E-cadherin* and impaired *Vimentin*, *SMAD4* and *SNAI1* expression in both cells (Figure 4.25). *OCLN* expression was enhanced in MDA-MB-231 cells but not MCF7 cells. Meanwhile, the expression of the *ZEB2* gene was suppressed only in transfected-MCF7 cells. Taken together, these observations illustrate that miR-941 may facilitate the inhibition of breast cancer cell migration and invasion via MET regulation and strongly suggest that miR-941 has tumor suppressor function in both breast cancer subtypes.

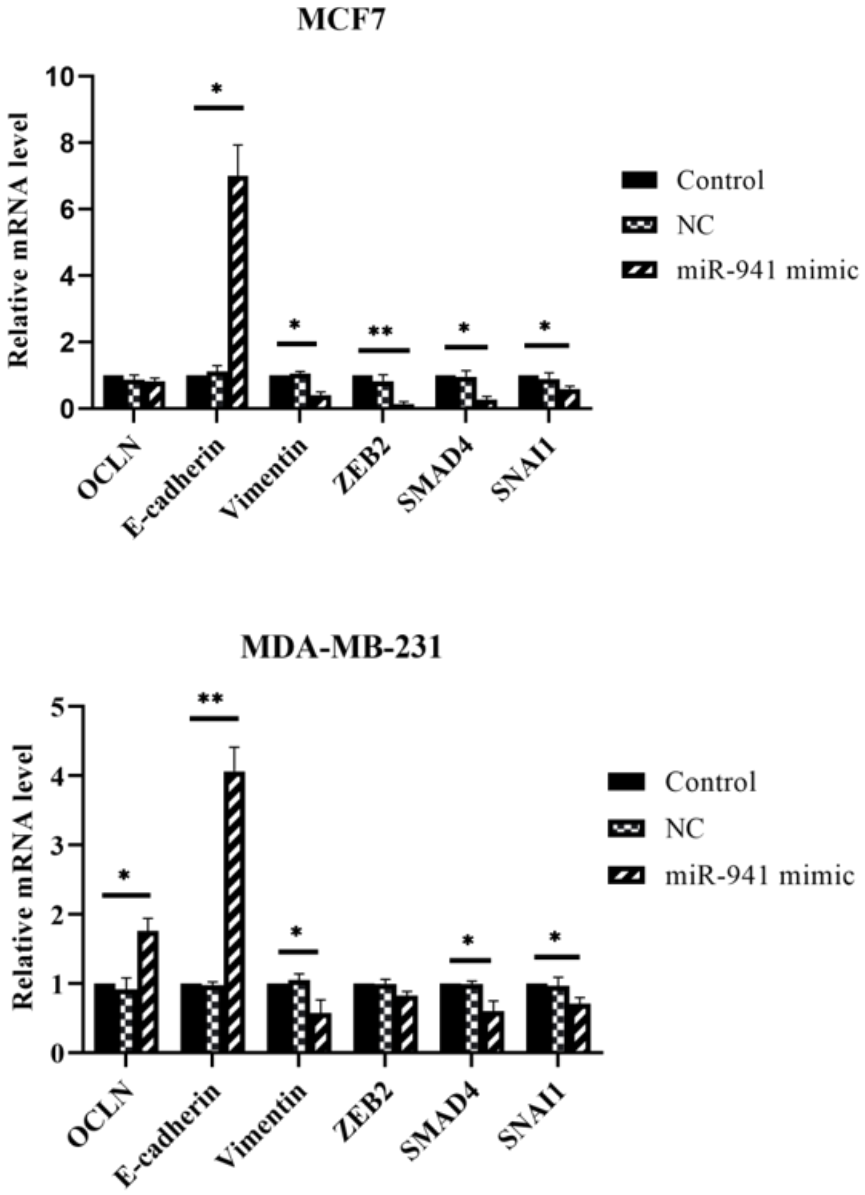

Figure 4.25. The effect of miR-941 mimic transfection on EMT markers expression. Mir-941 mimic led to the reduction of mesenchymal genes and an increase in epithelial genes expression level. The results were analyzed using ANOVA with mean values ± SD. *p<0.05 and **p<0.01.

CHAPTER 5

DISCUSSION AND CONCLUSION

5.1 Indirect Co-culture Promotes Dormancy of Breast Cancer by Inducing Cell Cycle Arrest

In breast cancer research, MCF7 and MDA-MB-231 cells are the classic cell lines of two clinical breast tumor subtypes. Their regulation depends on their interaction with surrounding cells present in the tumor microenvironment. The interaction can affect cancer progression and thus influences patient prognosis and survival. Although ADMSCs represent the most prominent cell type in the breast tumor microenvironment, very little attention has been given to the ADMSCs population. Interestingly, growing research interest was noted in exploiting ADMSCs in the cancer biology field due to their dual role as cancer promoters and suppressors (Chen et al., 2019; Reza et al., 2016).

Breast cancer cells are likely to disseminate during cancer progression and interact with ADMSCs in TME, releasing molecular signals contributing to the emergence of a subpopulation of cells that may go into the dormancy stage. The cell's subpopulation can avoid chemotherapy treatment and reawaken in response to signals and transform into the aggressive phenotype, resulting in recurrence and metastasis. The risk of developing distant metastasis may vary over time across different subgroups of breast cancer cells.

Several types of *in-vitro* co-culture models have been developed to study the interaction between cancer cells and microenvironment components such as extracellular matrix (ECM), fibroblast and MSCs. These components have demonstrated the importance of the microenvironment in governing cancer cell growth (Bartosh et al., 2016; Koh et al., 2019; Hwang et al., 2019). The most common interaction models to elucidate the interaction between two distinct cells include direct co-culture (Koh et al., 2019) and indirect co-culture.

The indirect method employs culture insert separating cells in space but sharing similar culture conditions, similar to our study (Bliss et al., 2016). There are also previous studies that have been carried out using conditioned mediums from MSCs and were incubated with cancer cells (Farahmand et al., 2018; Wang et al., 2019). However, this method lacks feedback-loop-dependent signaling or bi-directional cross-talk. There is also a 3D co-culture model established to recapitulate the complexity of interaction between breast cancer and bone marrow MSCs where it promotes dormancy (Marlow et al., 2013; Bartosh et al., 2016).

Even though *in vivo* animal is a better model in representing the complexity and significance of the interaction between the cells, *in vitro* model is still required for preliminary study. Very few models have been developed concentrating on cellular dormancy and metastasis property (Ono et al., 2014; Bliss et al., 2016). Despite those remarkable findings, the complex interaction

of ADMSCs on metastasis and dormancy of breast cancer subtypes remain unanswered.

In this study, an indirect co-culture transwell system was used to simulate and investigate non-contact interaction between ADMSCs and breast cancer subtypes affecting cancer progression and metastasis. The findings demonstrated that when both breast cancer subtypes interact with ADMSCs indirectly, a reduction in cell proliferation, drastic change in MDA-MB-231 cells' cell morphology, and induction of cell cycle arrest was noted.

Tumor dormancy was reported to occur when cancer cells exit the cell cycle, survive in a quiescence state and cease to divide under an unfavorable microenvironment (Yuan et al., 2018). This implies that ADMSCs promote dormancy of breast cancer by suppressing cancer proliferation mediated by cell cycle arrest. The present findings were consistent with that reported by Yuan et al. (2018) where umbilical cord MSCs successfully prevented lung cancer cycle regulation, decreased cellular activity and increased the dormant population.

5.2 Indirect Co-culture Promotes Chemoresistance in Breast Cancer Cells

The decrease in metabolic and cellular activities of dormant cells can be further linked to the increase in drug resistance against doxorubicin, tamoxifen, cisplatin and 5HNQ. This could be due to the design of drugs that target the rapidly proliferating cells, resulting in less effective chemotherapy drugs in eliminating resting dormant cells (Yadav et al., 2018). Besides, it was found that the ADMSCs served as the guardians for the breast cancer cells, thus protecting them from chemotherapy effects.

It was previously described that CD44+/CD24− breast cancer stem cells (CSCs) have a slow proliferating population, tumorigenicity and higher resistance to drugs (Boo et al., 2017). However, the associated features of dormancy do not indicate CSCs in the co-culture of breast cancer with ADMSCs. It was confirmed by aldehyde dehydrogenase-1 (ALDH1) gene expression, a functional regulator of CSCs and the surface marker expression CD44+/CD24− of the cells population. Both characteristic markers of breast CSCs significantly decreased in co-culture of MDA-MB-231 cells that acquired dormant phenotypes.

Additionally, the proliferative activity of both co-culture subtypes (MCF7 and MDA-MB-231) was restored when the cells were placed in the non-inhibitory culture environment without the presence of ADMSCs (Appendix E). The results supported the concept of dormancy, where cells can

re-entering cell regulation when conditions become favorable (Ono et al., 2014).

3D sphere formation assay was used to enrich and select the slow proliferating cells that include both CSCs and dormant cells and evaluate their ability to grow from single cells into colonies in a favorable environment. Indeed, cells cultured in a 3D model system more closely mimick the *in vivo* conditions and address most of the factors that can impact cancer dormancy, such as cell-to-cell and cell-to-microenvironment interactions, tissue architecture, proteomic and metabolomics profiles and oxygen levels. When subjected to the 3D sphere enrichment model, co-cultured MDA-MB-231 cells displayed higher sphere forming ability than MCF7. The MCF7 cells maintained their slow-proliferation and epithelial characteristic in contrast to MDA-MB-231 cells that could exit dormancy and restore their mesenchymal appearances once removed from the inhibitory niche.

It was also noted that co-cultured MDA-MB-231 cells were able to form spheres much more quickly after reverting to their proliferating state. On the contrary, MCF7 had a lower sphere formation capability than its parental counterpart after exiting the resting stage. This explains the higher recurrence and the lowest survival rate of MDA-MB-231 basal subtype in the first five years of treatment in contrast to lower recurrence and higher survival period (>10 years) in MCF7-luminal patients (Ignatov et al., 2018). This confirms that ADMSCs serves as an inhibitory niche for breast cancer, resulting in a temporary cell-cycle arrest. At the same time, the upregulation of drug

resistance gene (*ABCG2)*, DNA repair gene (*PARP1)* and regulator Cyclin D2 *(CCND2)* indicates the resistance to apoptosis leading to cell survival. It is supported by the previous finding which suggested the association between drug resistance and dormancy that represent an inhibitory phenotype of breast cancer (Yuan et al., 2018).

5.3 Exosomes Mediate the Transfer of microRNAs During Intercellular Communication Between ADMSCs and Breast Cancer Cells

Mechanisms by which ADMSCs inhibit breast cancer proliferation through the transfer of exosomes carrying miRNAs from ADMSCs to breast cancer were elucidated in this study. Changes in microenvironment following co-culture translate into rearrangements in the miRNA cargo within exosomes. MicroRNAs which can be found in cells and exosomes was shown to act as signaling molecules that control entire gene networks and were commonly expressed in a cell-type-specific and cancer subtype-specific manner (Shi et al., 2017).

With the aid of fluorescence tracking dyes, we discovered that throughout co-culture interaction, cells communicate via the transfer of exosomes in a direction from ADMSCs to breast cancer cells creating a feedback loop. The transmission direction depends on the cell-specific interaction and the signal released by the cells (Dioufa et al., 2017).

Findings from this study further revealed that cell-to-cell interaction is the key to communication between ADMSCs and breast cancer that inhibited cancer progression and facilitated dormancy acquisition. When cancer cells were subjected to non-co-culture exosomes isolated from ADMSCs, a less inhibitory effect was observed relative to co-culture-derived exosomes. It should be noted that the findings could also be due to other factors beyond exosomes.

The inhibition effect of co-cultured exosomes on proliferation, metastasis, invasion and wound healing property closely resembles the inhibitory activity of exosomes from indirect transwell culture compared to non-co-cultured exosomes. This event indicates that inhibition effects on breast cancer are majorly attributed to the soluble factors released during the interaction between those two cells types in the same microenvironment. The soluble factors that are readily excreted by ADMSCs without interaction with cancer cells are also contributing to the inhibitory effect but at a lesser degree. This confirms that interaction with surrounding cells in TME is important for tumor progression and metastasis.

Interpretation of the miRNAs heat map profiles showed an interaction between ADMSCs and breast cancer resulted in different clusters of miRNAs being exported, transported and received by recipient cells compared to miRNAs-derived exosomes from ADMSCs alone which may cause the disparity in cancer suppression level and dormancy effects among these cells (Fig 5A).

Results from this study were consistent with that reported previously for a related research on the implication of miRNAs from ADMSCs derived exosomes which showed induction of cycling dormancy and early BCC quiescent in the bone marrow that gives rise to drug resistance. Nevertheless, the distinction in breast cancer subtypes was not emphasized (Bliss et al., 2016).

The latest technique of transcriptomic study using the Next Generation Sequencing (NGS) has shown the differences in miRNAs and gene expression profiles between the subtypes which explained the stronger invasiveness of the MDA-MB-231 cell line compared to MCF-7 cells (Shi et al., 2017). Using a similar platform, miRNAs expression of indirect co-culture exosomes and cells were profiled in this study to investigate the effects of miRNAs specific subtypes signaling mechanism on cancer proliferation and dormancy.

Sequencing results revealed a distinct proportion of small RNA population in exosomes and cells, while miRNAs were found to be one of the main RNA populations involved in a cell-to-cell transfer. Furthermore, global microRNA expression profiles exhibited differential and subtype-specific microRNA expression profiles upon co-culture.

5.4 Exosomal microRNAs Regulate Mesenchymal-to-Epithelial Transition and Inhibit Breast Cancer Progression

The fundamental step in cancer metastasis involves EMT transition, where MSCs have been reported to affect the transition in the invasive and metastatic types of cancers (Scioli et al., 2019). A mesenchymal phenotype is characterized by its increased motility, metastatic expansion and all the essential adaptations required in facilitating circulatory survival. Conversely, MET is the reverse of EMT where cells acquire epithelial features and lose mesenchymal characteristics, including spindle-shaped and flattened phenotypes. The transition was known to impact cells in a metastatic niche to develop secondary tumors and has been associated with the acquisition of chemoresistance and recurrence (Roche, 2018).

Both breast cancer subtypes MCF7 and MDA-MB-231 are of epithelial origin. MCF7 cells express the epithelial phenotype in contrast to MDA-MB-231 cells that are more mesenchymal (Gjerdrum et al., 2010). MDA-MB-231 cells acquire fibroblast-like properties and exhibit reduced cell-cell adhesion and increased motility via EMT.

During co-culture, ADMSCs induce MET in MDA-MB-231 and establish maintenance of epithelial in MCF7. MET is a type of plasticity characterized by long-lasting morphological and molecular changes in mesenchymal cells due to transdifferentiation towards an epithelial cell type. The stabilization of either an epithelial or mesenchymal phenotype depends on

interaction and signaling factors released by ADMSCs during co-culture. The MET transition in breast cancer cells was consistent with the morphologic changes following co-culture with ADMSCs. Furthermore, data from this study revealed that dysregulation of miRNAs subset following co-culture affects not only the growth of breast cancer but also metastasis events by inhibiting EMT regulation.

As part of MET, dysregulation of miRNA maintained the epithelial phenotype by blocking mesenchymal transcriptional regulators, specifically *ZEB-2, Vimentin, SMAD4* and *SNAI1*. The substantial miRNAs that have been dysregulated in co-culture MCF7 includes tumor suppressor miRNAs (miR-200 family, miR-941, miR-629-5p, miR-7, and miR-185-5p) and oncomiRs (miR-155-5p, miR-224-5p, miR-486-5p and miR-10b) (Table 3).

Meanwhile, in co-culture MDA-MB-231 cells, tumor suppressor miRNAs (miR-146a-5p, miR-941, miR-629-5p) and oncomiRs (miR-10b and miR-486-5p) were dysregulated. This resulted in the repression of *Vimentin* and *SMAD4* of mesenchymal transcription factor and substantial augmentation of *OCLN* and *E-cadherin* of epithelial transcriptional regulators. Increased expression of tumor suppressor miRNAs and reduced expression of oncogenic miRNAs in co-culture cells prevented cancer progression by miRNAs' participation in a complex regulatory network which affected the epithelial acquisition. An increase in epithelial gene expression and reduction in mesenchymal gene expression has led to a mesenchymal transition to epithelial

in MDA-MB-231 cells and maintenance of epithelial characteristics in MCF7 co-cultured cells.

Among the cluster of dysregulated miRNAs in co-culture MCF7 cells, miR-200 family has been identified as the master key where it has been linked to chemoresistance, tumor metastasis and dormancy by targeting the signaling pathways including Wnt and transforming growth factor β (TGF-β), thus impeding metastasis, cell adhesion and epithelial-to-mesenchymal transition (EMT). As an EMT inhibitor, miR-200 targets *ZEB2* transcription factors controlled the expression of gene clusters, including *E-cadherin* and *Vimentin* (Chen and Zhang, 2017).

Likewise, the downregulation of oncomiR-155 contributed to the increase in chemoresistance through TGF-β-induced MET and MAPK signaling pathways (Yu et al., 2015). Also, it has been reported that upregulation of miR-7 and miR-185 contributed to a similar outcome where miR-7 was negatively connected with Vimentin expression levels in breast carcinoma tissues by inhibiting EMT via focal adhesion pathway (Cui et al., 2017; Shi et al., 2017; Yin et al., 2018).

Meanwhile, in MDA-MB-231, selective enrichment of miR-146a-5p was found in co-culture exosomes and cells, suggesting a possible involvement of miR-146a in pathogenesis and recurrence. The miR-146a-5p implicates toll-like receptors and chemokines signaling pathways that prompt the entry of cells into dormancy. The present result was in agreement with that reported in

the previous study where miR-146a-mediated downregulation of *SMAD4* target gene could inhibit proliferation, migration, invasion and EMT in TNBC via TGF-β and Notch pathways (Si et al., 2018).

Another study has found that serum miR-146a level was correlated with drug resistance and higher recurrence, while their expression was classified as subtype-specific in breast cancer (Iacona and Lutz, 2019). Therefore, a therapeutic approach targeting miR146a could be a promising treatment for high recurrence and poor prognosis in MDA-MB-231 cells. The output from cluster analysis of microRNA expression in breast cancer subtypes in this study showed a complete separation of luminal and basal into two separate groups.

Apart from the uniquely expressed miRNAs present in both cells, five other miRNAs were detected as mutually dysregulated in MCF7-luminal and MDA-MB-231-basal cancer cells. The expression of oncomiR miR-10b-5p and miR-486-5p was downregulated and tumor suppressors such as miR-941, miR-200a-5p and miR-629-5p were upregulated accordingly. High expression of miR-629-5p has been linked to drug resistance and inhibition of metastasis and cancer growth, but none was related to the EMT regulation (Yan et al., 2019).

Meanwhile, the expression of miR-486-5p which is a cancer type-specific, acts as a tumor suppressor in lung cancer and oncomiR in colorectal cancer (Loh et al., 2019). It was found in this study that miR-486-5p expression was downregulated in both subtypes and can be classified as oncomiR. miR-486-5p were predicted to target tumor suppressor genes such as *MAP3K7* and

NFAT5. Recently, it was reported that miR-486-5p inhibited EMT by down-regulating *SMAD2* and EMT regulators, *Vimentin* and *E-cadherin* in breast cancer (ElKhouly et al., 2020). Reduced *E-cadherin* expression was attributed to increased miR-10b expression leading to the mesenchymal acquisition and vice versa (Sheedy and Medarova, 2018).

As discussed earlier, miR-200a-5p that belongs to the miR-200 family can suppress EMT. Also, Yu et al. (2018) demonstrated that miR-200a promoted chemoresistance by inhibiting DNA damage-induced apoptosis in breast cancer (Yu et al., 2018). In another study, overexpression of miR-941 was shown to cause substantial inhibition of metastasis in hepatoma and gastric cancers (Kim et al., 2014; Zhang et al., 2014b). To date, the effect of miRNAs on breast cancer cells, particularly in EMT regulation has not been reported despite miRNAs' ability to suppress tumor growth.

Interestingly, both subtypes shared 7 out of 10 of the most enriched KEGG pathways despite having only five mutually dysregulated miRNAs. This implies that although different clusters of miRNAs were uniquely expressed in the co-culture of MCF7 and MDA-MB-231, the enriched gene sets led to similarly associated pathways related to MET and tumor dormancy pathways. The group of dysregulated miRNAs controlled cell dormancy by inhibiting mitogen-activated protein kinase (MAPK), TGF-β and Wnt signaling pathways, followed by the initiation of MET transcriptional regulation, epithelial phenotype stabilization and cellular proliferation and metastasis

repression which may lead to chemoresistance and relapse in treatment (Li et al., 2013; Yuan et al., 2018; Prunier et al., 2019).

Other signaling pathways that can indirectly contribute to the aforementioned effects include ErbB, a pathway in cancer and neurotrophin signaling, which plays a crucial role in the initiation and progression of many cancers (Appert-Collin et al., 2015; Triaca et al., 2019). Axon guidance, focal adhesion and insulin signaling pathways were reported to affect multiple cell types connected through the tumor microenvironment and act as the major mediator of signal transduction in the metastasis and promotion of tumors (Luo and Guan, 2010; Wang et al., 2016; Hopkins et al., 2020).

Subsequent activation of Toll-like-receptors (TLRs) in cancer cells and the resulting signaling cascade effect along with chemokine production could play an important role in promoting cancer cell survival and chemoresistance (Huang et al., 2005). Besides, the participation of B and T cell receptors in the regulation of immune cells-mediated metastatic dormancy with the direct involvement of the immune system in protecting cancer cells was reported by (Romero et al., 2014).

Overall, the present study has successfully identified exosomal miRNAs signatures from the interaction of ADMSCs that can differentiate between MCF7 and MDA-MB-231 subtypes. A portion of those signatures miRNAs has been identified as EMT regulators, which regulate cancer progression, metastasis activity and chemoresistance, as illustrated in Figure

5.1. Although most of the miRNAs listed in Table 5.1 have been widely shown to be involved in cellular communication between MSC and cancer cells via exosomes, little attention has been focused on miR-941. Despite miR-941 involvement in mediating EMT regulation, DNA methylation and histone phosphorylation in cancer, it has not been specifically associated with MSC and cancer interaction (Kim et al., 2014; Zhang et al., 2014b; Surapaneni et al., 2020). In this study, miR-941 has been successfully identified in exosomes secreted by ADMSCs and taken up by both breast cancer subtypes during co-culture interaction.

Table 5.1. Comparison of the functional miRNAs identified in cross-talk between MSCs and cancer cells. The table summarized miRNAs signatures identified in this study *vs*. data from other findings from various sources of MSCs and cancer types. The listed miRNAs' signatures have been assessed to modulate EMT regulation and cancer progression (N/A=Not available).

MicroRNA Identified in following co-culture ADMSCs and Breast Cancer Subtype		**Role of miRNA**	**Co-culture cells from other published data**	**Associated Events**	**Reference**
miRNA	**BC Subtypes**				
miR-200 a,b,c	MCF7	Tumor suppressor	Adipose MSC with Breast cancer MCF7	Overexpression inhibits metastasis and EMT transition	(Xu et al., 2012)
miR-155-5p	MCF7	OncomiR	Adipose MSC with Prostate cancer	Low expression promotes drug resistance and EMT transition	(Abd Elmageed et al., 2014)
miR-7	MCF7	Tumor suppressor	MSC with Hepatocellular carcinoma	Overexpression inhibits metastasis and proliferation	(Shang et al., 2019)
miR-185-5p	MCF7	Tumor suppressor	MSC with Oral cancer	Overexpression inhibits cancer proliferation, angiogenesis and induce apoptosis	(Wang et al., 2019)
miR-146a-5p	MDA-MB-231	Tumor suppressor	Human umbilical cord MSC with Ovarian cancer	Overexpression increase sensitivity to chemotherapy, inhibit cancer growth	(Qiu et al., 2020)
miR-941	Both	Tumor suppressor	N/A	Overexpression inhibits cancer proliferation and metastasis	N/A
miR-629-5p	Both	Tumor suppressor	Adipose MSC with Hepatocellular carcinoma	Overexpression impede cancer migration and modulate EMT regulation	(Zhang et al., 2018b)
miR-10b	Both	Oncomir	Adipose MSC with Breast cancer	Overexpression promotes cell invasion and metastasis	(Singh et al., 2014)
miR-486-5p	Both	Dual role	Bone Marrow MSC with Prostate cancer	Drug resistance	(ElKhouly et al., 2020; Qiu et al., 2018)

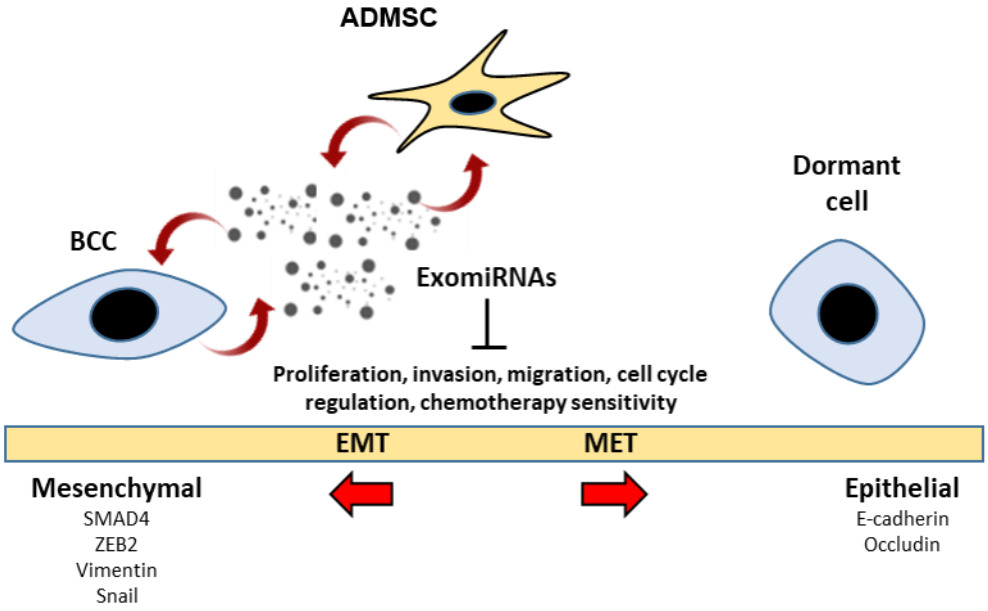

Figure 5.1. Schematic diagram of breast cancer cells interact with ADMSCs in the microenvironment. The interaction leading the cells to maintain/acquire epithelial characteristics and become dormant cells. During the reversible process, a consensus of exosomal miRNAs is postulated to acts as a switch to modulate signaling pathways responsible for the cells' transition to MET state that allow cells to enter dormancy.

The limitations of cell lines in breast cancer research are well-documented including the fact that immortalized cells may acquire genetic variances during the unlimited passaging compared to patient-derived tissues (Van Staveren et al., 2009). However, the use of cell lines is important as an in vitro model. It emerges as a feasible alternative to overcome sample size limitations and clearance consent from patients. In addition, the collection of tumor tissue of adequate quality for analysis is difficult to source, particularly the metastatic breast cancer tissue, as patients who develop the symptoms usually are already at stage IV. Besides, establishing the procedures and facility for tissue collection is challenging to implement; still, it is required to ensure the collection of sufficient high-quality samples as assurance for the success of downstream molecular analysis (Gelao et al., 2013).

Following advancements in cancer diagnostic using approaches such as transcriptome sequencing analysis of biomarkers, breast cancer can be detected before pathological symptoms develop. The use of more than single breast cancer-related marker can enhance the sensitivity and specificity of cancer detection for early diagnosis. This information can greatly contribute to the personalized clinical approaches in which specific treatment regimens can be designed based on the clinical history and stage of cancer identified from profiles of markers discovered in cell lines (Verma, 2012).

Furthermore, the involvement of exosomes as biomarker carriers has significantly contribute to the advancement of breast cancer diagnostic and management (Ono et al., 2014; Dioufa et al., 2017; Wang et al., 2019).

Transition into the clinical phase requires the isolation of circulating exosomes from bodily fluids and serum, and their miRNA content has been shown to reflect their breast cancer cells' origin (Bliss et al., 2016). Therefore, it is reasonable to rationalize the use of cell lines to assess the progression of breast cancer and crucially contribute to clinical predictive values.

Amongst the mutually dysregulated miRNAs that are critically involved in the associated pathways of MET and dormancy, miR-941 was selected as molecular markers to represent both cancer subtypes for further investigation. In the current study, the downstream effects of miR-941 overexpression in MCF7 and MDA-MB-231 cells were proven based on three pathways: inhibition of proliferation; inhibition of migration, invasion and wound healing; and promotion of MET.

In agreement with findings from this study, miR-941 was shown to act as a tumor suppressor by suppressing cancer growth and migration of gastric and hepatoma cells via direct target of EMT inducers *SNAIL1*, *ZEB1* and *ZEB2* and promotes *E-cadherin* expression in the cancer cells (Kim et al., 2014; Zhang et al., 2014b). It was confirmed that the expression of mesenchymal regulators was suppressed and epithelial regulators were augmented using the qPCR technique.

Association of miR-941 with cell proliferation and other biological processes through regulation of components involved in dormancy such as MAPK, TGF-β and Wnt signaling pathways was identified through

bioinformatics analysis. However, the direct relationship between miR-941 and the dormancy was not confirmed. From the findings, exosomal transfer of miR-941 and its suppression of mesenchymal characteristics was proposed as one of the principal mechanisms contributing to inhibiting cell proliferation and metastasis of luminal and basal breast cancer subtypes.

The unique miRNAs signatures between subtypes may allow researchers and clinicians to select the best regimen for breast cancer treatment, particularly for metastatic chemoresistant cells like TNBC. From there, researchers can develop miRNAs-based therapeutic strategies through miRNA replacement therapy using miRNA mimics or anti-miRNA therapy to target tumor suppressor miRNAs or oncomiRs (Nygren et al., 2014; Shu et al., 2015). Furthermore, the easy accessibility of circulating miRNAs may help in clinical settings as biomarkers for early diagnosis of cancer relapse and prognosis of treatment outcome. To sum up, miRNAs therapy can assist in addressing the alarming rate of cancer relapse and mortality linked with breast cancer cells.

5.5 Conclusion

In conclusion, the findings revealed the role of the miR-200 family, miR-146a-5p and miR-941 as molecular mediators of MCF7-luminal, MDA-basal subtypes and both subtypes, respectively. Owing to the complexity of exosomes contents, other small RNAs populations such as tRNAs, unknown small RNAs, proteins and DNA, which are not highlighted in this study may also contribute to the ability of BCCs to induce MET, dormancy and chemoresistance. This, however, requires further research.

To date, this is the first inclusive microRNA expression profiling study of MCF7-luminal versus MDA-MB-231-basal BCCs interaction with ADMSCs involving exosomes. This research delivers further understanding and framework for future clinical studies focusing on differential regulation of microRNA expression in breast cancer patients. It may help in the differentiation of breast cancer subtypes, lineages and malignant transformation.

Inhibition of breast cancer cell progression resulted from intercellular communication between ADMSCs and breast cancer cells has been reported many times describing the changes in breast cancer metastatic properties and phenotypes (Schweizer et al., 2015; Kucerova et al., 2013). However, this is the first study highlighting the miRNAs-dormancy markers that are unique and shared by both breast cancer subtypes, MCF7 and MDA-MB-231. Although

the question of when the dormant population of breast cancer transforms into an aggressive phenotype or stays permanently quiescent remains uncertain.

The influence of co-culture-derived exosomes and their corresponding miRNAs shows qualitative changes in breast cancer associated with a dormant-epithelial phenotype and low rates of metastasis contributing to high chemoresistance. Therefore, corresponding exosomal miRNAs are suitable miRNA biomarkers candidates for managing breast cancer metastasis and relapse.

Understanding the complex interaction of breast cancer cells and their microenvironment, their control by multifunctional miRNAs and the potential involvement of miRNAs contributes to the biological significance of cell-cell interaction between ADMSCs and breast cancer MCF7 and MDA-MB-231 cells. The study mimic the *in vivo* biological, spatial, biochemical, and biophysical features of tumor tissues. At the same time, it highlights the miRNAs and pathways involved in tumor dormancy and chemoresistance and the role of ADMSCs in paving the way for novel anti-cancer therapies. The development of miRNA-based treatment strategies specifically preventing recurrence and targeting the chemoresistant is an attractive therapeutic target for clinical application.

CHAPTER 6

LIMITATION AND FUTURE DIRECTION

There has been growing evidence *in vitro* and *in vivo* unfolding the potential role of ADMSCs as therapy for numerous diseases, particularly for cancer treatment. With their ability to be recruited to the tumor microenvironment, differentiate into various cell types and multiple effects in regulating EMT transcription factors leading to inhibition of breast cancer metastasis and induction of dormancy, ADMSC-based therapies have brought new hope to cancer patients by offering more targeted anti-cancer treatments.

As a model of breast cancer study, it is worthy to study the interaction of ADMSCs with breast cancer of different subtypes MCF7 and MDA-MB-231 and to elucidate the functional role of exosomes in transporting consensus of miRNAs. Furthermore, the study showed the effect of particular miRNAs signaling on metastatic and dormancy of breast cancer and the discovery of miRNAs biomarkers for breast cancer diagnosis and early intervention of relapse.

Despite its ability to mimic the interaction between ADMSCs and breast cancer in the tumor microenvironment, this classical two-dimensional (2D) co-culture has its limitations. The cell-extracellular environment interactions and architecture are not fully represented as they would be in the

tumor mass. For future study, an alternative cells interaction platform, a three-dimensional (3D) culture system, is an excellent model to better represent *in vivo*. Having said that, even a 3D system has its disadvantages. It is a complex system that restricts the number of cell populations used and requires a thorough experimental technique and analysis. Since it is still relatively new, researchers have difficulty standardizing and generating replicable and comparable results across a wide range of techniques.

Understanding the interaction between ADMSCs and breast cancer cells has shed light on the application of ADMSCs-derived exosomes as the clinical approach in cancer diagnosis and improving the clinical safety of MSC-based therapeutic approaches. Yet, there is still a great challenge to translate *in vitro* and *in vivo* studies to clinical. For future studies, the results need to be transferred to *in vivo* models to enlighten the interactions of breast cancer cells and ADMSCs in a systemic environment. Although countless fundamental researches have been conducted, more preclinical and clinical evidence is needed to determine their efficacy, safety, and impact on cancer progression.

LIST OF REFERENCES

Azizah, A.M., Nor Saleha, I.T., Noor Hashimah, A., Asmah, Z.A. and Mastulu, W., 2016. Malaysian national cancer registry report 2007-2011. *Malaysia cancer statistics, data and figure. Putrajaya: National Cancer Institute, Ministry of Health.*

Abd Elmageed, Z. Y., et al., 2014. Neoplastic reprogramming of patient-derived adipose stem cells by prostate cancer cell-associated exosomes. *Stem Cells,* 32(4), pp.983-997.

Ahmad, A., 2013. Pathways to breast cancer recurrence. *International Scholarly Research Notices,* 2013.

Al-Ejeh, F., et al., 2011. Breast cancer stem cells: treatment resistance and therapeutic opportunities. *Carcinogenesis,* 32(5), pp.650-658.

Al-Nbaheen, M., et al., 2013. Human stromal (mesenchymal) stem cells from bone marrow, adipose tissue and skin exhibit differences in molecular phenotype and differentiation potential. *Stem Cell Reviews and Reports,* 9(1), pp.32-43.

Al-Thoubaity, F. K., 2020. Molecular classification of breast cancer: A retrospective cohort study. *Annals of Medicine and Surgery,* 49(44-48.

Allahverdi, A., et al., 2020. MicroRNA-4731-5p delivered by AD-mesenchymal stem cells induces cell cycle arrest and apoptosis in glioblastoma. *Journal of cellular physiology,* 235(11), pp.8167-8175.

Appert-Collin, A., Hubert, P., Cremel, G. & Bennasroune, A., 2015. Role of ErbB receptors in cancer cell migration and invasion. *Frontiers in pharmacology,* 6, p.283.

Babicki, S., et al., 2016. Heatmapper: web-enabled heat mapping for all. *Nucleic acids research,* 44(W1), pp.W147-W153.

Baghban, R., et al., 2020. Tumor microenvironment complexity and therapeutic implications at a glance. *Cell Communication and Signaling,* 18(1), pp.1-19.

Bartosh, T. J., Ullah, M., Zeitouni, S., Beaver, J. & Prockop, D. J., 2016. Cancer cells enter dormancy after cannibalizing mesenchymal stem/stromal cells (MSCs). *Proceedings of the National Academy of Sciences,* 113(42), pp.E6447-E6456.

Belkacemi, Y., Hanna, N. E., Besnard, C., Majdoul, S. & Gligorov, J., 2018. Local and regional breast cancer recurrences: Salvage therapy options in the new era of molecular subtypes. *Frontiers in oncology*, 8, p.112.

Blenkiron, C., et al., 2007. MicroRNA expression profiling of human breast cancer identifies new markers of tumor subtype. *Genome biology*, 8(10), pp.1-16.

Bliss, S. A., et al., 2016. Mesenchymal Stem Cell-Derived Exosomes Stimulate Cycling Quiescence and Early Breast Cancer Dormancy in Bone Marrow. *Cancer research*, 76(19), pp.5832-5844.

Bogdanowicz, D. R. & Lu, H. H., 2013. Studying cell-cell communication in co-culture. *Biotechnology journal*, 8(4), pp. 395-396.

Boo, L., et al., 2017. Phenotypic and microRNA transcriptomic profiling of the MDA-MB-231 spheroid-enriched CSCs with comparison of MCF-7 microRNA profiling dataset. *PeerJ*, 5, p.e3551.

Brabletz, T., Kalluri, R., Nieto, M. A. & Weinberg, R. A., 2018. EMT in cancer. *Nature Reviews Cancer*, 18(2), pp. 128-134.

Bray, F., et al., 2018. Global cancer statistics 2018: GLOBOCAN estimates of incidence and mortality worldwide for 36 cancers in 185 countries. *CA: a cancer journal for clinicians*, 68(6), pp.394-424.

Caddeo, S., Boffito, M. and Sartori, S., 2017. Tissue engineering approaches in the design of healthy and pathological in vitro tissue models. *Frontiers in bioengineering and biotechnology*, 5, p.40.

Cardoso, F. and Castiglione, M., 2009. Locally recurrent or metastatic breast cancer: ESMO clinical recommendations for diagnosis, treatment and follow-up. *Annals of Oncology*, 20, pp.iv15-iv18.

Casson, J., Davies, O.G., Smith, C.A., Dalby, M.J. and Berry, C.C., 2018. Mesenchymal stem cell-derived extracellular vesicles may promote breast cancer cell dormancy. *Journal of tissue engineering*, 9, p.2041731418810093.

Chan, C.W., Law, B.M., So, W.K., Chow, K.M. and Waye, M.M., 2017. Novel strategies on personalized medicine for breast cancer treatment: an update. *International journal of molecular sciences*, 18(11), p.2423.

Chen, Y., He, Y., Wang, X., Lu, F. and Gao, J., 2019. Adipose-derived mesenchymal stem cells exhibit tumor tropism and promote tumorsphere formation of breast cancer cells. *Oncology reports*, 41(4), pp.2126-2136.

Chen, Y. and Zhang, L., 2017. Members of the microRNA-200 family are promising therapeutic targets in cancer. *Experimental and therapeutic medicine,* 14(1), pp.10-17.

Cocce, V., et al., 2017. Fluorescent Immortalized Human Adipose Derived Stromal Cells (hASCs-TS/GFP+) for Studying Cell Drug Delivery Mediated by Microvesicles. *Anti-Cancer Agents in Medicinal Chemistry (Formerly Current Medicinal Chemistry-Anti-Cancer Agents),* 17(11), pp.1578-1585.

Cui, Y. X., et al., 2017. MicroRNA-7 suppresses the homing and migration potential of human endothelial cells to highly metastatic human breast cancer cells. *British journal of cancer,* 117(1), pp.89-101.

Curtis, C., et al., 2012. The genomic and transcriptomic architecture of 2,000 breast tumours reveals novel subgroups. *Nature,* 486(7403), pp.346-352.

De Abreu, F. B., Wells, W. A. & Tsongalis, G. J., 2013. The emerging role of the molecular diagnostics laboratory in breast cancer personalized medicine. *The American journal of pathology,* 183(4), pp.1075-1083.

Degirmenci, U., Wang, M. & Hu, J. J., 2020. Targeting aberrant RAS/RAF/MEK/ERK signaling for cancer therapy. *Cells,* 9(1), p.198.

Detassis, S., Grasso, M., Del Vescovo, V. & Denti, M. A,. 2017. microRNAs make the call in cancer personalized medicine. *Frontiers in cell and developmental biology,* 5,p.86.

Ding, M., et al., 2018. Comparison of commercial exosome isolation kits for circulating exosomal microRNA profiling. *Analytical and bioanalytical chemistry,* 410(16), pp.3805-3814.

Ding, X. M. 2014. MicroRNAs: regulators of cancer metastasis and epithelial-mesenchymal transition (EMT). *Chinese journal of cancer,* 33(3), pp.140-147.

Dioufa, N., Clark, A. M., Ma, B., Beckwitt, C. H. & Wells, A., 2017. Bi-directional exosome-driven intercommunication between the hepatic niche and cancer cells. *Molecular cancer,* 16(1), pp.1-14.

Duroux-Richard, I., et al., 2014. Circulating miRNA-125b is a potential biomarker predicting response to rituximab in rheumatoid arthritis. *Mediators of inflammation,* 2014.

Elder, E., et al., 2006. Patterns of breast cancer relapse. *European Journal of Surgical Oncology (EJSO),* 32(9), pp.922-927.

ElKhouly, A. M., Youness, R. A. & Gad, M. Z., 2020. MicroRNA-486-5p and microRNA-486-3p: Multifaceted pleiotropic mediators in oncological and non-oncological conditions. *Non-coding RNA research,* 5(1), pp.11-21.

Farahmand, L., Esmaeili, R., Eini, L. & Majidzadeh, A. K., 2018. The effect of mesenchymal stem cell-conditioned medium on proliferation and apoptosis of breast cancer cell line. *Journal of cancer research and therapeutics,* 14(2), pp.341-344.

Figueroa-Magalhães, M. C., Jelovac, D., Connolly, R. M. & Wolff, A. C., 2014. Treatment of HER2-positive breast cancer. *The breast,* 23(2), pp.128-136.

Fischer, K. R., et al., 2015. Epithelial-to-mesenchymal transition is not required for lung metastasis but contributes to chemoresistance. *Nature,* 527(7579), pp.472-476.

Fletcher, J. I., Haber, M., Henderson, M. J. & Norris, M. D., 2010. ABC transporters in cancer: more than just drug efflux pumps. *Nature Reviews Cancer,* 10(2), pp.147-156.

Fouad, Y. A. & Aanei, C., 2017. Revisiting the hallmarks of cancer. *American journal of cancer research,* 7(5), pp.1016-1036.

Friedländer, M. R., Mackowiak, S. D., Li, N., Chen, W. & Rajewsky, N., 2011. miRDeep2 accurately identifies known and hundreds of novel microRNA genes in seven animal clades. *Nucleic acids research,* 40(1), pp.37-52.

Gal, A., et al., 2008. Sustained TGFβ exposure suppresses Smad and non-Smad signalling in mammary epithelial cells, leading to EMT and inhibition of growth arrest and apoptosis. *Oncogene,* 27(9), pp.1218-1230.

Gao, J. & Liu, Q.G., 2011. The role of miR-26 in tumors and normal tissues. *Oncology letters,* 2(6), pp.1019-1023.

Gelao, L., et al., 2013. Tumour dormancy and clinical implications in breast cancer. *Ecancermedicalscience,* 7.

Gjerdrum, C., et al., 2010. Axl is an essential epithelial-to-mesenchymal transition-induced regulator of breast cancer metastasis and patient survival. *Proceedings of the National Academy of Sciences,* 107(3), pp.1124-1129.

Godet, I., Gilkes, D. M., 2017. BRCA1 and BRCA2 mutations and treatment strategies for breast cancer. *Integrative cancer science and therapeutics,* 4(1).

Goers, L., Freemont, P. & Polizzi, K. M., 2014. Co-culture systems and technologies: taking synthetic biology to the next level. *Journal of The Royal Society, Interface,* 11(96), pp.20140065.

Goldhirsch, A., et al., 2011. Strategies for subtypes--dealing with the diversity of breast cancer: highlights of the St. Gallen International Expert Consensus on the Primary Therapy of Early Breast Cancer 2011. *Annals of oncology,* 22(8), pp.1736-1747.

Gordon, A. & Hannon, G. J., 2010. Fastx-toolkit. *FASTQ/A short-reads preprocessing tools (unpublished) http://hannonlab. cshl. edu/fastx_toolkit,* 5.

Graveel, C. R., Calderone, H. M., Westerhuis, J. J., Winn, M. E. & Sempere, L. F., 2015. Critical analysis of the potential for microRNA biomarkers in breast cancer management. *Breast cancer: targets and therapy,* 7, pp.59-79.

Grønbaek, K., Hother, C. & Jones, P. A., 2007. Epigenetic changes in cancer. *Apmis,* 115(10), pp.1039-1059.

Guay, C. & Regazzi, R., 2013. Circulating microRNAs as novel biomarkers for diabetes mellitus. *Nature Reviews Endocrinology,* 9(9), pp.513-521.

Harburg, G. C. & Hinck, L., 2011. Navigating breast cancer: axon guidance molecules as breast cancer tumor suppressors and oncogenes. *Journal of mammary gland biology and neoplasia,* 16(3), pp.257-270.

Hass, R., 2020. Role of MSC in the Tumor Microenvironment. *Cancers,* 12(8), p.2107.

Hass, R., von der Ohe, J. & Ungefroren, H., 2019. Potential role of MSC/cancer cell fusion and EMT for breast cancer stem cell formation. *Cancers,* 11(10), pp.1432.

He, M. & Zeng, Y., 2016. Microfluidic exosome analysis toward liquid biopsy for cancer. *Journal of laboratory automation, 21(4), pp.599-608.*

He, N., et al., 2018. MSCs inhibit tumor progression and enhance radiosensitivity of breast cancer cells by down-regulating Stat3 signaling pathway. *Cell death & disease,* 9(10), pp.1-14.

Higgins, M. J. & Baselga, J., 2011. Targeted therapies for breast cancer. *The Journal of clinical investigation,* 121(10), pp.3797-3803.

Hiramoto, H., et al., 2017. miR-509-5p and miR-1243 increase the sensitivity to gemcitabine by inhibiting epithelial-mesenchymal transition in pancreatic cancer. *Scientific reports,* 7(1), pp.1-12.

Hmadcha, A., Martin-Montalvo, A., Gauthier, B. R., Soria, B. & Capilla-Gonzalez, V., 2020. Therapeutic potential of mesenchymal stem cells for cancer therapy. *Frontiers in bioengineering and biotechnology*, 8, p.43.

Hopkins, B. D., Goncalves, M. D. & Cantley, L. C., 2020. Insulin-PI3K signalling: an evolutionarily insulated metabolic driver of cancer. *Nature Reviews Endocrinology*, 16(5), pp.276-283.

Hu, W., et al., 2018. Functional miRNAs in breast cancer drug resistance. *Oncotargets and therapy*, 11, pp.1529-1541.

Huang, B., et al., 2005. Toll-like receptors on tumor cells facilitate evasion of immune surveillance. *Cancer research*, 65(12), pp.5009-5014.

Huang, J., Li, H. & Ren, G., 2015. Epithelial-mesenchymal transition and drug resistance in breast cancer. *International journal of oncology*, 47(3), pp.840-848.

Hurvitz, S. A., Hu, Y., O'Brien, N. & Finn, R. S., 2013. Current approaches and future directions in the treatment of HER2-positive breast cancer. *Cancer treatment reviews*, 39(3), pp.219-229.

Hwang, H. J., Oh, M. S., Lee, D. W. & Kuh, H. J., 2019. Multiplex quantitative analysis of stroma-mediated cancer cell invasion, matrix remodeling, and drug response in a 3D co-culture model of pancreatic tumor spheroids and stellate cells. *Journal of Experimental & Clinical Cancer Research*, 38(1), pp.1-14.

Iacona, J. R. & Lutz, C. S., 2019. miR-146a-5p: Expression, regulation, and functions in cancer. *Wiley Interdisciplinary Reviews: RNA*, 10(4), pp.e1533.

Iacoviello, L., Bonaccio, M., de Gaetano, G. & Donati, M. B., 2020. Epidemiology of breast cancer, a paradigm of the "common soil" hypothesis. *Seminars in cancer biology*, (Vol. 72, pp.4-10). Academic Press.

Ignatov, A., Eggemann, H., Burger, E. & Ignatov, T., 2018. Patterns of breast cancer relapse in accordance to biological subtype. *Journal of cancer research and clinical oncology*, 144(7), pp.1347-1355.

Jensen, J., Kitlen, J. W., Briand, P., Labrie, F. & Lykkesfeldt, A. E., 2003. Effect of antiestrogens and aromatase inhibitor on basal growth of the human breast cancer cell line MCF-7 in serum-free medium. *The Journal of steroid biochemistry and molecular biology*, 84(4), pp.469-478.

Jiang, X., et al., 2020. The role of microenvironment in tumor angiogenesis. *Journal of Experimental & Clinical Cancer Research*, 39(1), pp.1-19.

Jiang, Z. S., Sun, Y. Z., Wang, S. M. & Ruan, J. S., 2017. Epithelial-mesenchymal transition: potential regulator of ABC transporters in tumor progression. *Journal of Cancer*, 8(12), pp.2319-2327.

Kim, J. G., et al., 2014. Epigenetically regulated MIR941 and MIR1247 target gastric cancer cell growth and migration. *Epigenetics*, 9(7), pp.1018-1030.

Kittaneh, M., Montero, A. J. & Glück, S., 2013. Molecular profiling for breast cancer: a comprehensive review. *Biomarkers in cancer*, 5, pp.61-70.

Kletukhina, S., Neustroeva, O., James, V., Rizvanov, A. & Gomzikova, M., 2019. Role of mesenchymal stem cell-derived extracellular vesicles in epithelial–mesenchymal transition. *International journal of molecular sciences*, 20(19), p.4813.

Koboldt, D.C.F.R., et al., 2012. Comprehensive molecular portraits of human breast tumours. *Nature*, 490(7418), pp.61-70.

Kodahl, A. R., et al., 2014. Novel circulating microRNA signature as a potential non-invasive multi-marker test in ER-positive early-stage breast cancer: a case control study. *Molecular oncology*, 8(5), pp.874-883.

Koh, B., Jeon, H., Kim, D., Kang, D. & Kim, K. R., 2019. Effect of fibroblast co-culture on the proliferation, viability and drug response of colon cancer cells. *Oncology letters*, 17(2), pp.2409-2417.

Kong, Y. W., Ferland-McCollough, D., Jackson, T. J. & Bushell, M., 2012. microRNAs in cancer management. *The lancet oncology*, 13(6), pp.e249-e258.

Kowal, J., Tkach, M. & Théry, C., 2014. Biogenesis and secretion of exosomes. *Current opinion in cell biology*, 29, pp.116-125.

Kucerova, L., Skolekova, S., Matuskova, M., Bohac, M. & Kozovska, Z., 2013. Altered features and increased chemosensitivity of human breast cancer cells mediated by adipose tissue-derived mesenchymal stromal cells. *BMC cancer*, 13(1), pp.1-13.

Kuhbier, J. W., et al., 2014. Observed changes in the morphology and phenotype of breast cancer cells in direct co-culture with adipose-derived stem cells. *Plastic and reconstructive surgery*, 134(3), pp.414-423.

Kumar, P., et al., 2013. Circulating miRNA biomarkers for Alzheimer's disease. *PloS one,* 8(7), p.e69807.

Lawrie, C. H., et al., 2008. Detection of elevated levels of tumour-associated microRNAs in serum of patients with diffuse large B-cell lymphoma. *British journal of haematology,* 141(5), pp.672-675.

Leung, E. Y., et al., 2017. Endocrine therapy of estrogen receptor-positive breast cancer cells: early differential effects on stem cell markers. *Frontier in oncology,* 7, p.184.

Li, L., et al., 2011. Human mesenchymal stem cells play a dual role on tumor cell growth in vitro and in vivo. *Journal of Cellular Physiology,* 226(7), pp.1860-1867.

Li, N. Y., et al., 2013. An MAPK-dependent pathway induces epithelial-mesenchymal transition via Twist activation in human breast cancer cell lines. *Surgery,* 154(2), pp.404-410.

Li, T., et al., 2020. Adipose-derived mesenchymal stem cells and extracellular vesicles confer antitumor activity in preclinical treatment of breast cancer. *Pharmacological research,* 157, p.104843.

Lo, H. C. & Zhang, X. H. F., 2018. EMT in metastasis: Finding the right balance. *Developmental Cell,* 45(6), pp.663-665.

Lobb, R. J., et al., 2015. Optimized exosome isolation protocol for cell culture supernatant and human plasma. *Journal of extracellular vesicles,* 4(1), p.27031.

Loh, H. Y., et al., 2019. The regulatory role of microRNAs in breast cancer. *International journal of molecular sciences,* 20(19), p.4940.

Lu, T. P., et al., 2012. miRSystem: an integrated system for characterizing enriched functions and pathways of microRNA targets. *PLoS One,* 7(8), p.e42390.

Luo, M. & Guan, J. L., 2010. Focal adhesion kinase: a prominent determinant in breast cancer initiation, progression and metastasis. *Cancer letters,* 289(2), pp.127-139.

Majidinia, M. & Yousefi, B., 2017. DNA repair and damage pathways in breast cancer development and therapy. *DNA repair,* 54, pp.22-29.

Malvezzi, M., et al., 2019. European cancer mortality predictions for the year 2019 with focus on breast cancer. *Annals of Oncology,* 30(5), pp.781-787.

Marlow, R., et al., 2013. A novel model of dormancy for bone metastatic breast cancer cells. *Cancer research,* 73(23), pp.6886-6899.

Martin, M., 2011. Cutadapt removes adapter sequences from high-throughput sequencing reads. *EMBnet. journal,* 17(1), pp.10-12.

Mi, H., Muruganujan, A., Casagrande, J. T. & Thomas, P. D., 2013. Large-scale gene function analysis with the PANTHER classification system. *Nature protocols,* 8(8), pp.1551-1566.

Milane, L., Singh, A., Mattheolabakis, G., Suresh, M. & Amiji, M. M., 2015. Exosome mediated communication within the tumor microenvironment. *Journal of Control Release,* 219, pp.278-294.

Morel, A. P., et al., 2012. EMT inducers catalyze malignant transformation of mammary epithelial cells and drive tumorigenesis towards claudin-low tumors in transgenic mice. *PLoS genetics,* 8(5), p.e1002723.

Muntean, A. G. & Hess, J. L., 2009. Epigenetic dysregulation in cancer. *The American journal of pathology,* 175(4), pp.1353-1361.

Neophytou, C. M., Kyriakou, T. C. & Papageorgis, P., 2019. Mechanisms of metastatic tumor dormancy and implications for cancer therapy. *International journal of molecular sciences,* 20(24), p.6158.

Nygren, M. K., et al., 2014. Identifying microRNAs regulating B7-H3 in breast cancer: the clinical impact of microRNA-29c. *British journal of cancer,* 110(8), pp.2072-2080.

Ono, M., et al., 2014. Exosomes from bone marrow mesenchymal stem cells contain a microRNA that promotes dormancy in metastatic breast cancer cells. *Science signaling,* 7(332), pp.ra63.

Ota, I., Li, X. Y., Hu, Y. & Weiss, S. J., 2009. Induction of a MT1-MMP and MT2-MMP-dependent basement membrane transmigration program in cancer cells by Snail1. *Proceedings of the National Academy of Sciences,* 106(48), pp.20318-20323.

Othman, N. & Nagoor, N. H., 2014. The role of microRNAs in the regulation of apoptosis in lung cancer and its application in cancer treatment. *BioMed research international,* 2014.

Pandey, A. C., et al., 2011. MicroRNA profiling reveals age-dependent differential expression of nuclear factor κB and mitogen-activated protein kinase in adipose and bone marrow-derived human mesenchymal stem cells. *Stem Cell Research & Therapy,* 2(6), pp.1-18.

Pantel, K. & Hayes, D. F., 2018. Disseminated breast tumour cells: biological and clinical meaning. *Nature Reviews Clinical Oncology*, 15(3), pp.129-131.

Park, S. Y. & Nam, J. S., 2020. The force awakens: metastatic dormant cancer cells. *Experimental & Molecular Medicine*, 52(4), pp.569-581.

Patel, G. K., et al., 2019. Comparative analysis of exosome isolation methods using culture supernatant for optimum yield, purity and downstream applications. *Scientific reports*, 9(1), pp.1-10.

Patrikoski, M., Mannerström, B. & Miettinen, S., 2019. Perspectives for clinical translation of adipose stromal/stem cells. *Stem cells international*, 2019.

Pfeffer, C. M. & Singh, A. T., 2018. Apoptosis: a target for anticancer therapy. *International journal of molecular sciences*, 19(2), p.448.

Phan, T. G. & Croucher, P. I., 2020. The dormant cancer cell life cycle. *Nature Reviews Cancer*, 20(7), pp.398-411.

Piccinin, S., et al., 2012. A "twist box" code of p53 inactivation: twist box: p53 interaction promotes p53 degradation. *Cancer cell*, 22(3), pp.404-415.

Plava, J., et al., 2019. Recent advances in understanding tumor stroma-mediated chemoresistance in breast cancer. *Molecular cancer*, 18(1), pp.1-10.

Prunier, C., Baker, D., Ten Dijke, P. & Ritsma, L., 2019. TGF-β family signaling pathways in cellular dormancy. *Trends in cancer*, 5(1), pp.66-78.

Qiu, G., et al., 2018. Mesenchymal stem cell-derived extracellular vesicles affect disease outcomes via transfer of microRNAs. *Stem Cell Research & Therapy*, 9(1), pp.1-9.

Qiu, L., Wang, J., Chen, M., Chen, F. & Tu, W., 2020. Exosomal microRNA-146a derived from mesenchymal stem cells increases the sensitivity of ovarian cancer cells to docetaxel and taxane via a LAMC2-mediated PI3K/Akt axis. *International journal of molecular medicine*, 46(2), pp.609-620.

Quail, D. F. & Joyce, J. A., 2013. Microenvironmental regulation of tumor progression and metastasis. *Nature Medicine*, 19(11), pp.1423-1437.

Rabbani, B., Nakaoka, H., Akhondzadeh, S., Tekin, M. & Mahdieh, N., 2016. Next generation sequencing: implications in personalized medicine and pharmacogenomics. *Molecular Biosystems*, 12(6), pp.1818-1830.

Ramdasi, S., Sarang, S. & Viswanathan, C., 2015. Potential of mesenchymal stem cell based application in cancer. *International journal of hematology-oncology and stem cell research*, 9(2), pp.95-103.

Reza, A. M. M. T., Choi, Y. J., Yasuda, H. & Kim, J. H., 2016. Human adipose mesenchymal stem cell-derived exosomal-miRNAs are critical factors for inducing anti-proliferation signalling to A2780 and SKOV-3 ovarian cancer cells. *Scientific Reports*, 6(1), pp.1-15.

Ribatti, D., Tamma, R. & Annese, T., 2020. Epithelial-mesenchymal transition in cancer: a historical overview. *Translational oncology*, 13(6), pp.100773.

Riggio, A. I., Varley, K. E. & Welm, A. L., 2021. The lingering mysteries of metastatic recurrence in breast cancer. *British Journal of Cancer*, 124(1), pp.13-26.

Roche, J., 2018. The epithelial-to-mesenchymal transition in cancer. *Cancers*, 10(3), p.79.

Romero, I., Garrido, F. & Garcia-Lora, A. M., 2014. Metastases in immune-mediated dormancy: a new opportunity for targeting cancer. *Cancer research*, 74(23), pp.6750-6757.

Rowan, B. G., et al., 2014. Human adipose tissue-derived stromal/stem cells promote migration and early metastasis of triple negative breast cancer xenografts. *PloS one*, 9(2), pp.e89595.

Rybinska, I., Agresti, R., Trapani, A., Tagliabue, E. & Triulzi, T., 2020. Adipocytes in breast cancer, the thick and the thin. *Cells*, 9(3), p.560.

Sabol, R. A., et al., 2018. Therapeutic potential of adipose stem cells. *Advances in experimental medicine and biology*, pp.1-11.

Sakha, S., Muramatsu, T., Ueda, K. & Inazawa, J., 2016. Exosomal microRNA miR-1246 induces cell motility and invasion through the regulation of DENND2D in oral squamous cell carcinoma. *Scientific reports*, 6(1), pp.1-11.

Santos, J. C., et al., 2018. Exosome-mediated breast cancer chemoresistance via miR-155 transfer. *Scientific reports*, 8(1), pp.1-11.

Saydam, O., et al., 2009. Downregulated microRNA-200a in meningiomas promotes tumor growth by reducing E-cadherin and activating the Wnt/β-catenin signaling pathway. *Molecular and cellular biology*, 29(21), pp.5923-5940.

Schweizer, R., et al., 2015. The role of adipose-derived stem cells in breast cancer progression and metastasis. *Stem cells international,* 2015(120949).

Scioli, M. G., et al., 2019. Adipose-derived stem cells in cancer progression: new perspectives and opportunities. *International journal of molecular sciences,* 20(13), p.3296.

Shang, B. Q., et al., 2019. Functional roles of circular RNAs during epithelial-to-mesenchymal transition. *Molecular cancer,* 18(1), pp.1-10.

Shao, S., et al., 2015. Notch1 signaling regulates the epithelial-mesenchymal transition and invasion of breast cancer in a Slug-dependent manner. *Molecular cancer,* 14(1), pp.1-17.

Sheedy, P. & Medarova, Z., 2018. The fundamental role of miR-10b in metastatic cancer. *American journal of cancer research,* 8(9), pp.1674-1688.

Shi, Y., Ye, P. & Long, X., 2017. Differential expression profiles of the transcriptome in breast cancer cell lines revealed by next generation sequencing. *Cellular Physiology and Biochemistry,* 44(2), pp.804-816.

Shu, D., et al., 2015. Systemic delivery of anti-miRNA for suppression of triple negative breast cancer utilizing RNA nanotechnology. *ACS nano,* 9(10), pp.9731-9740.

Si, C., Yu, Q. & Yao, Y., 2018. Effect of miR-146a-5p on proliferation and metastasis of triple-negative breast cancer via regulation of SOX5. *Experimental and therapeutic medicine,* 15(5), pp.4515-4521.

Siemens, H., et al., 2011. miR-34 and SNAIL form a double-negative feedback loop to regulate epithelial-mesenchymal transitions. *Cell cycle,* 10(24), pp.4256-4271.

Singh, R., Pochampally, R., Watabe, K., Lu, Z. & Mo, Y. Y., 2014. Exosome-mediated transfer of miR-10b promotes cell invasion in breast cancer. *Molecular cancer,* 13(1), pp.1-11.

Singletary, S. E., et al., 2003. Staging system for breast cancer: revisions for the 6th edition of the AJCC Cancer Staging Manual. *Surgical Clinics,* 83(4), pp.803-819.

Smid, M., et al., 2008. Subtypes of breast cancer show preferential site of relapse. *Cancer research,* 68(9), pp.3108-3114.

Søkilde, R., et al., 2019. Refinement of breast cancer molecular classification by miRNA expression profiles. *BMC genomics,* 20(1), pp.1-12.

Sung, H., et al., 2021. Global cancer statistics 2020: GLOBOCAN estimates of incidence and mortality worldwide for 36 cancers in 185 countries. *CA: a cancer journal for clinicians*, 71(3), pp.209-249.

Surapaneni, S. K., Bhat, Z. R. & Tikoo, K., 2020. MicroRNA-941 regulates the proliferation of breast cancer cells by altering histone H3 Ser 10 phosphorylation. *Scientific reports*, 10(1), pp.1-17.

Tanabe, S., Quader, S., Cabral, H. & Ono, R., 2020. Interplay of EMT and CSC in cancer and the potential therapeutic strategies. *Frontiers in pharmacology*, 11, p.904.

Tang, Q., Cheng, J., Cao, X., Surowy, H. & Burwinkel, B., 2016. Blood-based DNA methylation as biomarker for breast cancer: a systematic review. *Clinical epigenetics*, 8(1), pp.1-18.

Tang, Y. T., et al., 2017. Comparison of isolation methods of exosomes and exosomal RNA from cell culture medium and serum. *International journal of molecular medicine*, 40(3), pp.834-844.

Tang, Y. T., et al., 2018. Alterations in exosomal miRNA profile upon epithelial-mesenchymal transition in human lung cancer cell lines. *BMC genomics*, 19(1), pp.1-14.

Taylor, D. D., Zacharias, W. & Gercel-Taylor, C., 2011. Exosome isolation for proteomic analyses and RNA profiling. *Serum/plasma proteomics*, pp.235-246.

Théry, C., Amigorena, S., Raposo, G. & Clayton, A., 2006. Isolation and characterization of exosomes from cell culture supernatants and biological fluids. *Current protocols in cell biology*, 30(1), pp3-22.

Triaca, V., et al., 2019. Cancer stem cells-driven tumor growth and immune escape: the Janus face of neurotrophins. *Aging (Albany NY)*, 11(23), pp.11770-11792.

Van Staveren, W., et al., 2009. Human cancer cell lines: Experimental models for cancer cells in situ? For cancer stem cells? *Biochimica et Biophysica Acta (BBA)-Reviews on Cancer*, 1795(2), pp.92-103.

Vega, S., et al., 2004. Snail blocks the cell cycle and confers resistance to cell death. *Genes & development*, 18(10), pp.1131-1143.

Verma, M., 2012. Personalized medicine and cancer. *Journal of personalized medicine*, 2(1), pp.1-14.

Villarroya-Beltri, C., et al., 2013. Sumoylated hnRNPA2B1 controls the sorting of miRNAs into exosomes through binding to specific motifs. *Nature communications*, 4(1), pp.1-10.

Voduc, K. D., et al., 2010. Breast cancer subtypes and the risk of local and regional relapse. *Journal of clinical oncology,* 28(10), pp.1684-1691.

Wang, F. E., et al., 2010. MicroRNA-204/211 alters epithelial physiology. The *FASEB Journal,* 24(5), pp.1552-1571.

Wang, L., et al., 2019. Delivery of mesenchymal stem cells-derived extracellular vesicles with enriched miR-185 inhibits progression of OPMD. *Artificial cells, nanomedicine, and biotechnology,* 47(1), pp.2481-2491.

Wang, S., et al., 2019. Exosomes secreted by mesenchymal stromal/stem cell-derived adipocytes promote breast cancer cell growth via activation of Hippo signaling pathway. *Stem cell research therapy,* 10(1), pp.1-12.

Wang, Z., et al., 2016. Axon guidance molecule semaphorin3A is a novel tumor suppressor in head and neck squamous cell carcinoma. *Oncotarget,* 7(5), pp.6048-6062.

Wangchinda, P. & Ithimakin, S., 2016. Factors that predict recurrence later than 5 years after initial treatment in operable breast cancer. *World journal of surgical oncology,* 14(1), pp.1-8.

WHO, W. H. O. 2020. Global Health Estimates 2020: Deaths by Cause, Age, Sex, by Country and by Region, 2000-2019. *WHO*.

Xiong, D. D., et al., 2017. A nine-miRNA signature as a potential diagnostic marker for breast carcinoma: An integrated study of 1,110 cases. *Oncology reports,* 37(6), pp.3297-3304.

Xu, Q., et al., 2012. Mesenchymal stem cells play a potential role in regulating the establishment and maintenance of epithelial-mesenchymal transition in MCF7 human breast cancer cells by paracrine and induced autocrine TGF-β. *International journal of oncology,* 41(3), pp.959-968.

Xu, X., et al., 2018. TGF-β plays a vital role in triple-negative breast cancer (TNBC) drug-resistance through regulating stemness, EMT and apoptosis. *Biochemical and biophysical research communications,* 502(1), pp.160-165.

Yadav, A. S., et al., 2018. The biology and therapeutic implications of tumor dormancy and reactivation. *Frontiers in oncology,* 8, p.72.

Yan, G., Li, C., Zhao, Y., Yue, M. & Wang, L., 2019. Downregulation of microRNA6295p in colorectal cancer and prevention of the malignant phenotype by direct targeting of lowdensity lipoprotein receptorrelated protein 6. *International journal of molecular medicine,* 44(3), pp.1139-1150.

Yang, L., et al., 2020. Targeting cancer stem cell pathways for cancer therapy. *Signal transduction and targeted therapy,* 5(1), pp.1-35.

Yates, L. R., et al., 2017. Genomic evolution of breast cancer metastasis and relapse. *Cancer cell,* 32(2), pp.169-184.

Ye, X. & Weinberg, R. A., 2015. Epithelial-mesenchymal plasticity: a central regulator of cancer progression. *Trends in cell biology,* 25(11), pp.675-686.

Yin, C., et al., 2018. miR1855p inhibits Factin polymerization and reverses epithelial mesenchymal transition of human breast cancer cells by modulating RAGE. *Molecular medicine reports,* 18(3), pp.2621-2630.

Yip, C. H., Taib, N. & Mohamed, I., 2006. Epidemiology of breast cancer in Malaysia. *Asian pacific journal of cancer prevention,* 7(3), p.369.

Yu, D. D., et al., 2015. Role of miR-155 in drug resistance of breast cancer. *Tumor biology,* 36(3), pp.1395-1401.

Yu, S. J., et al., 2018. MicroRNA-200a confers chemoresistance by antagonizing TP53INP1 and YAP1 in human breast cancer. *BMC cancer,* 18(1), pp.1-11.

Yuan, Y., et al., 2018. Suppression of tumor cell proliferation and migration by human umbilical cord mesenchymal stem cells: A possible role for apoptosis and Wnt signaling. *Oncology letters,* 15(6), pp.8536-8544.

Zaravinos, A., 2015. The regulatory role of microRNAs in EMT and cancer. *Journal of oncology,* 2015.

Zhang, J. P., et al., 2014. MicroRNA-148a suppresses the epithelial–mesenchymal transition and metastasis of hepatoma cells by targeting Met/Snail signaling. *Oncogene,* 33(31), pp.4069-4076.

Zhang, L., et al., 2015. A circulating miRNA signature as a diagnostic biomarker for non-invasive early detection of breast cancer. *Breast cancer research and treatment,* 154(2), pp.423-434.

Zhang, M., et al., 2018. Methods and technologies for exosome isolation and characterization. *Small methods*, 2(9), p.1800021.

Zhang, P. P., et al., 2014. DNA methylation-mediated repression of miR-941 enhances lysine (K)-specific demethylase 6B expression in hepatoma cells. *Journal of biological chemistry,* 289(35), pp.24724-24735.

Zhang, X., et al., 2018. circSMAD2 inhibits the epithelial–mesenchymal transition by targeting miR-629 in hepatocellular carcinoma. *OncoTargets and therapy,* 11, pp.2853-2863.

Zhang, X., et al., 2015. Exosomes in cancer: small particle, big player. *Journal of hematology & oncology*, 8(1), pp.1-13.

Zhang, Y., Liu, Y., Liu, H. & Tang, W. H., 2019. Exosomes: biogenesis, biologic function and clinical potential. *Cell & bioscience,* 9(1), pp.1-18.

LIST OF SCIENTIFIC PAPERS

First Author

1. **Mohd Ali, N.**, et al. 2020. Adipose MSCs Suppress MCF7 and MDA-MB-231 Breast Cancer Metastasis and EMT Pathways Leading to Dormancy via Exosomal-miRNAs Following Co-Culture Interaction. *Pharmaceuticals (Basel)*, 14(1), pp.

   Tier 1, IF: 4.286 (2019)

2. **Mohd Ali, N**., et al. 2016. Probable impact of age and hypoxia on proliferation and microRNA expression profile of bone marrow-derived human mesenchymal stem cells. *PeerJ*, 4(e1536-e1536.

   Tier 1/2, IF: 2.2 (2016)

Co-Authors

1. Boo, L., et al. 2016. MiRNA Transcriptome Profiling of Spheroid-Enriched Cells with Cancer Stem Cell Properties in Human Breast MCF-7 Cell Line. *Int J Biol Sci*, 12(4), pp 427-45.

   Tier 1, IF: 4.5

2. Boo, L., et al. 2017. Phenotypic and microRNA transcriptomic profiling of the MDA-MB-231 spheroid-enriched CSCs with comparison of MCF-7 microRNA profiling dataset. *PeerJ*, 5(e3551

   Tier 2, IF: 2.2

3. Boo, L., et al. 2020. Phenotypic and microRNA characterization of the neglected CD24+ cell population in MCF-7 breast cancer 3-dimensional spheroid culture. *J Chin Med Assoc*, 83(1), pp 67-76.

   Tier 2, IF: 1.894

APPENDICES

APPENDIX A

List of Antibodies

Primary antibody (TEM)	Dilution	Company, catalogue number
Anti-CD63	1:5	Santa Cruz Biotechnology, USA
Anti-CD81	1:5	Santa Cruz Biotechnology, USA
Anti-CD9	1:5	Santa Cruz Biotechnology, USA

Secondary antibody (TEM)	Dilution	Company, catalogue number
Goat anti-mouse IgG (10nm gold)	1:20	ab39619, Abcam, USA

Primary antibody (Flow cytometry)	Dilution	Company, catalogue number
Anti-CD24-PE	1:11	130-095-953, Miltenyi Biotec, USA
Anti-CD44-FITC	1:11	130-095-195, Miltenyi Biotec, USA
Anti-CD90-PE	1:20	CS208185, Merck, USA
Anti-CD44- Alexa Fluor® 647	1:20	CS208200, Merck, USA
Anti-CD105-FITC	1:20	CS208189, Merck, USA

APPENDIX B

List of multidrug resistant (MDR), cancer stem cells (CSC) and DNA repair genes primers used in qRT-PCR

Genes	Target Sequence (5'→3')
Reference gene	
ACTB	FP: 5'-AGAGCTACGAGCTGCCTGAC-3' RP: 5'-AGCACTGTGTTGGCGTACAG-3'
Multi drug resistant-ABC transporter genes	
ABCC2	FP: 5'-TGCAGCCTCCATAACCATGAG-3' RP: 5'-GATGCCTGCCATTGGACCTA-3'
ABCG2	FP: 5'-CAGGTCTGTTGGTCAATCTCACA-3' RP: 5'-TCCATATCGTGGAATGCTGAAG-3'
ABCA3	FP: 5'-CAAAACCCTGGATCACGTGTT-3' RP: 5'-CCTCCGCGTCTCGTAGTTCT-3'
Cancer stem cell genes	
ALDH1A1	FP: 5'-AGCAGGAGTGTTTACCAAAGA-3' RP: 5'-CCCAGTTCTCTTCCATTTCCAG-3'
CD44	FP: 5'-CACAAATGGCTGGTACGTCTT-3' RP: 5'-TTCATCTTCATTTTCTTCATTTGG-3'
DNA repair genes	
TaqMan® probe	**Assay ID**
PARP1	Hs00242302_m1
PARP3	Hs00193946_m1
MLH1	Hs00979919_m1
CCND2	Hs00153380_m1

APPENDIX C

List of epithelial and mesenchymal gene primers used in qRT-PCR

Genes	Target Sequence (5'→3')
ACTB	FP: 5'-AGAGCTACGAGCTGCCTGAC-3' RP: 5'-AGCACTGTGTTGGCGTACAG-3'
E-cadherin	FP: 5'-ACAGGAACACAGGAGTCATCAG-3' RP: 5'- CCCTTGTACGTGGTGGGATT-3'
OCLN	FP: 5'-TGCCTAGCTACCCCCATCTT-3' RP: 5'-TGC ACC CAG CACAGATCAAT-3'
SNAIL	FP: 5'-AGTGGTTCTTCTGCGCTACTG-3' RP: 5'-TGCTGGAAGGTAAACTCTGGATTAG-3'
SMAD4	FP: 5'-CTCCAGCTATCAGTCTGTCA-3' RP: 5'-GATGCTCTGTCTTGGGTAATC-3'
Vimentin	FP: 5'-CCTGCAATCTTTCAGACAGG-3' RP: 5'-CTCCTGGATTTCCTCTTCGT-3'
ZEB2	FP: 5'-TTTCAGGGAGAATTGCTTGA-3' RP: 5'-CACATGCATACATGCCACTC-3'

APPENDIX D

List of miRNA primers used in RT-qPCR validation of NGS

miRNA	Sequence accession number	Target Sequence
hsa-miR-146a-5p	MIMAT 0000449	UGAGAACUGAAUUCCAUGGGUU
hsa-miR-941	MIMAT 0004984	CACCCGGCUGUGUGCACAUGUGC
hsa-miR-10b-5p	MIMAT 0000254	UACCCUGUAGAACCGAAUUUGUG
hsa-miR-760	MIMAT 0004957	CGGCUCUGGGUCUGUGGGGA
hsa-miR-205-5p	MIMAT 0000266	UCCUUCAUUCCACCGGAGUCUG

APPENDIX E

Percentage of cell proliferation (%)

Cell Type	Percentage of cell proliferation (%)				SD
	Replicate			Average	
	1	2	3		
MCF7	100	100	100	100	0
MCF7 Co-culture	69.77	80.00	73.33	74.37	5.19
MCF Re-culture without ADMSCs	81.3	85	92.3	86.20	5.60

Cell Type	Percentage of cell proliferation (%)				SD
	Replicate			Average	
	1	2	3		
MDA-MB-231	100	100	100	100	0
MDA-MB-231 Co-culture	52.78	62.96	54.69	56.81	5.41
MDA-MB-231 Re-culture without ADMSCs	110.00	108.89	97.89	105.59	6.69

APPENDIX F

Spheroid-forming ability (SFA)

Cell Type		Replicate			Average	SD
		1	2	3		
MCF7	Number of spheres	50 /10,000	48 /10,000	37 /10,000		
	Sphere forming efficiency %	0.50	0.48	0.37	0.45	0.07
MCF7 co-culture	Number of spheres	30 /10,000	20 /10,000	24 /10,000		
	Sphere forming efficiency %	0.30	0.20	0.24	0.25	0.05
MDA-MB-231	Number of spheres	57 /10,000	78 /10,000	60 /10,000		
	Sphere forming efficiency %	0.57	0.78	0.60	0.65	0.11
MDA-MB-231 co-culture	Number of spheres	118 /10,000	156 /10,000	135 /10,000		
	Sphere forming efficiency %	1.18	1.56	1.35	1.36	0.19

Three independent experiments were carried out. (Equivalent to Figure 4.5)

APPENDIX G

Pathway ranking summary of miR-941.

The pathway network analyses shows that miR-941 participates mainly in MAPK, regulation of B and T-cell receptor signaling and ErbB signaling pathways.

KEGG Pathway	Total Genes of The Term	Union Targets In The Term	Score
MAPK Signaling Pathway	272	3	3.227
Renal Cell Carcinoma	70	2	3.058
B Cell Receptor Signaling Pathway	75	2	2.999
ErbB Signaling Pathway	87	2	2.872
T Cell Receptor Signaling Pathway	108	2	2.689
Neurotrophin Signaling Pathway	127	2	2.552
Natural Killer Cell Mediated Cytotoxicity	140	2	2.47
Lysine Degradation	44	1	1.564
Long-Term Potentiation	70	1	1.369
VEGF Signaling Pathway	76	1	1.335
FC Epsilon RI Signaling Pathway	79	1	1.319
Apoptosis	88	1	1.274
Gap Junction	90	1	1.265
GnRH Signaling Pathway	101	1	1.218
Axon Guidance	129	1	1.119
Insulin Signaling Pathway	137	1	1.095
Wnt Signaling Pathway	150	1	1.059
JAK-STAT Signaling Pathway	155	1	1.046
Calcium Signaling Pathway	177	1	0.994
Chemokine Signaling Pathway	189	1	0.968
Focal Adhesion	199	1	0.949
Pathways in Cancer	325	1	0.768

APPENDIX H

Consent letter for mesenchymal stem cells use for research purpose

cryocord
premier stem cell bank

16th August 2013

Universiti Tunku Abdul Rahman
Lot PT 21144, Jalan Sungai Long,
Bandar Sg. Long, Cheras,
43000 Kajang, Selangor.

Dear Sir,

RE: A Collaboration between Cryocord Sdn. Bhd. and Associate Prof. Dr. Alan Ong Han Kiat on Research Projects Involving Laboratory Cultured Human Mesenchymal Stem Cells

With regards to the matter above, I would like to inform that Cryocord Sdn. Bhd. is currently collaborating with Associate Prof. Dr. Alan Ong Han Kiat from Universiti Tunku Abdul Rahman on research projects involving laboratory cultured human mesenchymal stem cells. In this collaboration, Cryocord Sdn. Bhd. will provide laboratory cultured human mesenchymal stem cells derived from bone marrow, umbilical cord, dental pulp or adipose tissue. These human mesenchymal stem cells are free from HIV, Hepatitis B and Hepatitis C.

The donors of the mesenchymal stem cells provided by Cryocord Sdn. Bhd. for these research projects had given their informed consent allowing the use of these cells for research purposes

Please do not hesitate to contact me if you have any questions.

Thank you,

James Then

Managing director